2.13.4 Seal Integrity

The maximum stress analyses in the previous sections are based on criteria for the accident conditions intended to prevent failures by excessive plastic deformation or by the rupture of the bolt. Using the yield stress as the stress limit for average tensile bolt stress, as per NUREG/CR-6007 [Ref. 10], implies that a small amount (0.02%) of plastic deformation is permitted. The following calculations show that the O-rings will continue to provide positive sealing of the closure lids even with this small plastic deformation.

2.13.4.1 Primary Lid Seals

The 0.02% bolt plastic deformation permitted in NUREG/CR-6007 [Ref. 10] is distributed over the 67 mm bolt shank dimension shown in Detail 1 of Drawing RT-100 PE 1001-1 Rev. G (Chapter 1, Appendix 1.4, Attachment 1.4-2). This may result in a separation between the primary lid and cask flange mating surfaces of 0.0134 mm (= 67mm × 0.0002). However, the primary lid seals are 12 +/-0.3 mm diameter EPDM rubber and the grooves for these seals are 9.4 +/- 0.15 mm deep (Drawing RT-100 PE 1001-1, Rev. G Appendix 1.4). Thus, the seal is minimally compressed 2.15 mm (= (12 - 0.3) - (9.4 + 0.15)). Considering that EPDM O-rings have a compression set of up to 45% at 150 °C (Figure 2.13.4-1), the minimum compression in the seal is 1.18 mm (= 2.15 – 0.45×2.15). Since the minimum seal compression greatly exceeds the separation due to possible plastic deformation, the primary lid/cask flange containment boundary will remain sealed following an HAC drop event.

2.13.4.2 Secondary Lid Seals

The 0.02% bolt plastic deformation permitted in NUREG/CR-6007 [Ref.10] is distributed over the 43 mm bolt shank dimension shown in Detail 2 of Drawing RT-100 PE 1001-1 Rev G, (Chapter 1, Appendix 1.4, Attachment 1.4-2). This may result in a separation between the secondary and primary lid mating surfaces of 0.0086 mm (= 43mm × 0.0002). However, the secondary seals are 12 +/-0.3 mm diameter EPDM rubber and the grooves for these seals are 9.4 +/- 0.15 mm deep (Drawing RT-100 PE 1001-1 Rev G (Chapter 1, Appendix 1.4, Attachment 1.4-2). Thus, the seal is minimally compressed 2.15 mm (= (12 - 0.3) - (9.4 + 0.15)). Considering that EPDM O-rings have a compression set of up to 45% (Figure 2.13.4-1) at 150 °C, the minimum compression in the seal is 1.18 mm (= 2.15 – 0.45×2.15). Since the minimum seal compression greatly exceeds the separation due to possible plastic deformation, the primary to secondary lid containment boundary will remain sealed following an HAC drop event.

Figure 2.13.4-1 Compression Set vs. Temperature

(Figure 2-13 from Parker O-ring Handbook [Ref. 50])

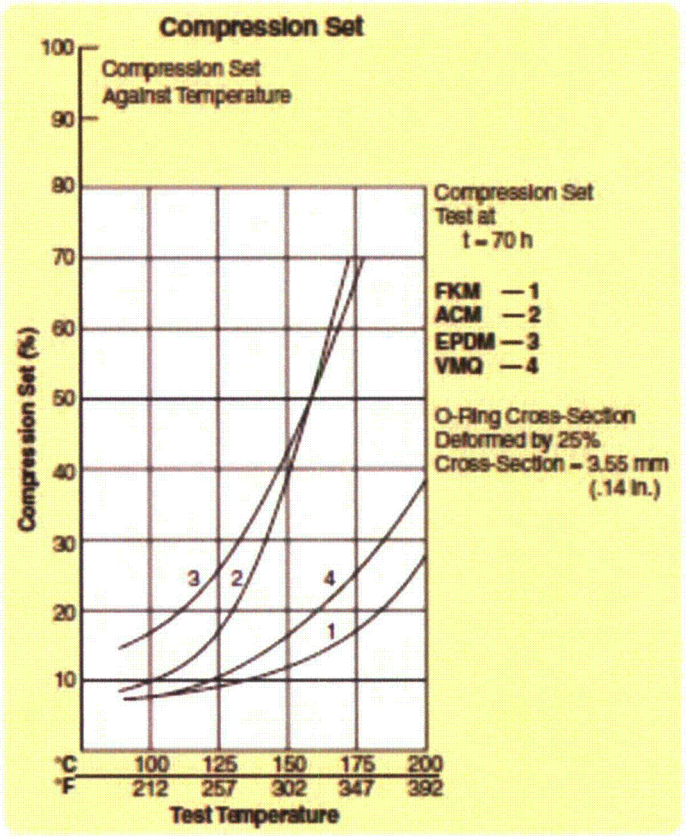

2.13.5 Vent Port Cover Plate O-Ring and Bolt Evaluation

The RT-100 cask port cover utilizes a double polymer (EPDM) O-ring configuration face seal to protect the leak test port. For this evaluation the diameter of the outer O-ring is considered to maximize the seating force (Calculation Package RTL-001-CALC-ST-0203, Rev. 6 [Ref.60]). The port cover is sealed with six DIN912 M10 x 30-A4-70 bolts.

2.13.5.1 Vent Port Cover Plate O-Ring Evaluation

This section evaluates the vent port cover sealing force and calculates the preload to maintain a tight seal (Calculation Package RTL-001-CALC-ST-0203, Rev. 6 [Ref 60]).

2.13.5.1.1 O-ring Sealing Force

The O-ring requires a minimum 3.7 N/mm sealing force (Trelleborg, Appendix 1 [Ref. 58]). The force required to seat the polymer O-ring seal is:

$$F_s = Y_r \times C = 3.7 \times (\pi \times 136.6) = 1{,}587.8 \text{ N}$$

Where,

Y_f = Sealing force
C = O-ring circumference

2.13.5.1.2 Vent Port Cover Plate Preload

The preload force available to maintain a tight seal that accounts for reduction in preload during HAC is:

$$P_L = F_c - P_{HAC} = 50{,}522 \text{ N}$$

Where,

F_c = Available closure force
= $P_{min} \times N_b$
P_{min} = Minimum preload per bolt
= $T_{min} / k / d$
T_{min} = Minimum torque (-10%, Chapter 7, Table 7.4.5-1)
= 24,300 N-mm
k = Nut factor – non-lubricated condition
= 0.3
d = Nominal bolt diameter
= 10 mm
N_b = Number of bolts
= 6
P_{HAC} = Loss of preload during HAC [Ref. 10]
= $0.0002 \times E \times A_T$
= 8,910 N
E = Modulus of elasticity
= 1.89×10^{11} Pa @ 100°C
A_t = Tensile area of the bolt [Ref. 27]

$$= 0.7854\left(d - \frac{0.97431}{n}\right)^2$$

= 77.6386 mm²
n = Number of threads per inch
= 16.93

2.13.5.1.3 Factor of Safety to Maintain a Tight Seal

Comparing the available preload force to the load required to maintain a tight seal, the factor of safety is:

$$FS = \frac{50{,}522}{1587.8} = 31.8$$

2.13.5.2 Bolt Evaluation

This section evaluates the vent port cover thread engagement and associate stress.

2.13.5.2.1 Thread Engagement

For the port cover, the mating internal and external threads are manufactured of materials of equal tensile strengths. To prevent stripping of the external threads, the minimum engagement length, L_e, is:

$$L_e = \frac{2 \times A_t}{\pi \times K_{n,max}\left[\frac{1}{2} + 0.57735 \times n \times \left(E_{s,min} - K_{n,max}\right)\right]}$$

$$= 2.46 \text{ mm}$$

Where,

$K_{n,max}$ = 8.676 mm (Machinery's Handbook [Ref. 27])
$E_{s,min}$ = 8.862 mm (Machinery's Handbook [Ref. 27])

The available thread length based on the drawings (RT-100 PE 1001-2 Rev G, Chapter 1, Appendix 1.4, Attachment 1.4-3) is 15.5 mm. Since 15.5 mm > 2.46 mm, there are sufficient threads to prevent stripping of the bolts.

2.13.5.2.2 Thread Shear Evaluation

The load necessary to shear the external threads due to the tensile force is:

$$P_S = 0.6 \times A_s \times S_y$$
$$= 121{,}044 \text{ N}$$

where,

$$A_s = \pi \times n \times L_e \times K_{n,max}\left[\frac{1}{2n} + 0.57735\left(E_{s,min} - K_{n,max}\right)\right]$$

L_e = 15.5 mm
S_y = 2.06×10^8 Pa @ 100°C

The tensile force generated in the bolt is:

$$P_B = \frac{T}{\left(\frac{l}{2\pi} + \frac{d_2\mu}{2\cos\alpha} + \frac{(d+b)\mu}{4}\right)}$$

$$= 16{,}791 \text{ N}$$

where,

T = Torque
= 29700 N-mm

d2	=	Min major diameter	[Ref. 27]
	=	d – 3/4H +EI	
D	=	10 mm	
H	=	Thread height ignoring flats	
	=	$\frac{\sqrt{3}}{2} \times P = 1.299$ mm	
EI	=	Fundamental deviation	[Ref.27]
	=	0.032	
P	=	Thread pitch	
	=	1.5 mm	
α	=	Half thread angle	
	=	30°	
μ	=	Coefficient of friction	[Ref. 27]
	=	0.15	

Comparing the load required to shear the external threads with the tensile force generated in the bolt, the factor of safety is:

$$FS = \frac{121{,}044}{16{,}791}$$
$$= 7.2$$

2.13.5.2.3 Load to Break Bolt

The load necessary to break the bolt is:

$$P = S_u \times A_t$$
$$= 48{,}058 \text{ N}$$

where,

$$S_u = 6.19 \times 10^8 \text{ Pa @ } 100°C$$

Since the load required to break the bolt is less than the applied force (48,058 N > 16,791 N), the bolts will not fail.

2.14 Appendix – Fabrication Stress Evaluation

Manufacturing the RT-100 can introduce thermal stresses in the inner shell during the lead pouring process. These thermal stresses are evaluated in this section to provide assurance that the manufacturing process does not adversely affect the normal operation of the cask, or its ability to survive an accident.

According to Regulatory Position 7 of Regulatory Guide 7.6 [Ref. 4], any residual stresses in the containment vessel shell resulting from inelastic strain associated with the secondary local bending stresses (which are due to the lead pour thermal gradient) must be considered in the total stress range for normal and accident load conditions. Residual stresses in the containment vessel (inner shell) induced by shrinkage of the lead shielding after the lead pouring operation are relieved early in the life of the cask because of the low creep strength of lead.

The lead pour process is accomplished by first welding the inner and outer shells to the flange, which forms an annular region between the shells. Prior to the lead pour process; the initial temperature of the inner and outer shells is pre-heated to approximately 350°C. The lead is heated until the molten temperature is between 390°C and 440°C. Molten lead is then poured continuously through the open end of the cask until the entire annular region is filled. Solidification is allowed only when the entire cavity is completely filled. Water is then used to cool the cask below 327°C, where solidification occurs. Following the pouring process, the cask is allowed to cool to ambient conditions.

2.14.1 Lead Pour

This section evaluates the stresses generated during the lead pouring process.

2.14.1.1 Cask Shell Geometry

At 21°C, the cask inner and outer shell geometry dimensions are:

Inner Shell

Inside Diameter ($d_{i\text{-}21}$)	= 1.730 m
Outside Diameter ($d_{o\text{-}21}$)	= 1.790 m
Shell Thickness (t_i)	= 0.030 m

Outer Shell

Inside Diameter ($D_{i\text{-}21}$)	= 1.970 m
Outside Diameter ($D_{o\text{-}21}$)	= 2.040 m
Shell Thickness (T_o)	= 0.035 m

2.14.1.2 Stresses Resulting from Lead Pour

The hydrostatic pressure, Q, produced by the column of lead is:

$$Q = \rho \times h \times g = 224.8 \text{ kPa}$$

Where:

ρ = 11340 kg/m^3 (lead density)

h = 2.021 m (maximum height of lead column)

g = 9.81 m/s^2

For this analysis, it is assumed that the lead reaches a maximum temperature of 440°C, and the shells, initially at 21°C, reach an equilibrium temperature of 440°C. At 440°C, key shell geometric dimensions are:

$$d_{o\text{-}400} = d_{o\text{-}21}(1+\alpha\Delta T) = 1.80 \text{ m}$$

$$D_{i\text{-}400} = D_{i\text{-}21}(1+\alpha\Delta T) = 1.99 \text{ m}$$

$$t_{i-400} = t_{i-21}(1+\alpha\Delta T) = 0.0302 \text{ m}$$

Where:

$\alpha = 1.824 \times 10^{-5}$ m/m/°C at 440°C (stainless steel)

$\Delta T = 400 - 21 = 419$°C.

The hydrostatic pressure of the molten lead subjects the inner shell to an external hydrostatic pressure. The hydrostatic pressure varies from a maximum of 224.8 kPa at the bottom of the inner shell to 0 psi at the top of the lead cylinder. Using Table 29, Case 6 of "Roark's Formula for Stress and Strain" [Ref. 29], the deformation at the bottom of the inner shell y_B is found to be -3.567×10^{-5} m. The maximum circumferential membrane stress in the inner shell is:

$$S_{\theta max} = \frac{y_B E}{R} = -6.67 \text{ MPa}$$

Where:

E = 168.5 GPa at 399°C

R = 1.80/2 = 0.90 m

This stress exists only as long as the lead is molten and produces no plastic deformation of the inner shell. When the lead solidifies and begins to cool, it shrinks and exerts a uniform external pressure on the inner shell due to the lead coefficient of expansion being larger than that of stainless steel.

2.14.2 Cool-down

This section evaluates the stresses that occur during the cool-down process.

2.14.2.1 Hoop (Circumferential) Stresses

Proprietary Information Content Withheld Under 10 CFR 2.390

Proprietary Content Withheld Under 10 CFR 2.390

Proprietary Information Content Withheld Under 10 CFR 2.390

2.14.2.2 Axial Stress

Axial stresses develop in the lead shell and inner shell during fabrication as a result of the unequal shrinkage of the lead and steel shells. Assuming that the lead bonds to the inner shell during the cool-down process after completion of lead pouring, the stress in the lead when cooled to 21°C is:

$$S_{lead} = \varepsilon E = 3.44 \times 10^{-3} \times 16.7 \times 10^{9} = 57.4 \text{ MPa}$$

Where:

$$\varepsilon_{lead} = (\alpha_{lead} - \alpha_{shell})\,\Delta T = 3.44 \times 10^{-3} \text{ m/m}$$
$$\alpha_{lead} = 2.90 \times 10^{-5} \text{ m/m/°C}$$
$$\alpha_{shell} = 1.78 \times 10^{-5} \text{ m/m/°C}$$
$$\Delta T = 327 - 21 = 327\text{°C}$$
$$E = E_{lead70} = 16.7 \text{ GPa}$$

The calculated stress is above the yield point of lead (ranging between 5 and 19 MPa at 21°C). The axial load placed on the steel inner shell by shrinkage of the lead is therefore limited by the yield strength of lead. The maximum load imposed by the lead is:

$$P_{lead} = 19 \times \pi\,(0.985^2 - 0.895^2) = 1.010 \times 10^{7} \text{ N}$$

The corresponding compression stress in the inner shell to maintain equilibrium is:

$$S_{shell} = \frac{P}{A} = \frac{-1.010 \times 10^{7}}{\pi\left((0.985)^2 - (0.895)^2\right)} = -60.9 \text{ MPa}$$

This value is conservative because the yield strength of lead is very low at elevated temperatures (approximately 3 MPa) and therefore, the creep rate is high. Also, complete bonding of the lead to the stainless steel inner shell is not expected to occur. This case bounds others axial loading configurations since the calculation is based on the yield strength of lead at 21°C.

2.14.2.3 Effects of Temperature Differential during Cool-down

The preceding analyses assume that the inner shell and lead are always at the same temperature at any time during the cool-down process. This assumption may not be true under actual conditions. Because of the high thermal conductivity of the stainless steel and the lead, the temperature differential between the lead and steel inner shell is kept to a minimum. If the inner shell is cooler than the lead, the interference and the corresponding interface pressure and resulting hoop stresses are less than the equal temperatures case. Hence, the preceding analysis is conservative. An analysis is required if the inner shell is hotter than the lead shield. Assuming the temperature of the inner shell is 59°C and the lead is 21°C, the inner radius of the stress-free lead shell at 21°C is 0.892 m; the outer radius of the inner shell at 59°C is:

$$r_o = 0.892\,[1 + (1.53 \times 10^{-5})(38)] = 0.893 \text{ m}$$

The interference between the inner shell and the lead is 0.893 – 0.892 = 0.001 m. To accommodate this interference, the lead must deform 0.001 m. For $\delta = 0.001$ m, the maximum circumferential stress $S_{\theta max}$ in the inner shell is:

$$S_{\theta max} = \frac{\delta(E)}{R} = 9.7\ MPa$$

where

$R = 1.784/2 = 0.892$ m

$E = E_{lead70} = 16.7$ GPa

2.14.3 Lead Creep

As discussed previously, cooling of the lead shell and inner shell introduces acceptably low hoop and axial stresses in the inner shell. These stresses are relieved early in the life of the cask since lead demonstrates a significant creep rate at both room and elevated temperatures.

2.15 Appendix – Seal Region Stress Evaluation

To provide assurance that the primary and secondary cask seals meet the linear elastic requirements of Regulatory Guide 7.6 [Ref. 4] the contact stresses that represent the maximum nodal stresses on the sealing surfaces and the linearized nodal stresses in the solid elements that comprise the seal regions are evaluated and compared to the yield strength of the material at the maximum NCT temperature. The evaluation shows that the RT-100 seal region does not undergo inelastic deformation.

2.15.1 Seal Region Post-Processing Methodology

The cask body calculation reports the primary membrane and membrane plus bending stress

intensities averages across linearized sections. To evaluate the stresses in the lid gasket region, the lid component is first selected as shown in Figure 2.15.4-1. As shown in Figure 2.15.4-2, the elements comprising the lid gasket region are then selected to evaluate the stresses specific to the primary gasket location. Visual inspection of the model shows the location of the peak stress in the gasket region and the nodes are identified to calculate the average stress. The ANSYS finite element program [Ref. 28] calculates the average stress across a section by identifying the nodal points using the ANSYS APDL commands PATH, PDEF and PPATH. Figure 2.15.4-2 provides an example of where 2 points are defined across the gasket region. Once the points and path are defined, the ANSYS APDL command PRSECT reports the average stresses.

2.15.2 Stress Concentration Factors

Trapezoidal grooves are cut into the primary and secondary lids to allow the gaskets to properly seat during the closure process. Figure 2.15.4-3 shows the lid/gasket geometry. Under load, the grooves can cause a stress riser at the radius, r, where the groove transitions from horizontal to vertical ("Standard Handbook for Mechanical Engineers" [Ref. 55]). For this evaluation, the load is in the form of a bending moment. Using the dimensions provided in Figure 2.15.4-3 and Table 2.15.4-1, the resulting stress concentration factors are calculated in terms of the ratios of D/d and r/d. For the primary and secondary lids, the stress concentration factors are 2.6 and 2.2, respectively.

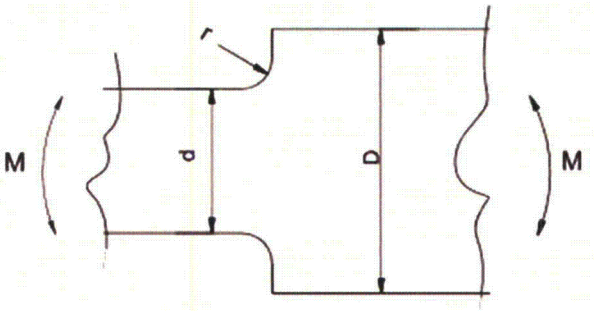

2.15.3 Seal Region Stress Results

The contact stresses that represent the maximum nodal stresses on the sealing surfaces are summarized in Table 2.15.4-2. The resulting membrane plus bending stresses are compared to the yield stress of the material at the maximum NCT temperature for each HAC case.

For the lid gasket grooves, the linearized stress is calculated for each peak stress location as described in Section 2.15.1 and multiplied by the stress concentration factor calculated in Section 2.15.2. Table 2.15.4-3 provides a summary of the resulting factored stress values. As the table shows the minimum factor of safety is 1.2 in accordance with Regulatory Guide 7.6 [Ref.4], the RT-100 seal region experiences no inelastic deformation during all HAC events.

2.15.4 Displacement Results

To determine whether the seal remains tight during HAC, the relative displacement of each sealing surface is determined. Table 2.15.4-4 calculates the relative displacement for each sealing surface and Figure 2.15.4-4 through Figure 2.15.4-9 provide graphical representations of the displacement for each case. From the containment evaluation, the permanent plastic deformation for the EPDM O-ring is approximately 25%. Therefore, based on the seal dimensions, the maximum permissible gap is 1.61mm. Reviewing the relative displacements from Table 2.15.4-4, the maximum separation that occurs is 0.07706mm. Since this maximum separation is less than the permissible gap, the seals are predicted to remain tight during all HAC events.

Table 2.15.4-1 Stress Concentration Factors

D/d	r/d							
	0.01	0.02	0.04	0.06	0.1	0.15	0.2	0.3
1.01	1.76	1.53	1.37	1.32	1.28	1.25	1.22	1.19
1.02	2.05	1.74	1.52	1.42	1.35	1.28	1.25	1.22
1.05	2.58	2.11	1.77	1.62	1.47	1.40	1.34	1.29
1.10	3.09	2.45	2.00	1.80	1.59	1.49	1.40	1.31
1.20	3.62	2.81	2.23	1.97	1.70	1.55	1.44	1.34
1.50	3.80	2.98	2.38	2.15	1.83	1.63	1.52	1.38
2.00		3.14	2.59	2.23	1.88	1.66	1.54	1.40
3.00		3.30	2.68	2.34	1.93	1.67	1.53	1.38

Table 2.15.4-2 Sealing Surface Stress Summary

Accident Condition	Yield Strength at Max. NCT Seal Temp (MPa)	Primary Sealing Surface Contact Stress (MPa)	FS	Primary Seal Linearized Stress Intensity P_m+P_b (MPa)	FS	Secondary Sealing Surface Contact Stress (MPa)	FS	Secondary Seal Linearized Stress Intensity P_m+P_b (MPa)	FS
Side Drop	184.2	40.1	4.6	15.6	11.8	5.7	32.3	33.7	5.5
End Drop	184.2	22.8	8.1	14.3	12.9	0.0	N/A	62.7	2.9
Puncture	184.2	93.2	2.0	77.0	2.4	83.4	2.2	89.7	2.1

Table 2.15.4-3 Lid Seal Groove Region Stresses

Accident Condition	Yield Strength at Max NCT Seal Temp (MPa)	Stress Concentration	Linearized Stress in Primary Lid Primary Seal (MPa)	Maximum Stress (MPa)	FS	Stress Concentration	Linearized Stress in Secondary Lid Primary Seal (MPa)	Maximum Stress (MPa)	FS
Side Drop	184.2	2.6	15.0	38.9	4.7	2.2	66.1	145.3	1.3
End Drop	184.2	2.6	45.1	115.9	1.6	2.2	47.7	102.6	1.8
Puncture	184.2	2.6	59.1	153.6	1.2	2.2	71.8	158.0	1.2

Table 2.15.4-4 HAC Seal Region Displacement

Location	Minimum Displacement (mm)	Maximum Displacement (mm)
HAC Side Drop		
Primary Lid Sealing Surface	-0.047281	-0.33065
Primary Seal Flange Surface	-0.043598	-0.40771
Relative Displacement	↓ -0.003683	↑ 0.07706
Secondary Lid Sealing Surface	-0.12481	-0.31864
Secondary Lid Sealing Surface on Primary Lid	-0.12238	-0.34072
Relative Displacement	↓ -0.00243	↑ 0.02208
HAC End Drop		
Primary Lid Sealing Surface	-0.27689	-0.43679
Primary Seal Flange Surface	-0.27867	-0.43227
Relative Displacement	↑ 0.00178	↓ -0.00452
Secondary Lid Sealing Surface	-0.93881	-1.08
Secondary Lid Sealing Surface on Primary Lid	-0.93328	-1.1009
Relative Displacement	↓ -0.00553	↑ 0.0209
Puncture		
Primary Lid Sealing Surface	0.044821	-0.12329
Primary Seal Flange Surface	0.046104	-0.1212
Relative Displacement	↑ -0.001283	↓ -0.00209
Secondary Lid Sealing Surface	-0.85594	-1.1537
Secondary Lid Sealing Surface on Primary Lid	-0.84898	-1.1475
Relative Displacement	↓ -0.00696	↑ -0.0062

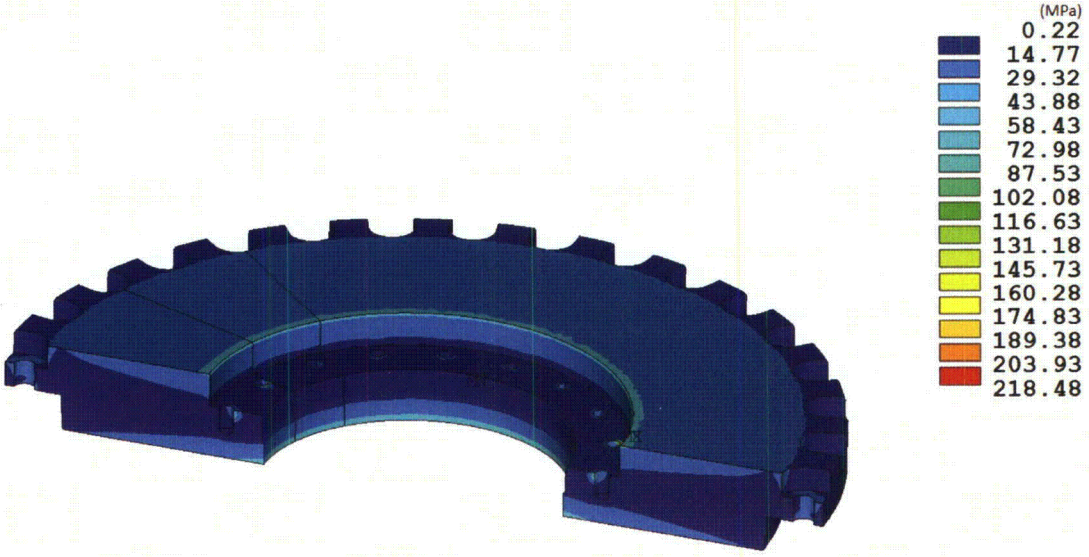

Figure 2.15.4-1 Stress Intensity Contour Plot of Primary Lid Following End Drop.

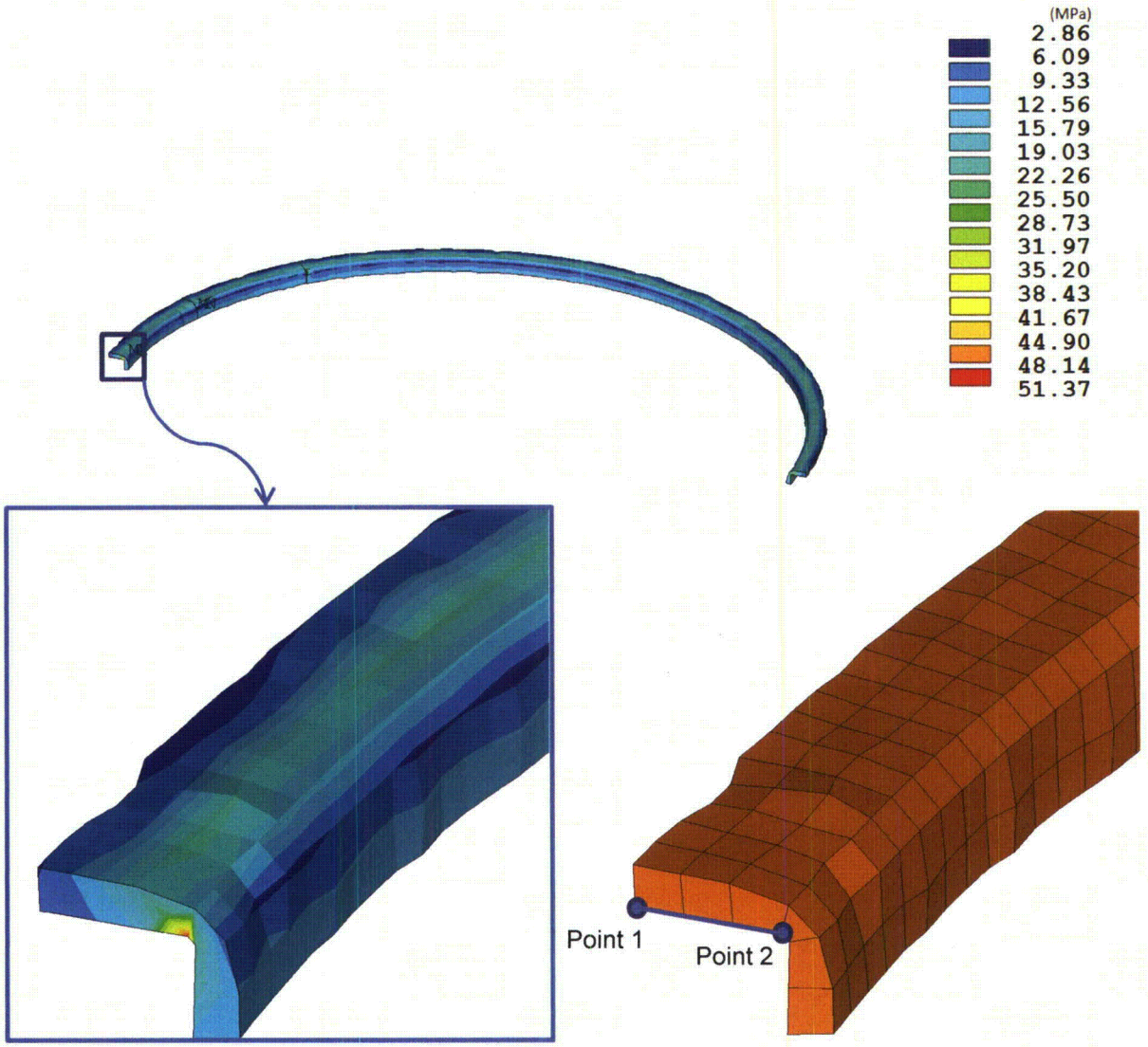

Figure 2.15.4-2 Stress Intensity Contour Plot of the Primary Seal Region

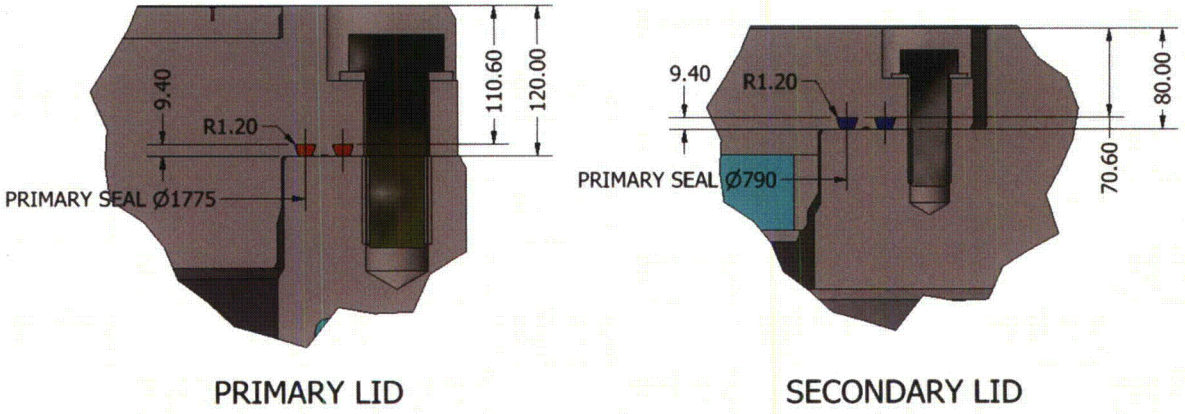

Figure 2.15.4-3 Lid Seal Geometry

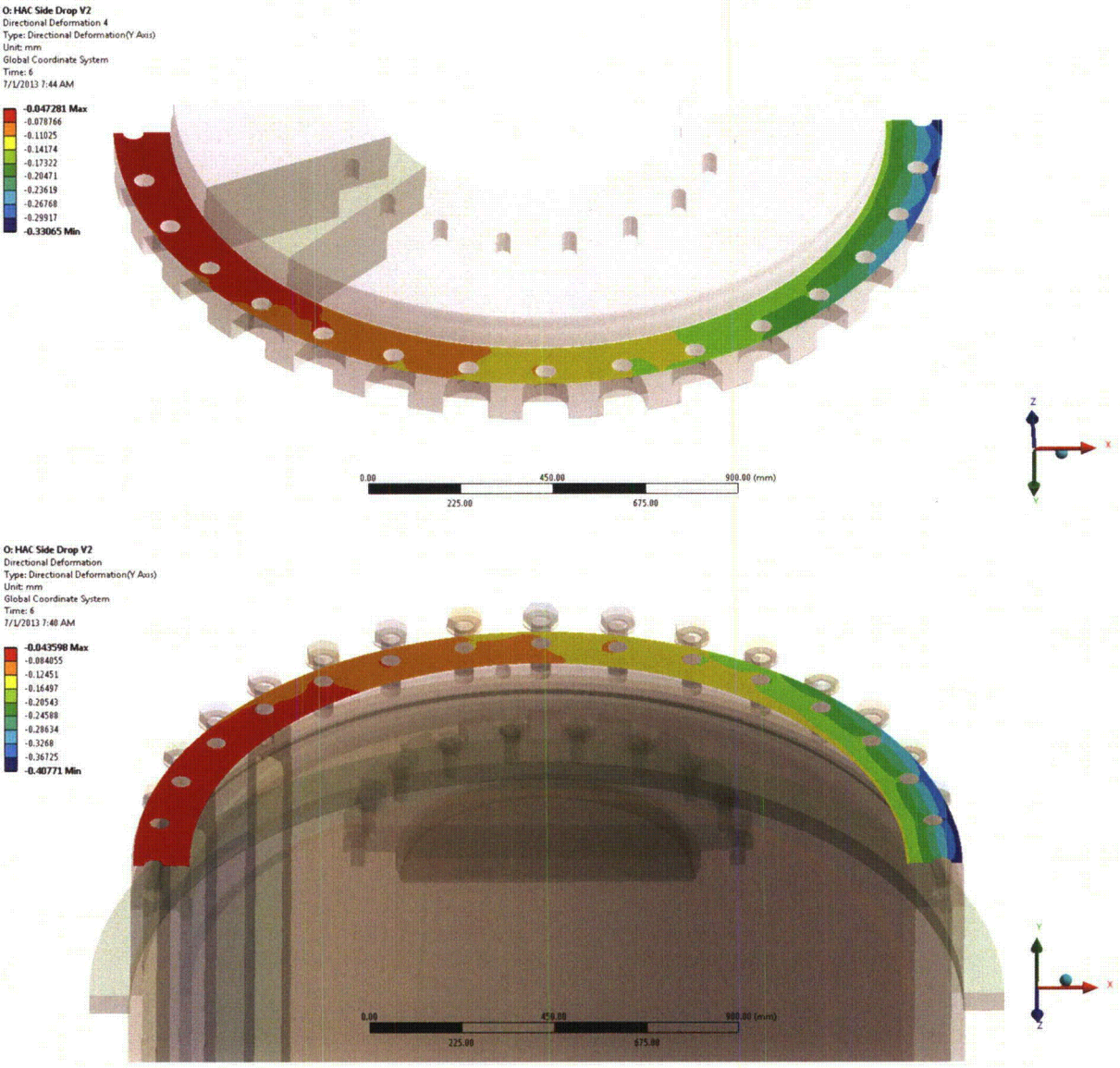

Figure 2.15.4-4 Primary Lid Sealing Surface Displacement during Side drop

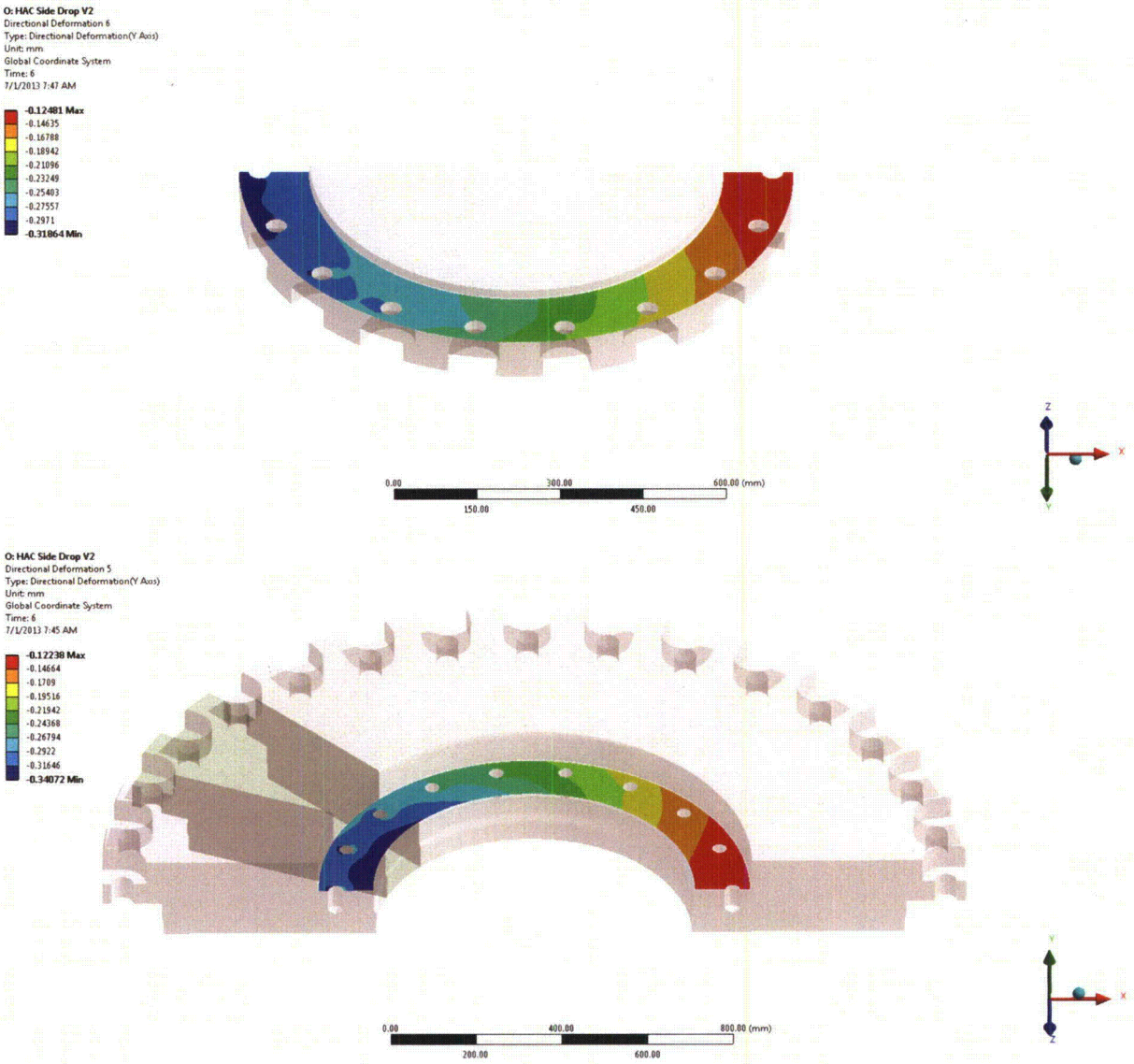

Figure 2.15.4-5 Secondary Lid Sealing Surface Displacement during Side drop

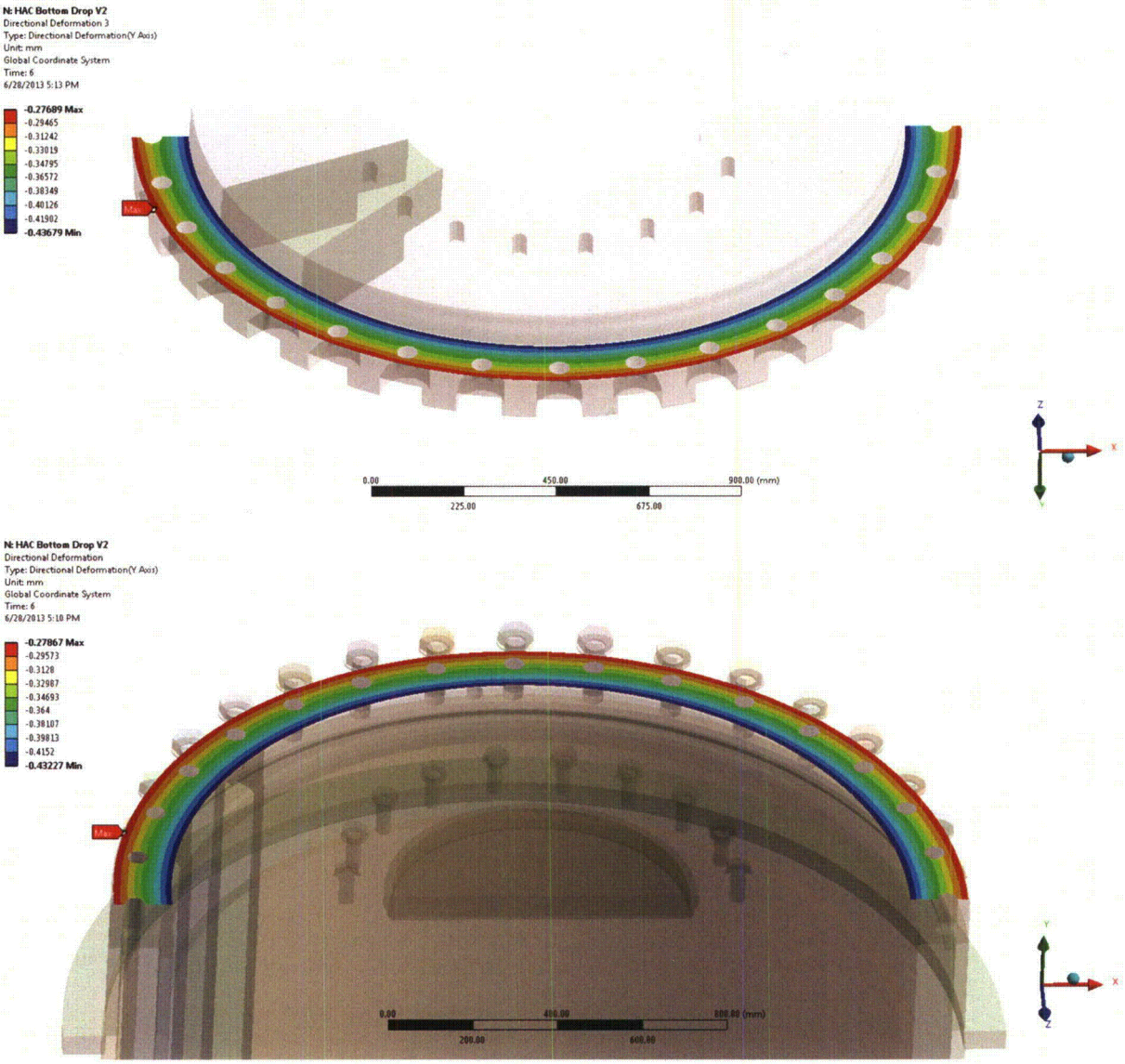

Figure 2.15.4-6 Primary Lid Sealing Surface Displacement during End drop

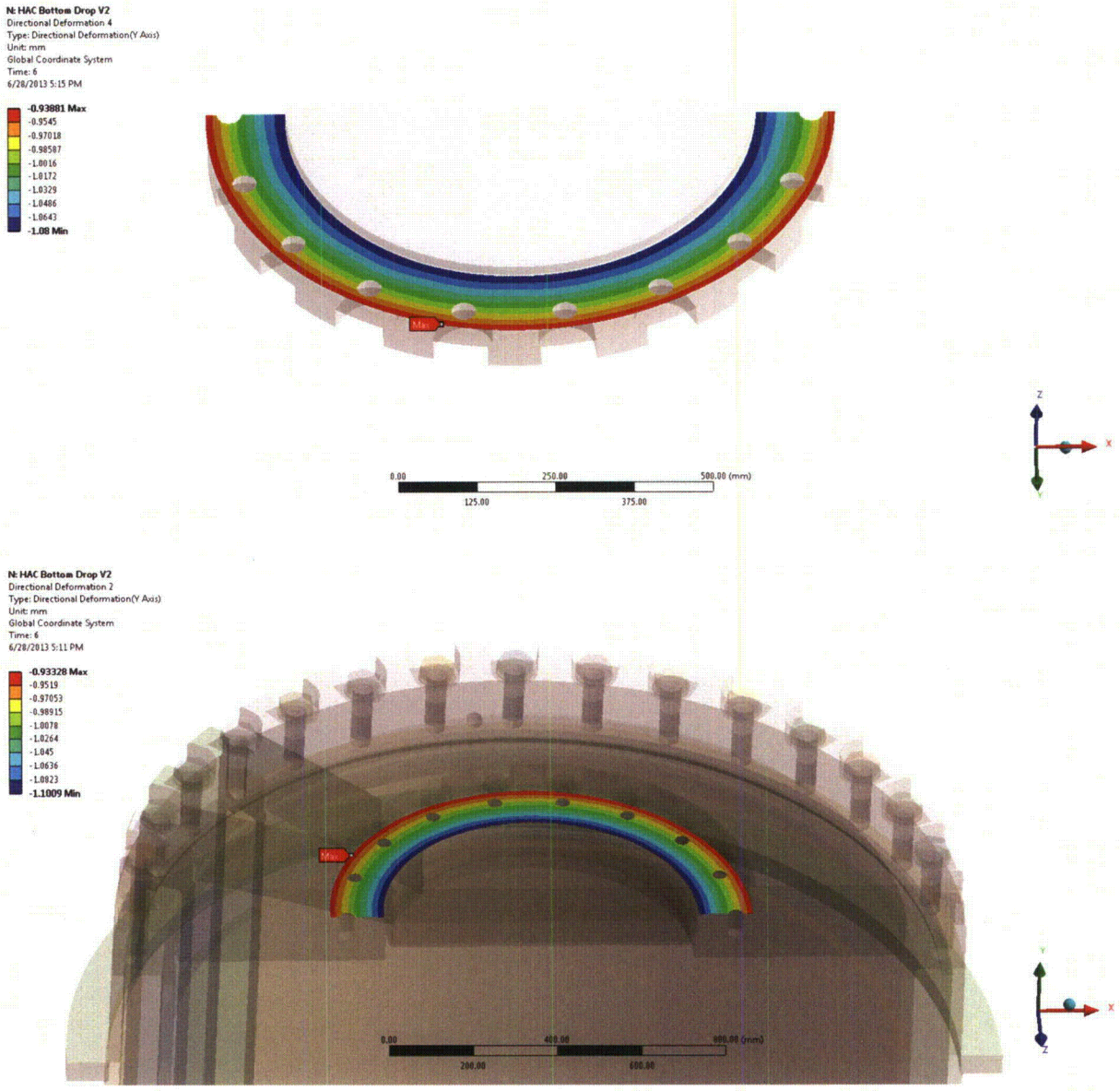

Figure 2.15.4-7 Secondary Lid Sealing Surface Displacement during End drop

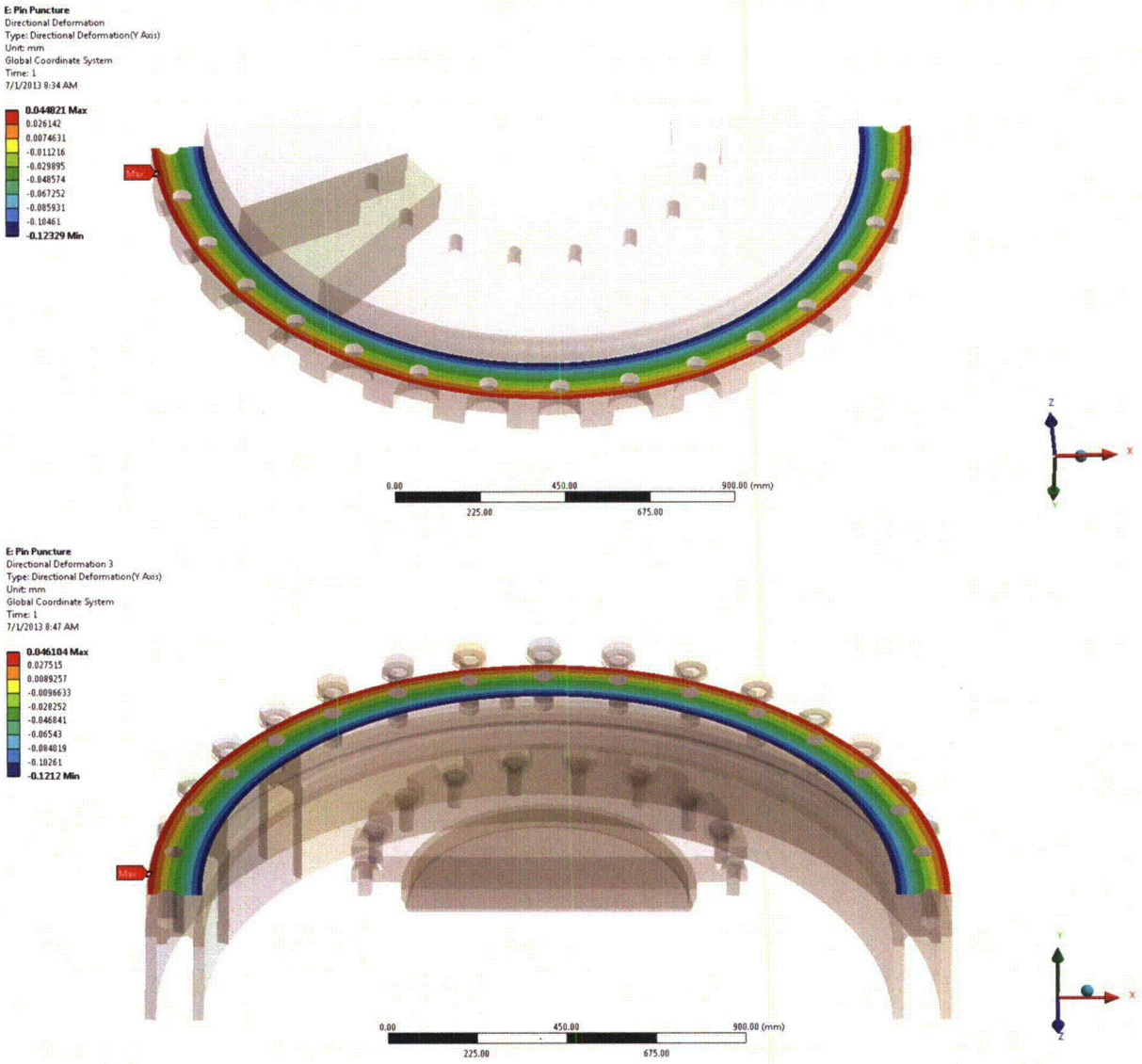

Figure 2.15.4-8 Primary Lid Sealing Surface Displacement during Puncture

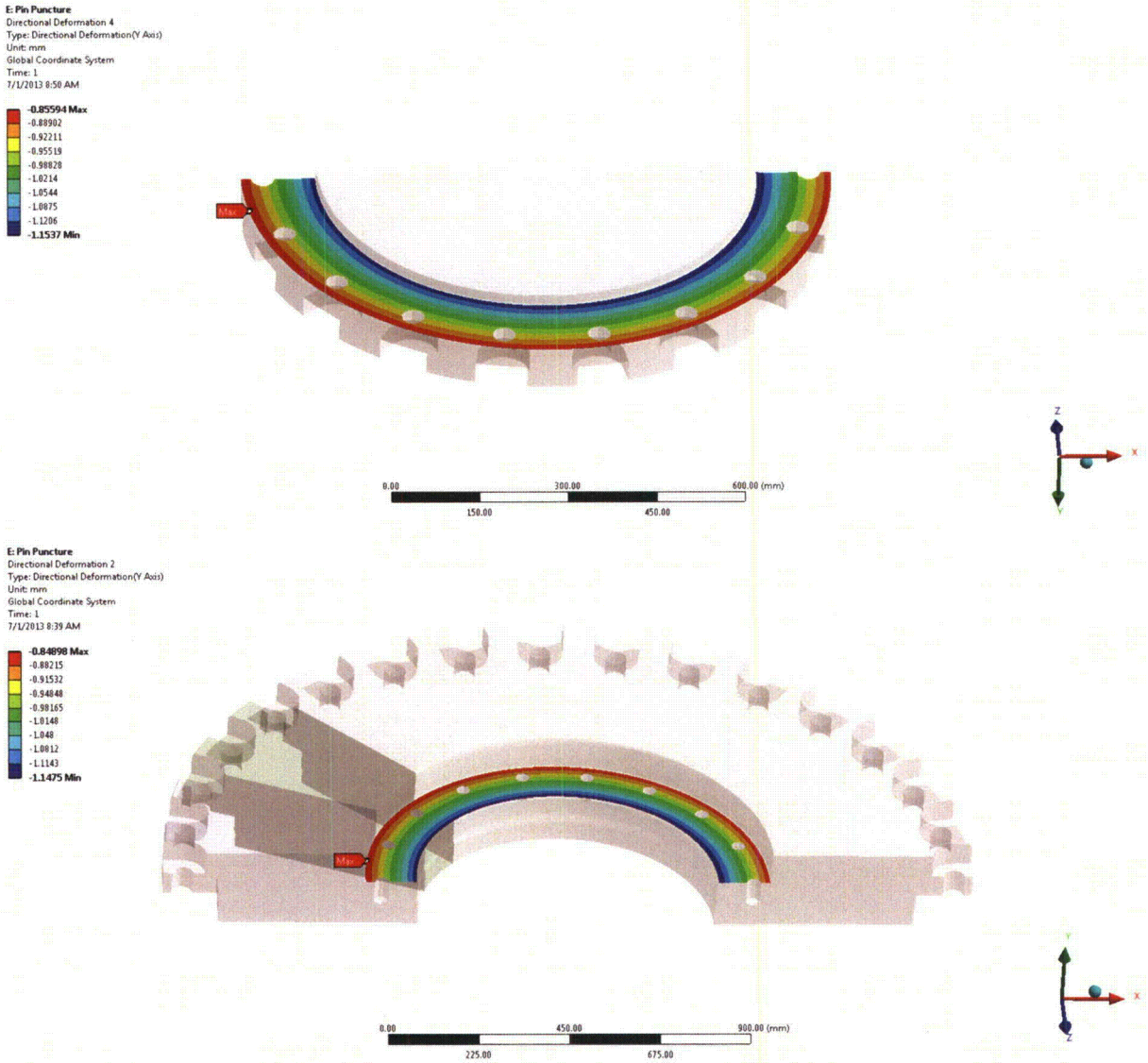

Figure 2.15.4-9 Secondary Lid Sealing Surface Displacement during Puncture

2.16 References

1. Robatel Technologies, LLC, Quality Assurance Program for Packaging and Transportation of Radioactive Material, 10 CFR 71 Subpart H, Dated January 31, 2012 and NRC Approved on March 21, 2012
2. U.S. Nuclear Regulatory Commission, 10 CFR Part 71--PACKAGING AND TRANSPORTATION OF RADIOACTIVE MATERIAL, dated March 7, 2012 and the following specific Sections:

71.31(a)(1)	71.31(a)(2)	71.33	71.35(a)
71.71	71.73	71.41(a)	71.45
71.85(b)	71.4	71.73(c)(1)	71.73(c)(3)
71.85	71.43	71.45(a)	71.45(b)
7.51	71.73(b)	71.71(c)	71.55(e)
71.59(a)(2)	71.85(b)	71.55	71.61
71.74	71.55(f)	71.75	

3. U.S. Nuclear Regulatory Commission, "Load Combinations for the Structural Analysis of Shipping Casks for Radioactive Material," Regulatory Guide 7.8.
4. U.S. Nuclear Regulatory Commission, "Design Criteria for the Structural Analysis of Shipping Cask Containment Vessels," Regulatory Guide 7.6.
5. U.S. Nuclear Regulatory Commission, "Fracture Toughness Criteria of Base Material for Ferritic Steel Shipping Cask Containment Vessels with a Maximum Wall Thickness of 4 Inches (0.1m)," Regulatory Guide 7.11.
6. U.S. Nuclear Regulatory Commission, "Fabrication Criteria for Shipping Containers," NUREG/CR-3854, March 1985.
7. ASME Boiler & Pressure Vessel Code 2007 Edition, Section III – Division 1 – Subsection ND, "Class 3 Components", The American Society of Mechanical Engineers, Three Park Avenue, New York, NY, www.asme.org.
8. ASME Boiler & Pressure Vessel Code 2007 Edition, Section III – Division 1 – Subsection NF, "Supports", The American Society of Mechanical Engineers, Three Park Avenue, New York, NY, www.asme.org.
9. U.S. Nuclear Regulatory Commission, "SCANS (Shipping Cask Analysis System): A Microcomputer Based Analysis System for Shipping Cask Design Review," NUREG/CR-4554, Volumes 3, 6 and 7, February 1990.
10. U.S. Nuclear Regulatory Commission, "Stress Analysis of Closure Bolts for Shipping Casks," NUREG/CR-6007, January 1993.
11. NUREG/CR-0481, "An Assessment of Stress-Strain Data Suitable for Finite-Element Elastic-Plastic Analysis of Shipping Containers," Rack, H. & Knorovsky, G., Sandia Laboratories, Albuquerque, NM, September 1978, Retrieved on August 28, 2013, Retrieved from http://rampac.energy.gov/docs/nrcinfo/NUREG_0481.pdf.

12. U.S. Nuclear Regulatory Commission, Standard Review Plan for Transportation Packages for Radioactive Material, NUREG-1609, March 31, 1999
13. U.S. Government Code of Federal Regulations, Request for Withholding Information Contained in License Application, 10 CFR 2.790
14. U.S. Nuclear Regulatory Commission, "Dynamic Analysis to Establish Normal Shock and Vibration of Radioactive Material Shipping Packages, Volume 3: Final Summary Report," NUREG/CR-2146, Vol. 3, October 1983.
15. U.S. Nuclear Regulatory Commission, "Engineering Drawings for 10 CFR Part 71 Package Approvals," NUREG/CR-5502, May 1998.
16. U.S. Nuclear Regulatory Commission, "Fracture Toughness Criteria of Base Material for Ferritic Steel Shipping Cask Containment Vessels with a Wall Thickness Greater than 4 Inches (0.1m)," Regulatory Guide 7.12.
17. U.S. Nuclear Regulatory Commission, "Methods for Impact Analysis of Shipping Containers," NUREG/CR-3966, November 1987.
18. U.S. Nuclear Regulatory Commission, "Puncture Testing of Shipping Packages under 10 CFR Part 71," Bulletin 97-02, September 23, 1997.
19. U.S. Nuclear Regulatory Commission, "Recommended Welding Criteria for Use in the Fabrication of Shipping Containers for Radioactive Materials," NUREG/CR-3019, March 1985.
20. U.S. Nuclear Regulatory Commission Bulletin, 97-02.
21. U.S. Nuclear Regulatory Commission, "Shock and Vibration Environments for a Large Shipping Container During Truck Transport (Part II)," NUREG/CR-0128, August 1978.
22. U.S. Nuclear Regulatory Commission, Dynamic Analysis to Establish Normal Shock and Vibration of Radioactive Material Shipping Packages, NUREG-2146, Volumes 1, 2 and 3, dated January 1, 1981-March 31, 1981; April 1, 1981-June 30, 1981; and October 1993, respectively.
23. U.S. Nuclear Regulatory Commission, International Agreement Report, International Code Assessment and Applications Program: Summary of Code Assessment Studies Concerning RELAP5/MOD2, RELAP5/MOD3, and TRAC-B, December 1993.
24. Bickford, J. & Looram, M., "Good Bolting Practices – A Reference Manual for Nuclear Power Plant Maintenance Personnel, Volume 1: Large Bolt Manual," Yalesville, CT: Electric Power Research Institute, 1987.
25. Blodgett, O. W., "Design of Welded Structures", The James F. Lincoln Arc Welding Foundation, Cleveland, Ohio.
26. AISC, "Guide to Design Criteria for Bolted and Riveted Joints", 2nd Edition, 2007.
27. Oberg, Erik, "Machinery's Handbook", 26th Edition.
28. ANSYS, Release 14.0, ANSYS, Inc., Canonsburg, PA, October, 2011
29. Young, Warren C., "Roark's Formulas for Stress and Strain", 6th Edition.

30. U.S. Nuclear Regulatory Commission, "Shock and Vibration Environments for a Large Shipping Container During Truck Transport" NUREG-0128.
31. ASME Boiler & Pressure Vessel Code 2010 Edition, Section II – Part D, "Materials", The American Society of Mechanical Engineers, Three Park Avenue, New York, NY, www.asme.org.
32. ASME Boiler & Pressure Vessel Code 2007 Edition, Section III – Division 1 – Subsection NB, "Class 1 Components", The American Society of Mechanical Engineers, Three Park Avenue, New York, NY, www.asme.org.
33. RTL-001-CALC-ST-0201, Rev. 5, "Lifting Structural Evaluation" (PROPRIETARY)
34. RTL-001-CALC-ST-0202, Rev. 4, "Tie-Down Evaluation" (PROPRIETARY)
35. RTL-001-CALC-ST-0402, Rev. 4, "Cask Body Structural Evaluation" (PROPRIETARY)
36. RTL-001-CALC-ST-0403, Rev. 4, "Pin Puncture Evaluation" (PROPRIETARY)
37. WM2001 Conference paper, "Benchmarking of LS-DYNA for Use with Impact Limiters," Joseph C. Nichols III, Michael E. Cohen, Robert A. Johnson, 2001.
38. RTL-001-CALC-TH-0102, Rev. 6, "RT-100 Cask Maximum Normal Operating Pressure Calculation" (PROPRIETARY)
39. Bickford, J. & Looram, M., "Good Bolting Practices – A Reference Manual for Nuclear Power Plant Maintenance Personnel, Volume 1: Large Bolt Manual," Yalesville, CT: Electric Power Research Institute, 1987.
40. RTL-001-CALC-ST-0401, Rev. 6, "RT-100 Cask Impact Limiter Drop Evaluation" (PROPRIETARY)
41. U.S. Nuclear Regulatory Commission, "Methods for Impact Analysis of Shipping Containers", NUREG/CR-3966.
42. RTL-001-CALC-TH-0102, Rev. 6, "RT-100 Cask Maximum Normal Operating Pressure Calculation" (PROPRIETARY)
43. RTL-001-CALC-TH-0202, Rev. 6, "RT-100 Cask Hypothetical Accident Condition Maximum Pressure Calculation" (PROPRIETARY)
44. ASME B1.13M-2005, METRIC SCREW THREADS: M PROFILE.
45. PAP 008, Specification D'approvisionnement - Mousse Polyurethane - Emballage de TRANSPORT RT-100 (Procurement Specification - Polyurethane Foam - Packaging of TRANSPORT RT-100), Rev. D, ROBATEL Industries (PROPRIETARY)
46. RES 001, Safety Analysis Robatel Package Model RT-100 Drop Test Report, Rev. E, ROBATEL Industries (PROPRIETARY)
47. Drawing 102885 MD 2021-06 Rev. D, "Robatel Transport Package RT100" (PROPRIETARY)
48. Certificate of Conformance for Purchase Order #117039 (Certificate for RT100 Scaled Foam Model) dated 09-07-2012 (PROPRIETARY)
49. U.S. Nuclear Regulatory Commission, "Standard Format and Content of Part 71 Applications for Approval of Packages for Radioactive Material," Regulatory Guide 7.9.

50. Parker O-Ring Handbook ORD 5700, Retrieved on August 28, 2013, Retrieved from http://www.parker.com/literature/ORD%205700%20Parker_O-Ring_Handbook.pdf.
51. Baumeister T. and Marks, L.S. "Standard Handbook for Mechanical Engineers, 7th Edition". New York: McGraw-Hill Book Co., 1967.
52. U.S. Nuclear Regulatory Commission Bulletin, 96-04.
53. U.S. Nuclear Regulatory Commission Interim Staff Guidance, "Use of Computational Modeling Software", ISG-21.
54. Glenn Lee, Radiation Resistance of Elastomers, IEEE Transactions on Nuclear Science, Vol. NS-32, No. 5, October 1985.
55. Baumeister T. and Marks, L.S. "Standard Handbook for Mechanical Engineers, 9th Edition". New York : McGraw-Hill Book Co., 1987.
56. ANSI N14.6-1978, "American National Standard for Special Lifting Devices for Shipping Containers Weighing 10000 pounds (4500 kg) or More for Nuclear Materials," American National Standards Institute, Inc., 11 West 42nd Street, New York, NY, www.ansi.org.
57. KTA 3905, "Load Attaching Points on Loads in Nuclear Power Plants," Safety Standards of the (German) Nuclear Safety Standards Commission, June 1999 Edition including rectification of July 2000.
58. TRELLEBORG Sealing Solutions O-Ring and Backup Rings Catalog, August 2011 Edition
59. Shappert, L.B. "The Radioactive Materials Packaging Handbook". Oak Ridge, Tennessee: Oak Ridge National Laboratory, 1988. ORNL/M-5003.
60. RTL-001-CALC-ST-0203, Rev. 6, "RT-100 Bolting Calculation" (PROPRIETARY)
61. GENERAL PLASTICS Design Guide for LAST-A-FOAM FR-3700 Crash & Fire Protection of Radioactive Material Shipping Containers, Rev. 02.20.12
62. J. F. Harvey, Theory and Design of Pressure Vessels, New York: Van Nostrand Reinhold, 1991.
63. CN-13039-203, Rev. 0, "RT-100 Cask Lead Shrinkage Evaluation" (PROPRIETARY)

This page is intentionally left blank.

3. THERMAL EVALUATION

Robatel has performed a thermal evaluation of the RT-100 using the Nuclear Industry standards and under the RT Company Quality Assurance Program [Ref. 1]. This thermal evaluation shows that the RT-100 meets or exceeds all the 10 CFR 71 regulatory requirements [Ref. 2]. The thermal review is based in part on the descriptions and evaluations presented in the General Information Chapter 1 and Structural Evaluation Chapter 2 of the application. Similarly, results of the thermal review are considered in the review of several other sections of the application. An example of information flow for the thermal review is shown in Figure 3-1.

RT identified, described, discussed, and analyzed the principal thermal engineering design of the RT-100, components, and systems that are important to safety. Section 3 describes how the package complies with the performance requirements of 10 CFR 71 [Ref. 2]. Results of the thermal evaluation verified that the thermal performance of the RT-100 design (for both NCT and HAC) meets the thermal regulatory requirements as follows:

- The RT-100 design is evaluated to demonstrate that it satisfies the thermal requirements of 10 CFR 71.31(a)(1)]; 10 CFR 71.31(a)(2); 10 CFR 71.33, and 10 CFR 71.35(a) [*all* Ref. 2].

- The application identifies the established codes and standards used for the thermal design according to 10 CFR 71.31(c) [Ref. 2].

- The performance of the RT-100 is evaluated under the tests specified in 10 CFR Part 71.71 [Ref. 2] for NCT and 10 CFR Part 71.73 [Ref. 2] for HAC and also referenced 10 CFR 71.41(a) [Ref. 2].

- The RT-100 is designed, constructed, and prepared for transport so that there is no significant decrease in packaging effectiveness under the tests specified in 10 CFR 71.71 (NCT) and references in 10 CFR 71.43(f) and 71.51(a)(1) [*all* Ref. 2].

- The RT-100 is designed, constructed, and prepared for transport so that the accessible surface temperature does not exceed the regulatory limits specified in 10 CFR 71.43(g) [Ref. 2].

- The RT-100 design does not rely on mechanical cooling systems to meet containment requirements in reference to 10 CFR 71.51(c) [Ref. 2].

- The RT-100 has adequate thermal performance to meet the containment, shielding, sub-criticality, and temperature requirements of 10 CFR 71 [Ref. 2] for (NCT/HAC).

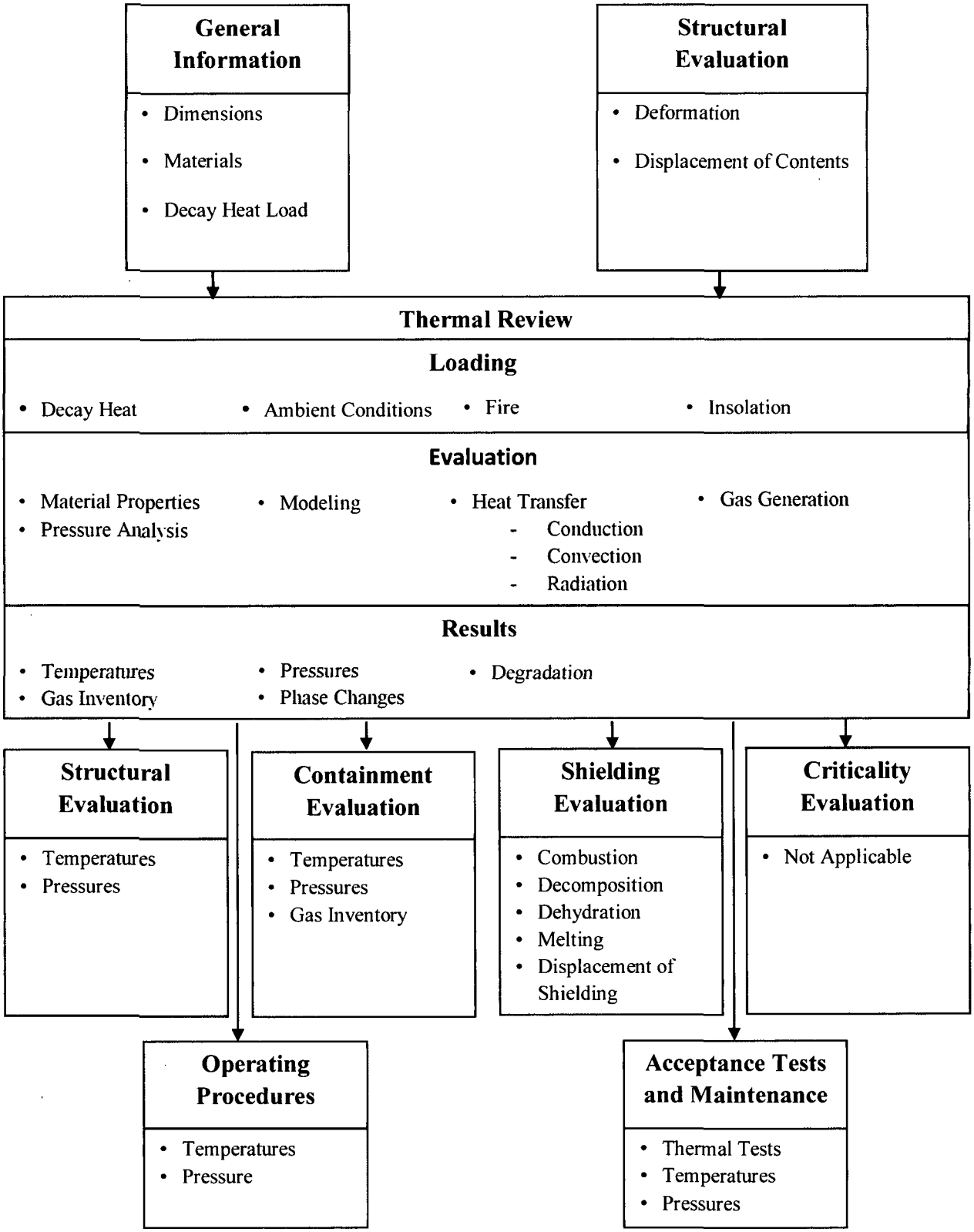

Figure 3-1 Information Flow for the Thermal Review

3.1 Description of Thermal Design

The thermal design aspects of the RT-100 are related primarily to protecting the sensitive components of the cask and the contents from the elevated temperatures produced by the hypothetical fire accident. The primary thermal criteria that are applied to the thermal evaluation are maintaining the lead shielding in the cask body and secondary lid below the melting temperature of lead, and the maximum temperature of the O-ring seals below their maximum operating temperature. The components primarily responsible for maintaining the temperatures of these components below their acceptance criteria are the impact limiters covering the top and bottom of the cask, and the thermal shield on the radial cask surface.

The impact limiters are made from a polyurethane foam material that has a low thermal conductivity. The impact limiters cover the top and bottom ends of the cask. They protect the lead in the bottom of the cask body and the O-rings in the primary lid, secondary lid, and the vent port cover plate. The impact limiters are designed to remain attached to the cask during normal operations and hypothetical accident conditions, and to insulate the lead and O-rings from the high temperatures of the hypothetical fire accident. The thermal shield covering the radial cask surface is made of a ceramic fiber material with a very low thermal conductivity. The ceramic fiber is covered by a thin, stainless steel cover that protects it from damage during normal handling. The ceramic fiber material is designed for use in insulating refractory furnaces, and providing an excellent thermal barrier for the fire accident, thus preventing the radial lead from exceeding its melting point.

The RT-100 is designed to accommodate contents with a maximum decay heat of 200 watts. This low decay heat value does not produce a significant temperature gradient through the cask body, and as a result, no specific design features are required to facilitate removing the heat from the cavity.

3.1.1 Design Features

As briefly described in Section 3.1, the RT-100 design has two primary thermal design features: the impact limiters and the radial thermal shield. These features are identified in Chapter 1, Figure 1.2.1-1 which highlights the primary components of the cask.

3.1.1.1 RT-100 Description

The RT-100 cask body consists of inner and outer shells constructed of 304/304L stainless steel. Lead shielding is provided between these radial shells, as well as between the 304/304L stainless steel bottom forging and bottom plate. The upper end of the cask comprises the upper 304/304L stainless steel forging that is attached to the inner and outer shells, and contains the mating surface for the primary lid. The primary and secondary lids are constructed of 304L stainless steel, as is the cover plate. The primary lid is attached using thirty-two (32) M48 hex head bolts and the secondary lid is secured using eighteen (18) M36 hex head bolts. The upper and lower impact limiter cover each end of the cask, and are constructed of 304L stainless steel shells containing polyurethane foam blocks. The impact limiters are secured to the body via twelve (12) M24 threaded studs. The RT-100 is described in greater detail in Chapter 1, Section 1.2.1.

Most of the outer shell of the cask is covered by a ceramic fiber thermal shield that is secured by a thin 304L stainless steel cover. Other portions of the radial cask surface are covered by the 318

stainless steel tie-down arms and tie-down arm baseplate, and by the 304L stainless steel lifting blocks. The exposed surfaces of the tie-down arm baseplate are covered by the ceramic fiber thermal shield and 304L stainless steel cover.

3.1.1.2 RT-100 Dimensions

The RT-100 thermal analysis is performed using the basic cask dimensions as presented in Appendix 1.4. The inner and outer shell thicknesses at the side of the cask are reduced to account for minimum thickness due to manufacturing tolerances. Specifically, the following material thicknesses are reduced by 2mm:

- Thicknesses of the cask body inner and outer stainless steel shells
- Bottom end of the cask body
- Stainless steel bottom forging welded to the inner shell
- Stainless steel bottom plate welded to the outer shell.

To represent the condition of undersized shells with a poured lead fill, lead thickness in both the sidewalls and the cask bottom end are simultaneously increased by 4 mm. This approach is conservative as it reduces the amount of stainless steel material protecting the lead from the HAC fire temperatures and thus, maximizes temperatures in the lead.

In order to maximize the amount of heat that can enter the cask body during the fire, no gaps are assumed between the lead and the outer shell. The lead and stainless steel outer shell are assumed to be in perfect contact. No other gaps are assumed in the thermal evaluation between the various components of the cask.

3.1.2 Content's Decay Heat

The RT-100 is designed for a maximum decay heat of 200 watts. This value is selected as the design basis, and is conservative for the contaminated resin and filter contents that are transported in the cask.

The analysis of the cask for normal condition of transport (NCT) and hypothetical accident conditions (HAC) is performed using the ANSYS finite element computer code [Ref. 3]. In this analysis, the decay heat of the contents is modeled as a uniform heat flux on the internal surfaces of the cask cavity.

To calculate this uniform heat flux over the inside surface of the cask, the inside diameter and the height of the cask cavity is used.

$$A_{in} = \pi dL + 2(\pi d^2/4)$$

where

A_{in} = inside surface area of the cask (m^2)
d = inside diameter of the cask (m)

L = height of the cavity (m)

Based on the RT-100 drawing provided in Appendix 1.4, the cask inside diameter is 1.730 m and the height of the cavity is 1.956 m. The area is then

$$A_{in} = \pi \times 1.730 \times 1.956 + 2(\pi \times 1.730^2/4) = 15.332 \text{ m}^2$$

The uniform internal heat flux, q_{int}, is then

$$q_{int} = 200\text{W} / 15.332 \text{ m}^2 = 13.04 \text{ W/m}^2$$

3.1.3 Summary Tables of Temperatures

Section 3.1.3 presents summary tables of maximum temperatures occurring in the RT-100 as a result of the NCT and HAC evaluations described in detail in Sections 3.3 and 3.4. Limiting temperatures for consideration in the structural and containment evaluations are the maximum temperatures. Therefore, the following tables present maximum temperatures that occur in the various cask components under NCT and HAC. Table 3.1.3-1 presents the NCT maximum temperatures while Table 3.1.3-2 and Table 3.1.3-3 present the maximum temperatures HAC. For the fire accident evaluation, the time at which the component reaches its maximum temperature is listed along with the temperature. In some cases, temperatures are after cessation of the fire transient.

The tables also present the maximum averaged surface temperature of the inner shell at the cavity side. These averaged surface temperatures are used to predict the cavity pressure under normal and hypothetical conditions, respectively.

Table 3.1.3-1 RT-100 Maximum Normal Condition Temperature Summary

Component	Hot Case 1 (°C)	Hot Case 2 (°C)	Cold Case 1 (°C)	Cold Case 2 (°C)	Allowable Temperature (°C)	Reference
Primary Seal	68.7	42.1	-35.5	-24.5	150	Ref. 8
Secondary Seal	70.3	42.9	-34.7	-23.8	150	Ref. 8
Quick Disc. Valve Cover Seal	72.5[a]	—[a]	—[a]	—[a]	150	Ref. 8
Lead Shield	73.2	43.1	-34.5	-23.6	328	Ref. 5 (p. 907)
Closure Bolts	70.0	42.8	-34.9	-23.9	—	—
Outer Surface	93.0	41.3	-36.3	-25.4	50/85[b]	10 CFR 71.43(g)
Inner Shell Maximum	73.1	42.6	-35.1	-24.1	—	—
Inner Shell Average	71.0	41.7	-36.0	-25.0	—	—
Total Impact Limiter Average	67.4	39.5	-38.3	-27.3	—	—
Top Impact Limiter Average	72.5	39.5	-38.3	-27.4	—	—

a. The NCT maximum temperature of the components surrounding the cover plate is the upper impact limiter average temperature (reported in Table 3.1.3-1) where the temperatures are higher on the external surfaces of the impact limiter. Thus the maximum temperature of the cover plate containment O-ring is considered to be 72.5°C with no further analysis. Since Hot Case 1 is the bounding upper temperature of this O-ring, the other NCT cases are not considered.

b. 10 CFR 71.43(g)—A package must be designed, constructed, and prepared for transport so that in still air at 38°C (100°F) and in the shade, no accessible surface of a package would have a temperature exceeding 50°C (122°F) in a nonexclusive use shipment, or 85°C (185°F) in an exclusive use shipment.

Table 3.1.3-2 RT-100 Maximum Calculated Temperature of Cask under HAC with Pin Puncture Damage on Top Impact Limiter

Component	Temperature (°C)	Time After Start of Fire (Minutes)	Allowable Temperature (°C)	Reference
Primary Seal Maximum	110.8	291.6	150	Ref. 8
Secondary Seal Maximum	131.1	33.4	150	Ref. 8
Quick Disc. Valve Cover Seal	133.1[c]	33.4[c]	150	Ref. 8
Lead Shield Maximum	304.8	34.5	328	Ref. 5 (p. 907)
Closure Bolts Maximum	133.1	33.4	—	—
Cask Body Maximum	799.1	30.0	—	—
Inner Shell Average	136.3	—	—	—

c. The port cover plate location is on the primary lid, close to the primary lid closure bolts. The cover plate is thermally insulated by the upper impact limiter. The highest temperature reported on the primary and secondary lid are the closure bolts (where the puncture bar penetrates the impact limiter) with a maximum temperature of 133.1°C (reported in Table 3.1.3-2). This temperature of 133.1°C being bonding to all the lids and cover plate recorded temperatures, the maximum temperature of the cover plate containment O-ring during HAC is considered to be 133.1°C with no further analysis.

Table 3.1.3-3 RT-100 Maximum Calculated Temperature of Cask under HAC with Pin Puncture Damage at the Side of the Cask Body

Component	Temperature (°C)	Time After Start of Fire (minutes)	Allowable Temperature (°C)	Reference
Primary Seal Maximum	110.3	285.1	150	Ref. 8
Secondary Seal Maximum	91.3	1624.4	150	Ref. 8
Quick Disc. Valve Cover Seal	— [d]	— [d]	150	Ref. 8
Lead Shield Maximum	304.7	34.5	328	Ref. 5 (p. 907)
Closure Bolts Maximum	91.9	1302.5	—	—
Cask Body Maximum	799.1	30.0	—	—
Inner Shell Average	137.0	—	—	—

d. The Quick-Disconnect Valve Cover Plate Seal maximum temperature is considered bounded by the result of the top impact limiter pin puncture HAC. Thus, the side puncture result is not reported.

3.1.4 Summary Tables of Maximum Pressures

The maximum internal pressures in the RT-100 are determined using the maximum temperatures presented in Table 3.1.3-1, Table 3.1.3-2, and Table 3.1.3-3 above. Details of these pressure calculations are presented in Section 3.3.2 for NCT and in Section 3.4.3 for HAC. Table 3.1.4-1 presents a summary of the maximum pressure calculations for normal and accident conditions. These pressures are utilized in the structural evaluation presented for the cask body in Sections 2.6 and 2.7.

Table 3.1.4-1 RT-100 Summary of Maximum Normal and Hypothetical Accident Condition Pressures

Condition	Maximum Pressure
Normal Conditions of Transport (MNOP)	342.7 kPa (49.7 psia)
Hypothetical Accident Conditions	689.4 kPa (100 psia)

3.2 Material Properties and Component Specifications

The material properties and specifications for the RT-100 materials of construction are presented in this section. The determination of material properties are carefully evaluated to ensure that for each thermal analysis:

- The appropriate thermal properties for the package materials are correctly incorporated into the thermal evaluations.
- Appropriate expressions are used for conductive, convective, and radiative heat transfer among package components, and from the surfaces of the package to the environment.

3.2.1 Material Properties

The thermal evaluation of the RT-100 is performed using material properties taken from standard industry references or manufacturer provided data in Tables 3.2.1-1 through 3.2.1-4. The thermal absorptivities and emissivities are appropriate for the package surface conditions and each thermal condition. When reporting a property as a single value, the evaluation shows that this value bounds the equivalent temperature-dependent property. This section includes references for the data provided.

Only room temperature values of conductivity, density, and specific heat are available for General Plastics FR-3700 series LAST-A-FOAM [Ref. 10, 11, and 12]. Quantitative temperature dependent material properties are not provided. However, most of the foam remains at temperatures close to ambient due to the dimensions of the RT-100 impact limiters which result in long heat conduction paths (see Figure 3.3.1-3). Thus, reduction in the foam thermal properties due to elevated temperatures will not be significant. Therefore, the use of temperature-independent thermal properties is justified.

Information on the EPDM O-ring material is provided in TRELLEBORG, Aug. 2011 Edition [Ref. 8] and PARKER O-RING Handbook [Ref. 16] for two different suppliers. The temperature range specified in Table 3.2.1-1 is conservative from the values specified in those two references. Additional information on the O-rings is presented in Appendices Attachment 3.5-1 and Attachment 3.5-2.

Table 3.2.1-1 Temperature-Independent Material Properties

Material	Properties	Reference Page Number	Value
Stainless Steel 304	Density	Ref.24: Page 744	8030 kg/m^3
	Emissivity (fire)	Ref. 2	0.9
	Emissivity (cool-down)	Ref. 2	0.8
	Emissivity (normal condition)	Ref. 5: Page 750 and 929	0.2
Lead	Density	Ref. 5: Page 907	11340 kg/m^3
	Melting Point	Ref. 5: Page 907	328°C (601 K)
Ceramic Paper	Density	Ref. 9	176.2 kg/m^3 (11 lb/ft^3)
	Specific Heat		1172.5 J/kg-K @1366.5K (0.28 BTU/lb-°F @ 2000°F)

Proprietary Information Content Withheld Under 10 CFR 2.390

Seal (EPDM)	Working Temperature	Ref. 8 & 16	-45°C to 150°C

Table 3.2.1-2 Temperature-Dependent Material Properties—Stainless Steel 304

[Ref. 13, page 765]

Temperature (°C)	Specific Heat (J/kg-K)	Thermal Conductivity (W/m-K)
20	472.6	14.8
50	483.6	15.3
75	493.1	15.8
100	499.4	16.2
125	506.7	16.6
150	511.4	17.0
175	520.1	17.5
200	525.7	17.9
225	530.0	18.3
250	532.5	18.6
275	536.5	19.0
300	541.7	19.4
325	545.5	19.8
350	547.7	20.1
375	551.4	20.5
400	552.3	20.8
425	557.0	21.2
450	557.8	21.5
475	562.3	21.9
500	563.1	22.2
525	566.3	22.6
550	568.1	22.9
575	571.2	23.3
600	572.9	23.6
625	575.9	24.0
650	577.5	24.3
675	580.4	24.7
700	581.9	25.0
725	585.8	25.4
750	587.2	25.7

Table 3.2.1-3 Temperature-dependent Material Properties—Lead

[Ref. 5, page 907]

Temperature (°C)	Specific Heat (J/kg- K)	Thermal Conductivity (W/m- K)
-173.15	118	3.97E+01
-73.15	125	3.67E+01
26.85	129	3.53E+01
126.8	132	3.40E+01
326.8	142	3.14E+01

Table 3.2.1-4 Temperature-dependent Material Properties—Ceramic Paper

[Ref. 9]

Temperature (°C)	Thermal Conductivity (W/m-K)
93.3	4.759E-02
204.4	5.206E-02
315.6	5.912E-02
426.7	6.907E-02
537.8	8.219E-02
648.9	9.834E-02
760.0	1.174E-01
871.1	1.396E-01

3.2.2 Component Specifications

This section includes the technical specifications of RT-100 components that are important to the thermal performance, as illustrated by the following examples:

- In the case of seals, the operation temperature limits
- Maximum allowable service temperatures for package components
- Minimum allowable service temperature of all components, which are less than or equal to -40 °C (-40 °F).

Table 3.2.2-1 lists the maximum and/or minimum allowable temperatures for the critical cask components.

Table 3.2.2-1 Component Specifications – Minimum and Maximum Temperatures

Material	Min. Temp.	Max. Temp.	Reference
304/ 304L SS	-	>1400°C (Melting Temp.)	Ref. 14
Lead	-	328°C (Melting Temp.)	Ref. 5
Polyurethane Foam	-	1093°C (2000°F of Foam Char Temp.)	Ref. 15
Seal (EPDM)	-45°C	150°C	Ref. 8 & 16

3.2.3 Content Properties

As described in Chapter 1, Section 1.2.2.3 (Physical and Chemical Form – Density, Moisture Content and Moderators), the RT-100 is designed to transport contents that include contaminated resins and filters. The contents include secondary containers and may also include shoring. Resins are made of thermoplastics such as polystyrene, or material such as inorganic carbon or zeolite. Filters may be constructed from thermoplastics such as nylon, polyester, or polypropylene, or paper. Secondary containers are constructed of either coated/painted carbon steel or stainless steel, or a thermoplastic such as polyethylene or polypropylene. The filter media may be held within a stainless steel cartridge. Shoring can be made of wood or one or several of the materials comprising the secondary containers.

Based on the ASME code, Section II-D [Ref. 13], the acceptable temperature of the carbon steel and stainless steel material is approximately 525°C (977°F) for the range of loads and stresses occurring under NCT and HAC.

The melting temperatures of thermoplastics range from 100°C (212°F) up to 250°C (482°F) SFPE Handbook of Fire Protection Engineering, [Ref. 21], which typically soften at these temperatures and do not produce volatiles that could react with any of the contents. The auto-ignition temperature of thermoplastics is above 300°C (572°F) [Ref. 21].

The auto-ignition temperatures of paper and wood vary widely and are a function of their specific composition and moisture content. A commonly accepted value for the auto-ignition point for paper is 232°C (450°F) "Fundamentals of Combustion Processes," [Ref. 22]. The auto-ignition point for wood has been shown to be at least 300°C (572°F) An Experimental Study of Autoignition of Wood, T. Poespowati, World Academy of Science, Engineering and Technology 23, 2008. [Ref. 23].

A summary of the maximum temperature specifications for the RT-100 contents is provided in Table 3.2.3-1.

Table 3.2.3-1 Maximum Temperature Limits for RT-100 Content Materials

Material	Maximum Temperature	Reference
Carbon/Stainless Steel	525°C	Ref. 13
Thermoplastics	300°C	Ref. 21
Paper	232°C	Ref. 22
Wood	300°C	Ref. 23

3.3 Thermal Evaluation under Normal Conditions of Transport

This section describes the thermal evaluations performed for the RT-100 for the NCT specified in 10 CFR 71.71 [Ref. 2]. The evaluation considers the response of the RT-100 to a range of temperature and environmental conditions as described in Section 3.3.1. The results are compared with allowable limits of temperature, pressure, etc., for the package components. The information is presented in summary tables, along with statements and appropriate comments. Information that is to be used in other sections of the review is identified. The margins of safety for package temperatures, pressures, and thermal stresses, including the effects of uncertainties in thermal properties, test conditions and diagnostics, and analytical methods are addressed.

The analyses are shown to be reliable and repeatable.

The following general information is considered and included in addressing the sections below, as appropriate:

- Assumptions that are used in the analysis are clearly described and justified.
- For computer analyses, including finite element analyses, the computer program is described and shown to be well benchmarked, widely used for thermal analyses, and applicable to the evaluation.
- Models and modeling details are clearly described.
- The methods used are properly referenced or developed in the application.
- These methods are correctly applied.
- The evaluation considers changes in package geometry and material properties resulting from structural and thermal tests under NCT and HAC.
- The required temperature and thermal boundary conditions for normal conditions of transport and hypothetical accident conditions are correctly applied.
- The time interval after the fire test is adequate to assure that maximum component temperatures and post-fire steady-state temperatures are achieved.

- The maximum temperatures and pressures of the components do not exceed their allowable values.
- Combustion of package components are considered, including the heat produced.
- Temperature data is reported at gaskets, valves, and other containment boundaries, particularly for temperature-sensitive materials as well as, for the overall package.
- Appropriate corrections and evaluations that account for differences in the thermal test are included for conditions like ambient temperature, decay heat of the contents, or package emissivity or absorptivity.
- Both interior and exterior temperatures are included.
- The damage caused by the tests and the results of any measurements made is reported in detail, including photographs of the testing and the test specimen.

3.3.1 Heat and Cold

Section 3.3.1 demonstrates that the tests for NCT do not result in a significant reduction in the RT-100 effectiveness. The following items are considered and addressed:

- Degradation of the heat-transfer capability of the packaging (such as creation of new gaps between components)
- Changes in material conditions or properties (e.g., expansion, contraction, gas generation, and thermal stresses) affecting structural performance
- Changes in the packaging affecting containment, shielding, or criticality (such as thermal decomposition or melting of materials)
- Ability of the packaging to withstand the tests under HAC

The component temperatures and pressures are compared to their allowable values and do not exceed them. This section explicitly shows that the package meets the maximum temperature of the accessible package surface is less than 50 °C (122 °F) for non-exclusive-use shipment or 85 °C (185 °F) for exclusive use shipment when the package is subjected to the heat conditions of 10 CFR 71.43(g) [Ref. 2].

3.3.1.1 Load Cases

Four load cases are analyzed in order to evaluate the RT-100 for the range of temperature and solar insolation conditions specified in 10 CFR 71.71 [Ref. 2] for normal conditions:

- Hot Case 1
- Hot Case 2
- Cold Case 1

- Cold Case 2

Hot case 1 is based on the requirements of 10 CFR 71.71(c)(1) [Ref. 2], which is one of the extreme initial conditions for normal conditions and a precursor for the hypothetical fire accident evaluation. It has the following conditions:

- Ambient temperature, 38°C (100°F)
- Initial temperature, 38°C (100°F)
- Heat transfer to ambient by natural convection, still air
- Heat transfer to ambient by radiation
- Steady-state solar insolation, 776 W/m^2 for flat surface and 388 W/m^2 for curved surface
- Internal heat load as a uniform heat flux, 13.04 W/m^2

Hot case 2 is based on the requirements of 10 CFR 71.43(g) [Ref. 2] and has the following conditions:

- Ambient temperature, 38°C (100°F)
- Initial temperature, 38°C (100°F)
- Heat transfer to ambient by natural convection, still air
- Heat transfer to ambient by radiation
- No solar insolation, in shade
- Internal heat load as a uniform heat flux, 13.04 W/m^2

Cold case 1 is based on the requirements of 10 CFR 71.71(c)(2) [Ref. 2], which is another extreme initial condition for the NCT test evaluation. It has the following conditions:

- Ambient temperature, -40°C (-40°F)
- Initial temperature, -40°C (-40°F)
- Heat transfer to ambient by natural convection, still air
- Heat transfer to ambient by radiation
- No solar insolation, in shade
- Internal heat load as a uniform heat flux, 13.04 W/m^2

Cold case 2 is based on requirements of 10 CFR 71.71(b) [Ref. 2] and has the following conditions:

- Ambient temperature, -29°C (-20°F)
- Initial temperature, -29°C (-20°F)
- Heat transfer to ambient by natural convection, still air
- Heat transfer to ambient by radiation
- No solar insolation
- Internal heat load as a uniform heat flux, 13.04 W/m^2

Among them, Hot case 1 and Cold case 1 are two extreme conditions for the analyses. Hot case 1

is also referred to as the "normal hot" condition on which conservative boundary conditions are applied. This case provides the highest temperature distributions within the cask, and is used as initial conditions for evaluation of the hypothetical fire accident event as described in Section 3.4.

3.3.1.2 Analytical Model

The thermal evaluation of the RT-100 is performed using the ANSYS finite element computer software [Ref. 3]. The cask model is made of 3D thermal solid elements (SOLID90) that represent the major components of the cask. Contact between the lead and the inner and outer shells are modeled as bonded surfaces for thermal analyses in order to maximize heat input to the lead. The contact between the upper flange and the primary lid is modeled by a pair of 3D thermal contact elements (CONTA174) and 3D target elements (TARGE170), as are the other contacts between the primary lid and the secondary lid, the bolts with the primary lid, and the bolts with the secondary lid.

For conservatism, the top impact limiter is modeled as without the stainless steel plate covering the central hollow portion of the limiter. Thus, the concave area on the top impact limiter is exposed to solar insolation and/or fire. This approach leads to a conservatively high temperature over the top impact limiter. The contacts between the impact limiters and the cask body are also modeled by pairs of 3D thermal contact elements (CONTA174) and 3D target elements (TARGE170) between the relative surfaces.

A depiction of the ANSYS thermal model of the RT-100 is provided in Figure 3.3.1-1 and Figure 3.3.1-2. Additional details regarding the modeling and analysis of the RT-100 are presented in Calculation Package RTL-001-CALC-TH-0201, Rev. 6 [Ref. 4].

Proprietary Content Withheld Under
10 CFR 2.390

3.3.1.3 Analysis Results

The results of the steady state analyses of the cask model with impact limiters are presented in the form of temperature contour plots. Figure 3.3.1-3 through Figure 3.3.1-6 show the temperature contour plots for Hot case 1. Hot case 1 predicts the maximum temperatures experienced during NCT. The figures show the package, cask body, inner shell surface and lead shielding material, respectively. Figure 3.3.1-7 and Figure 3.3.1-8 provide the results for Hot case 2. Figure 3.3.1-9 and Figure 3.3.1-10 provide the results for Cold case 1. Cold case 1 represents the temperatures experienced by the package during extreme cold conditions. Figure 3.3.1-11 and Figure 3.3.1-12 provide the results for Cold case 2. Maximum temperature results are obtained by selecting the FE model component or material of interest and sorting the nodal results. Table 3.1.3-1 shows the maximum temperatures of the cask under NCT based on the steady state solution.

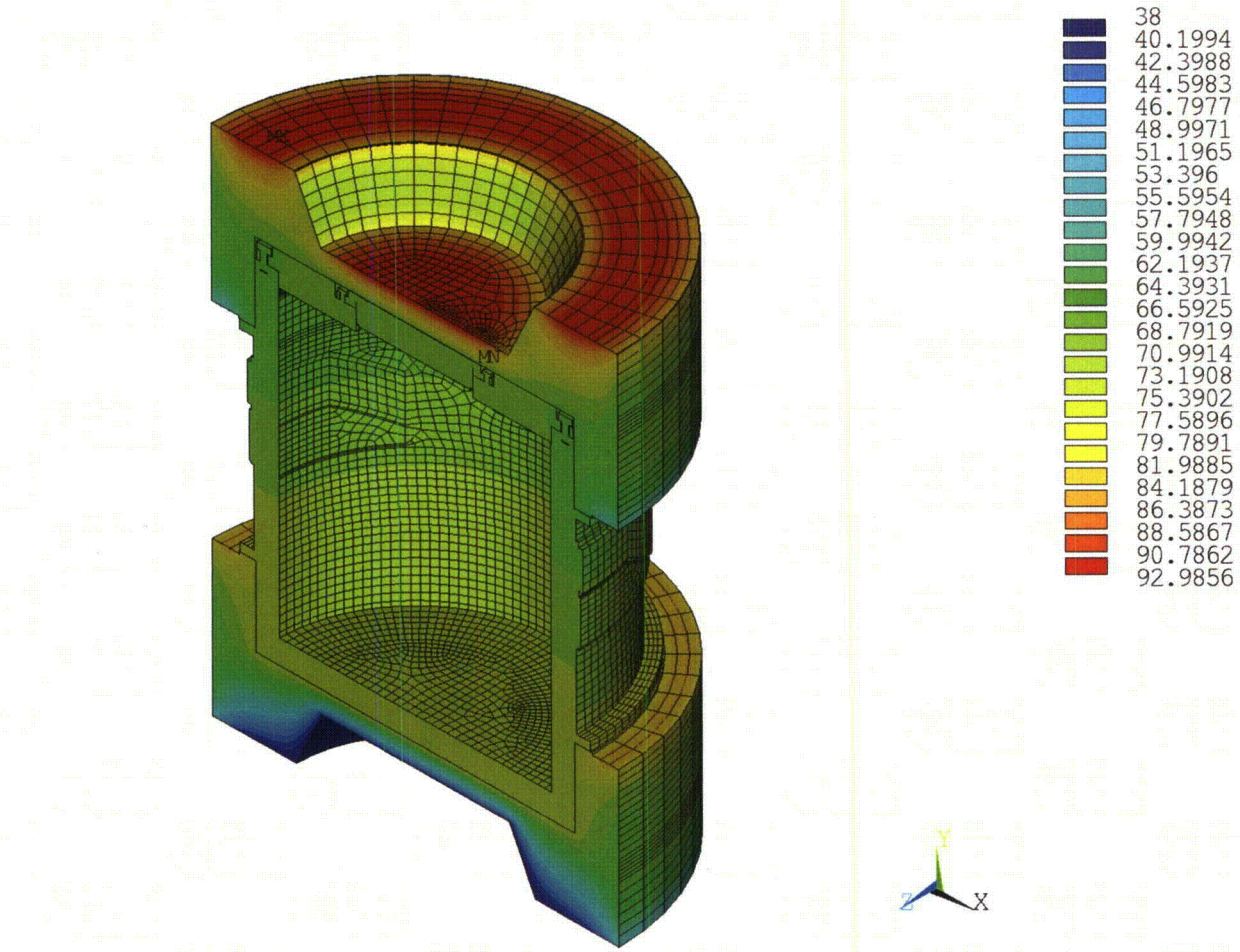

Figure 3.3.1-3 Temperature Contour Plot of Package—Hot Case 1

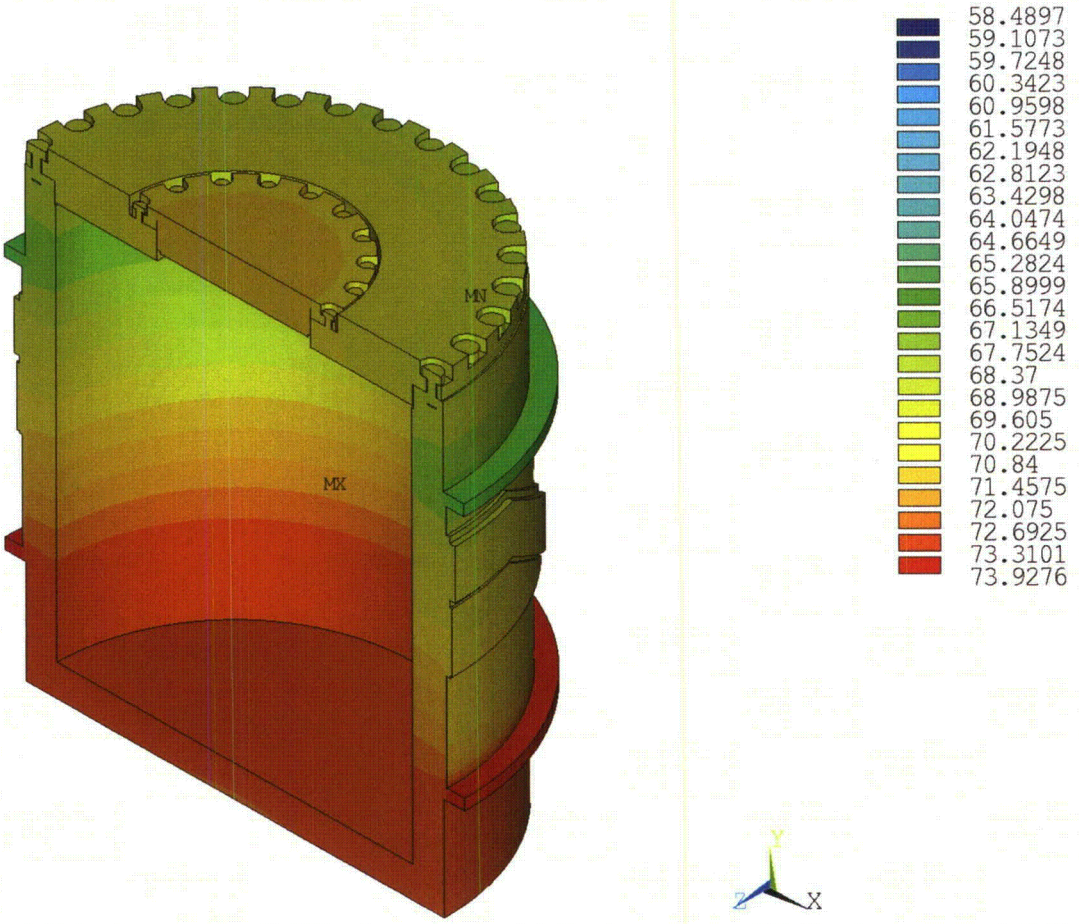

NCT--Case 1, Steady-State Boundary Conditions (Degrees Celsius)

Figure 3.3.1-4 Temperature Contour Plot of Cask Body—Hot Case 1

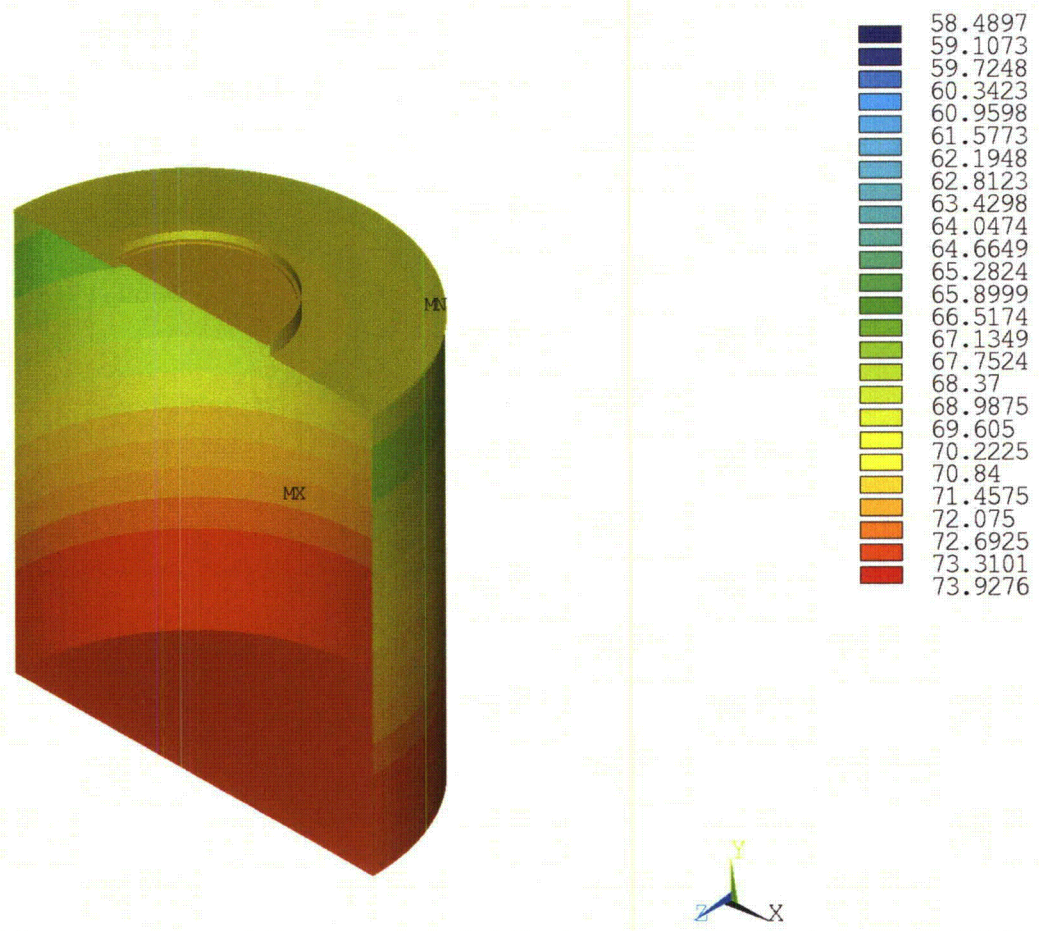

Figure 3.3.1-5 Temperature Contour Plot of Inner Shell Surface—Hot Case 1

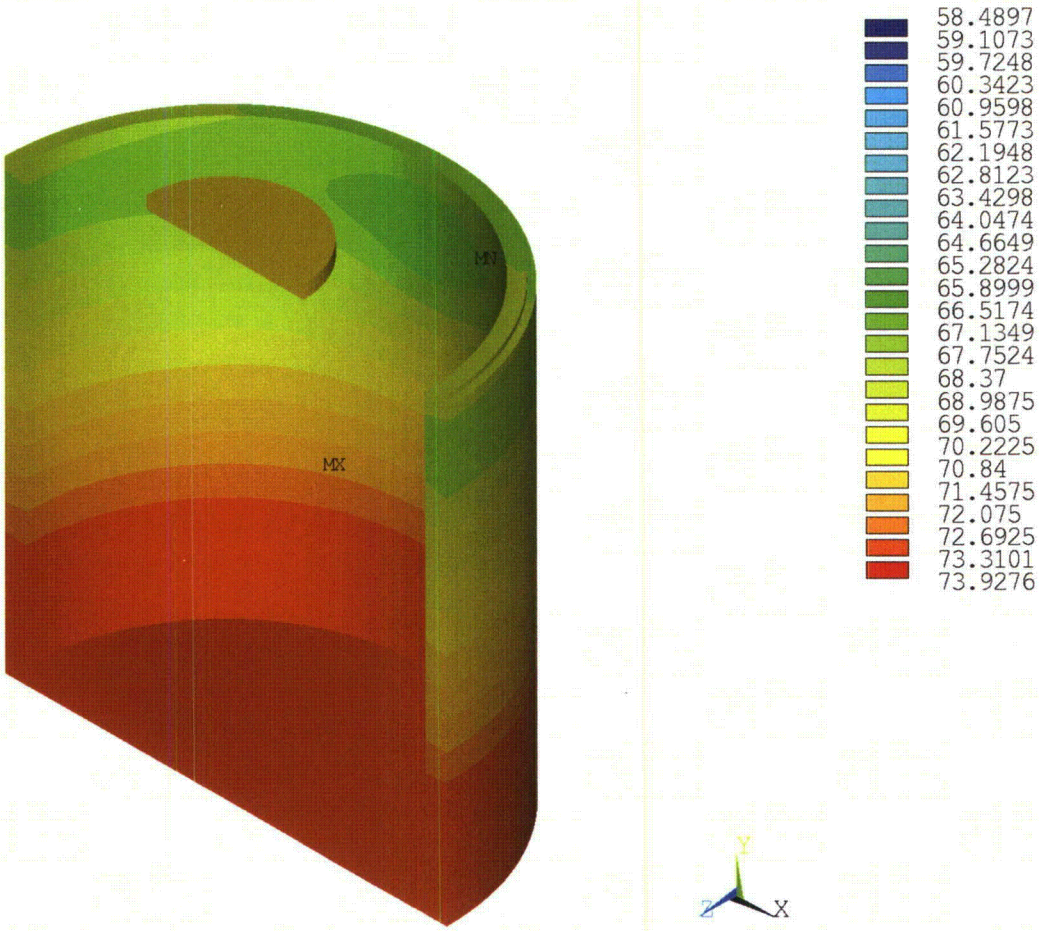

NCT--Case 1, Steady-State Boundary Conditions (Degrees Celsius)

Figure 3.3.1-6 Temperature Contour Plot of Lead Shielding—Hot Case 1

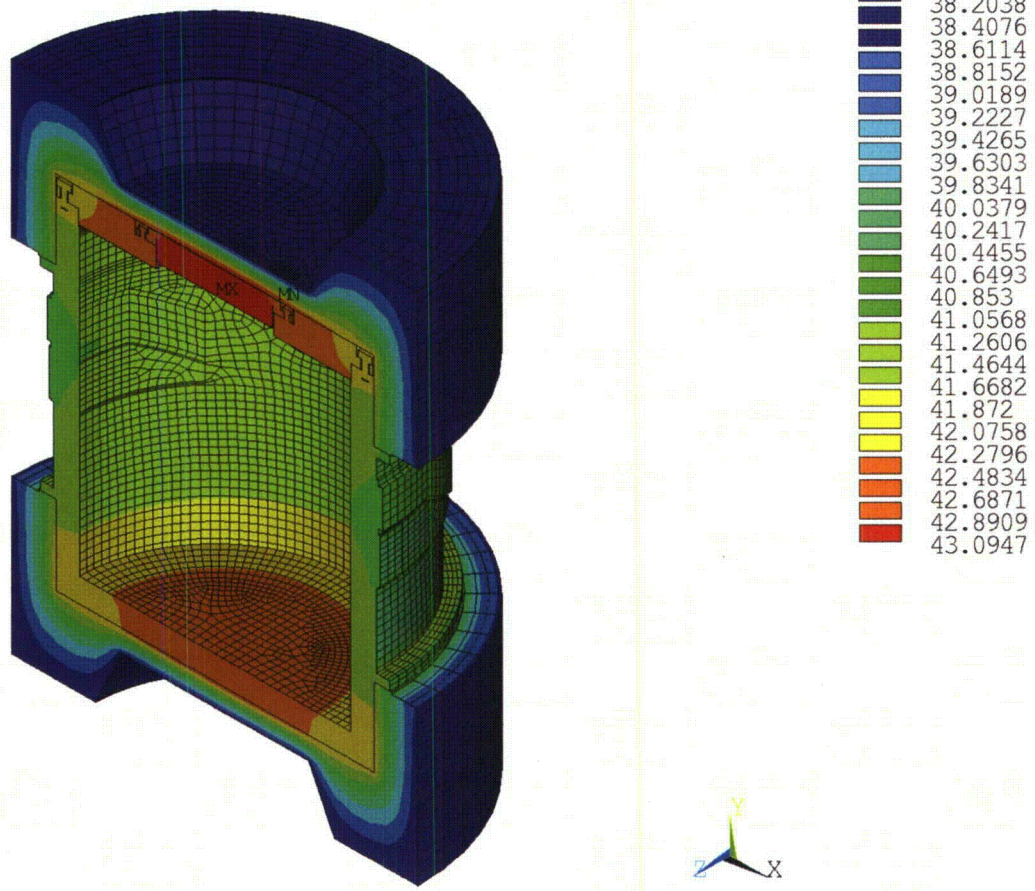

NCT--Case 2, Steady-State Boundary Conditions (Degrees Celsius)

Figure 3.3.1-7 Temperature Contour Plot of Package—Hot Case 2

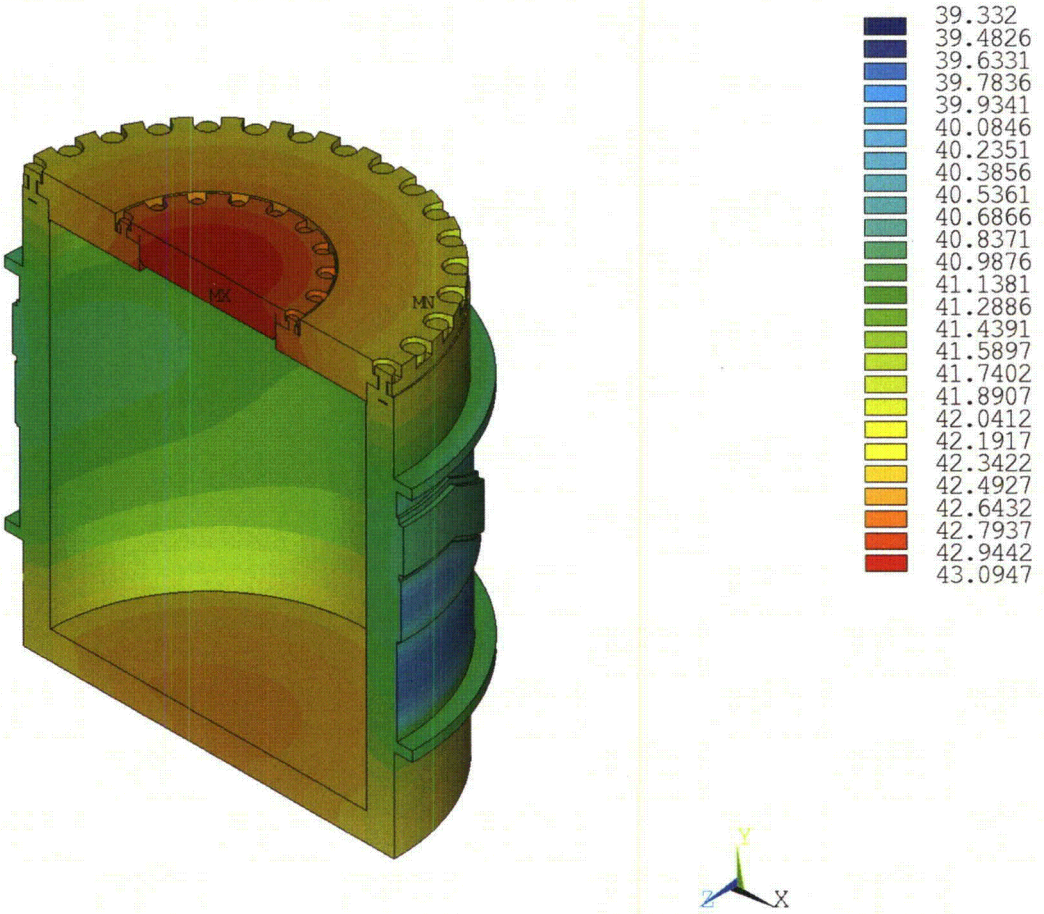

Figure 3.3.1-8 Temperature Contour Plot of Cask Body—Hot Case 2

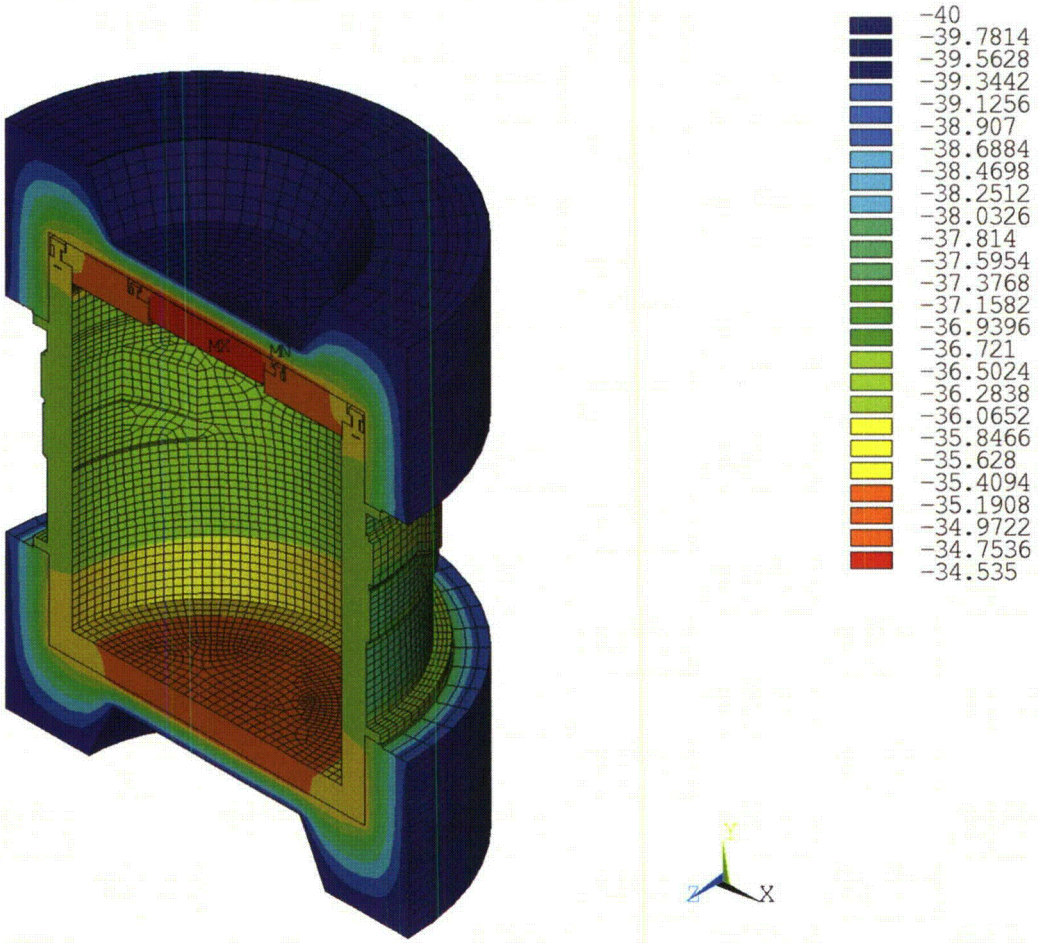

Figure 3.3.1-9 Temperature Contour Plot of Package—Cold Case 1

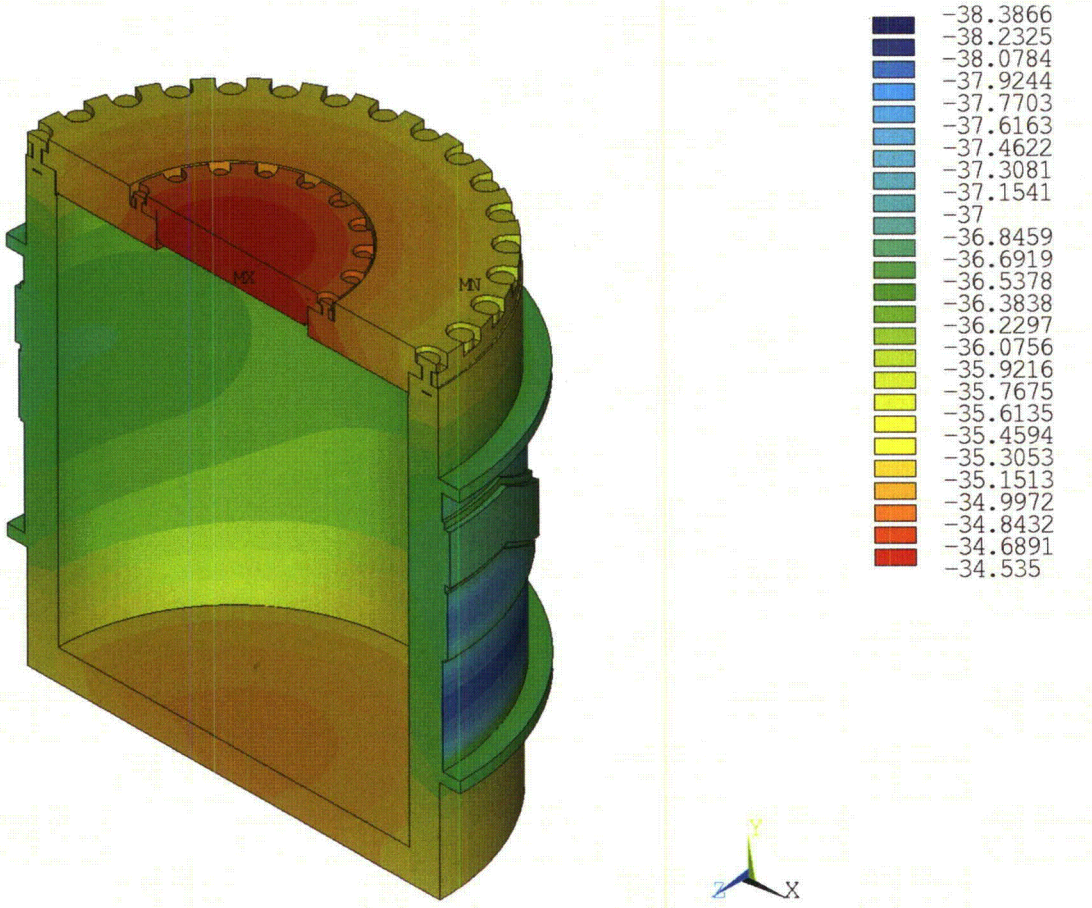

Figure 3.3.1-10 Temperature Contour Plot of Cask Body—Cold Case 1

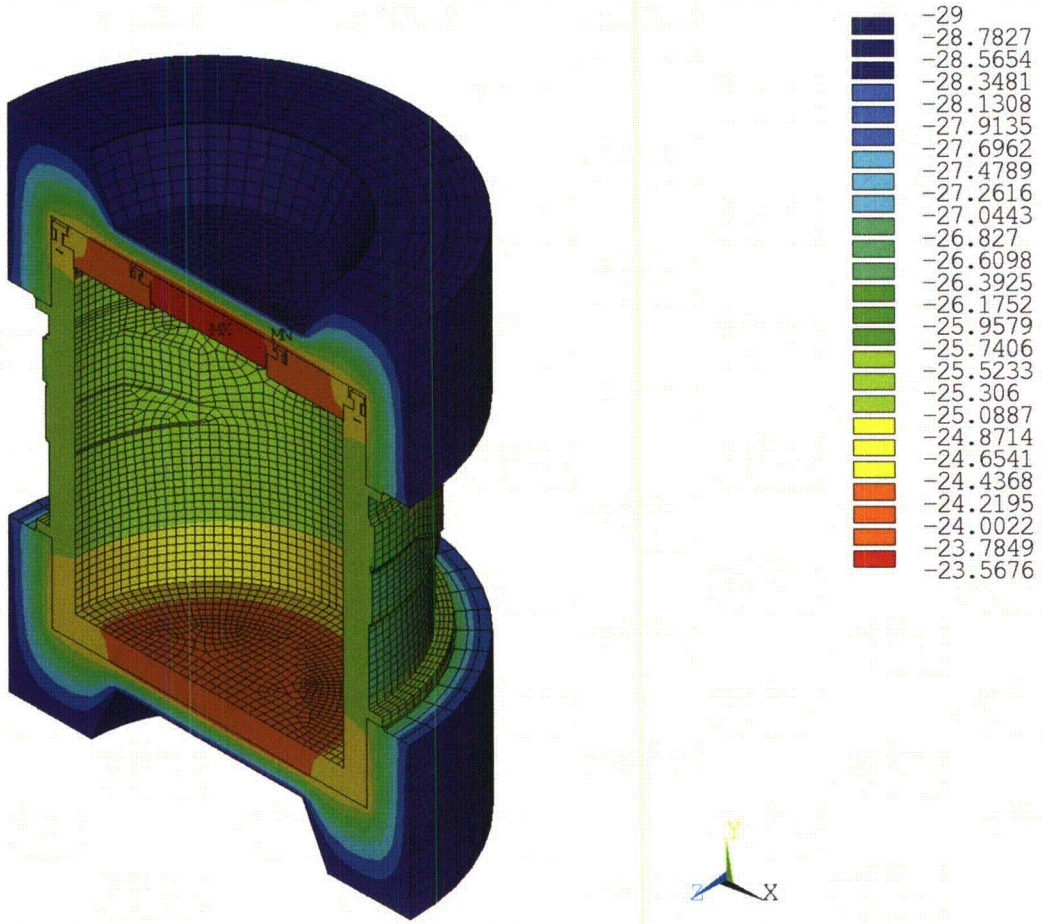

NCT—Case 4, Steady-State Boundary Conditions (Degrees Celsius)

Figure 3.3.1-11 Temperature Contour Plot of Package—Cold Case 2

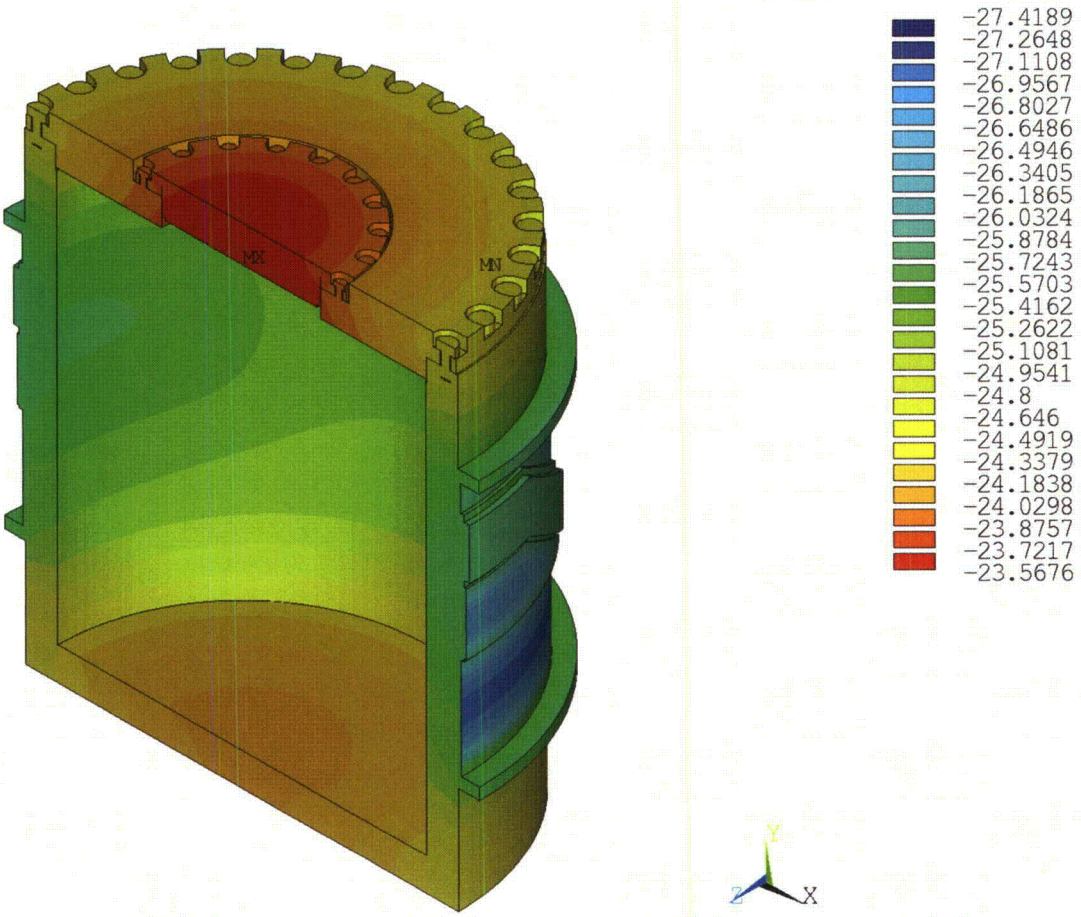

Figure 3.3.1-12 Temperature Contour Plot of Cask Body Cold Case 2

3.3.2 Maximum Normal Operating Pressure

The maximum pressure in the RT-100 for NCT is calculated using the maximum temperatures determined for the range of normal condition load cases. The calculation considers possible sources of gases including the following:

- Gases initially present in the package
- Saturated vapor, including water vapor from the contents or packaging
- Hydrogen or other gases resulting from thermal- or radiation-induced decomposition of materials such as water or plastics

Summary of the pressure calculation is provided in the following sections. Additional details are provided in Calculation Package RTL-001-CALC-TH-0102, Rev. 6 [Ref. 6].

3.3.2.1 Calculation Method

To determine the maximum normal operating pressure, the temperature of gas mixture within the cask is evaluated. Maximum temperature of the cask cavity under normal condition is bounded by the upper and lower temperature range of 80 °C (176°F) to -29 °C (-20°F). The total pressure in the cavity is represented by the sum of the primary contributors to the pressure. These are the pressure due to the increased temperature of the cavity gas (ideal gas law), the pressure due to the presence of water vapor, and the pressure due to the generation of gas via radiolysis.

The restriction of the contents to inorganic materials eliminates the potential for gas generation due to thermal degradation or biological activity. Thus, these gas sources are not considered in the evaluation. However, water vapor is present in trace quantities. Therefore, the analysis considers the contribution from the radiolytic decomposition of residual water in the cask cavity.

Per the ideal gas law, air pressure and water vapor pressure are directly proportional to the temperature, and with increase in temperature the pressure also increases. The upper bound temperature results in a higher maximum normal operating pressure for the cask compared to the lower bound. The gas mixture in the cavity is conservatively assumed to be at 80 °C (176°F).

3.3.2.2 Pressure Due to the Initially Sealed Air in the Cavity

Per the ideal gas law, the partial pressure of the air (P_{air}) initially sealed in the fixed volume of the cask at the ambient temperature as it is heated to 80 °C (176 °F) is:

$$P_1 \times T_2 = P_2 \times T_1$$

$$P_{air} = 101.35 \text{ kPa}[(353.15 \text{ K}) / (294.25 \text{ K})] = 121.64 \text{ kPa (17.64 psia)}$$

3.3.2.3 Pressure Due to the Water Vapor in the Cask

The cask cavity is assumed to contain a small amount of water. By conservatively assuming a condensing surface temperature of 80 °C (176 °F), the water vapor pressure, P_{wv}, at this temperature is:

47.34 kPa [6.87 psia], Fundamentals of Fluid Mechanics, Table B.2, pg. 831 [Ref. 17], Attachment 3.5-3.

Adding the water vapor pressure at 80 °C (176 °F) to the partial pressure of the air in the sealed cask at this temperature gives:

$P_2 = P_{air} + P_{wv} = 121.64 + 47.34 = 169.0$ kPa

$= 169.0$ kPa$\times$ 0.145 psi/kPa = [24.51 psia]

3.3.2.4 Pressure Due to Generation of Gas

Solidified or dewatered material may contain some water. Therefore, radiolytic generation of gases from this water could occur. Hydrogen and oxygen may be produced in the cask by radiolytic decomposition of residual water in the cask contents. As described in Chapter 1, Section 1.2.2.6, the maximum quantity of hydrogen must be limited to less than 5% to ensure that an explosive quantity does not accumulate.

The cask atmosphere can be assumed to contain 5% of hydrogen (H_2) gas due to radiolysis of the water. By stoichiometry of the water molecule (H_2O), the cask atmosphere will also contain 2.5% oxygen (O_2) gas generated by radiolysis. Partial pressures in an ideal gas mixture are additive and behave the same as ideal gas volume fraction or mole fractions. Therefore, the partial pressure of hydrogen is described by the following equation:

$P_{H2} = 0.05\ P_{pt}$

Where, $P_{pt} = P_{air} + P_{wv} + P_{H2} + P_{O2}$

Combining $P_{air} + P_{wv} = P_2$ and noting that $P_{O2} = 0.5 \times P_{H2}$.

$P_{H2} = 0.05 \times (P_2 + 1.5\ P_{H2})$

Solving the equation explicitly for P_{H2} give:

$P_{H2} = [0.05\ P_2] / [1 - 0.05\ (1.5)]$

$= [0.05 * 169.0 \text{ kPa}] / [1 - 0.05\ (1.5)]$

$= 9.14$ kPa [1.32 psia]

3.3.2.5 Total Pressure

Based on the stoichiometric relationship between hydrogen and oxygen liberated by radiolysis of water, and again combining the pressure of the initially sealed air and water vapor as P_2, the total pressure in the cask at 80°C (176°F) is:

$P_{Total} = P_2 + 1.5\ P_{H2}$

$= 169.0 \text{ kPa} + 1.5 * 9.14 \text{ kPa}$

$= 182.71$ kPa [26.5 psia] (actual calculated MNOP)

The design basis maximum normal operating pressure (MNOP) value is conservatively set at 342.7 kPa (49.7 psia or 35 psig) for use in the cask structural analyses for NCT.

3.4 Thermal Evaluation under Hypothetical Accident Conditions

This section describes the thermal evaluation of the RT-100 under hypothetical accident conditions. The RT-100 is evaluated by finite element computer analysis rather than physical testing to demonstrate the performance of the cask in response to the fire test conditions specified in 10 CFR 71.73(c) [Ref. 2]. The HAC defined in 10 CFR 71.73(c) [Ref. 2] are applied sequentially, considering the damaged condition of the packaging following the 30-foot free drop and pin puncture accident events prior to the fire transient. For the accident condition thermal evaluation, the general comments in Section 3.3 are considered and addressed, as appropriate.

As described in Chapter 2, Section 2.7.3 (Puncture), different pin puncture configurations are considered in order to determine the worst case for the accident event. For the structural evaluation, the orientations considered are directly in the middle of the secondary lid to maximize the bending loads in the primary and secondary lids and prying forces in the bolts. The second configuration considers the pin impact directly into the side of the RT-100 to ensure that the outer shell is not punctured by the pin. For the thermal analysis, these two events are also considered to be limiting. The differences are in the location of the pin at impact.

3.4.1 HAC Fire Analysis—Pin Puncture Damage to Top Impact Limiter

The analytical model described in Section 3.3.1.2 is used to evaluate the RT-100 package with damage on the top impact limiter. For this case, the limiting configuration for the thermal analysis considers a pin puncture through the top impact limiter directly into the secondary lid at the location of the O-rings. The model placed a 150 mm (6 in) diameter hole through the upper impact limiter, directly exposing the secondary lid to the thermal environment of the hypothetical accident fire. The following section evaluates both pin puncture orientations to determine the effect to critical components such as the seal locations and lead shielding.

3.4.1.1 Initial Conditions—Pin Puncture Damage to Top Impact Limiter

Per Regulatory Position 1.1 in Regulatory Guide 7.8 [Ref. 20], the initial cask temperature distribution is considered to be at steady state with an ambient temperature of 38°C (100°F) and solar insolation prior to the HAC fire accident. To meet this requirement, the steady-state solution for NCT hot case 1 is used, obtained to the initial temperatures of the cask prior to the fire. The steady-state temperatures are applied as the first load step of the transient solutions. To account for damage to the package that results during the sequential drop accidents, damage due to pin puncture is considered during the top and side puncture. For the top impact limiter 150 mm diameter volume of material including the steel shell and FR3740 foam is removed at the point closest to the elastomer O-ring. This is a conservative approach since the puncture probe will not penetrate through the top skin of the impact limiter and compressed foam will remain beneath the point of impact. Figure 3.4.1-1 shows the temperature contour of the package prior to the fire accident and localized higher temperatures in the region of the damaged impact limiter. Figure 3.4.1-2 and Figure 3.4.1-3 show the cask body and inner shell cavity temperature distribution prior to the fire accident.

3.4.1.2 HAC Fire and Cool-down Analysis—Pin Puncture Damage to Top Impact Limiter

The thermal analysis for HAC includes a 30 minute transient fire followed by the prescribed post-fire cool-down period. The FE model described in Section 3.3.1.2 is analyzed by applying

the following boundary conditions. Following the initial load step in which the steady-state temperatures are applied, the analysis proceeds with the HAC fire transient for 30 minutes (1,800 seconds) followed by a cool-down period with the boundary conditions associated with NCT Hot case 1. The NCT Hot case 1 boundary conditions are applied as constants ignoring the day/night cool-down cycle. The following is a summary of the fire transient boundary conditions:

- Environment temperature, 800°C (1472°F)
- No solar insolation, 0 W/m^2
- Forced convection, heat transfer coefficient = 10 $W/m^2 \cdot °C$
- Radiation from the environment to package surface, flame emissivity = 0.9
- Internal heat load as a uniform heat flux, 13.04 W/m^2

The cool-down analysis is performed for 216,000 seconds (2.5 days) with the following boundary conditions:

- Environment temperature, 38°C (100°F)
- Solar insolation applied as constant, 776 W/m^2 for flat surfaces and 388 W/m^2 for curved surfaces.
- Natural convection, heat transfer coefficient = 5 $W/m^2 \cdot °C$
- Radiation from package surface to the environment, package emissivity = 0.8
- Internal heat load as a uniform heat flux, 13.04 W/m^2

3.4.1.3 HAC Fire Analysis Results—Pin Puncture Damage to Top Impact Limiter

The temperature contour plots of the RT-100 package and cask body at the end of fire are shown in Figure 3.4.1-4 and Figure 3.4.1-5, respectively. Figure 3.4.1-6 and Figure 3.4.1-7 show the package and cask body temperature contours after the cool-down period. Figure 3.4.1-8 shows the temperature time-history from the start of the fire through the cool-down. As Figure 3.3.1-8 shows, the average inner shell temperature is 136.3°C (277.3°F) and is representative of the contents during the fire/cool-down transient. Figure 3.4.1-9 provides an enhanced view of the time-history data through the 30 minute fire and 2.5 hours of the cool down process. Figure 3.4.1-10 identifies the highest inner shell temperature at the point that it occurs, 48 minutes from the start of the fire. Figure 3.4.1-11 identifies the maximum lead shield temperature occurring 35 minutes after the start of the fire, at a point underneath the tie-down arms. This figure indicates that no melting of the lead shield occurs during the HAC fire.

Table 3.1.3-2 summarizes the maximum temperatures of the cask under HAC fire with pin puncture damage at the side of the cask body.

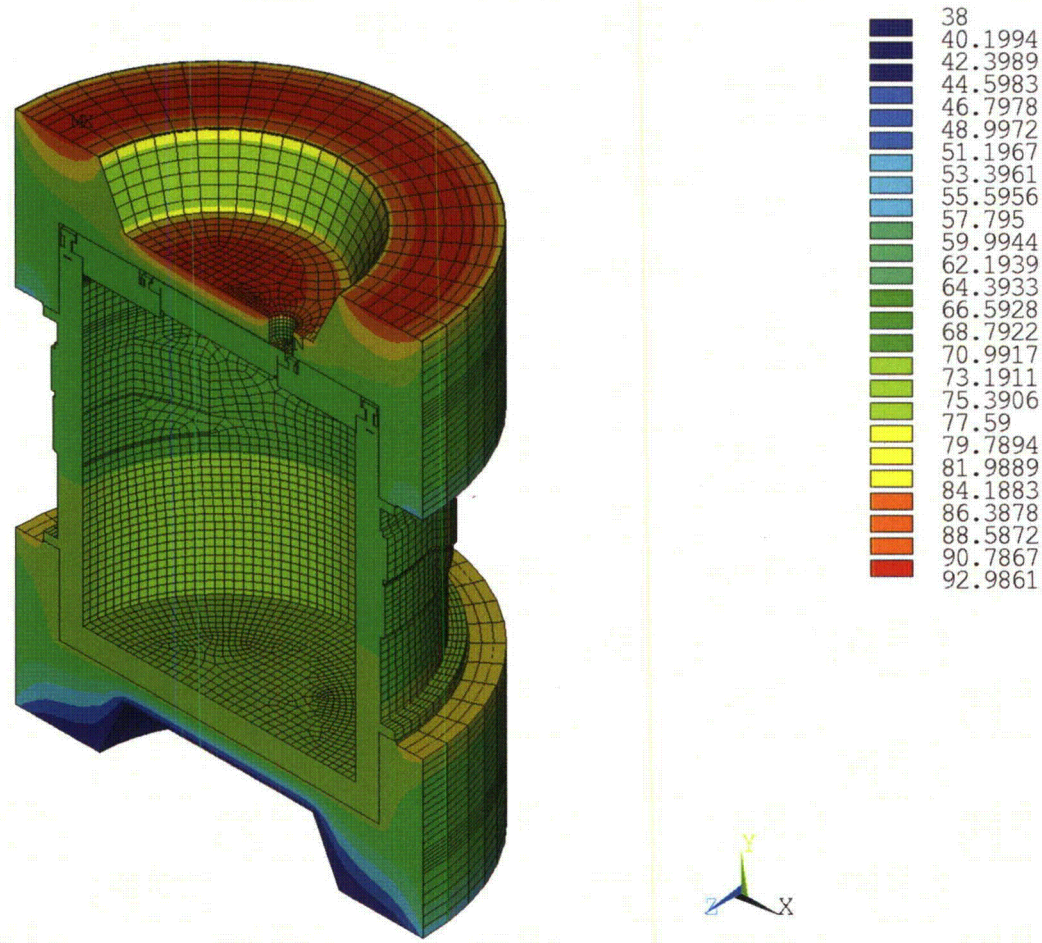

HAC--Fire Top Puncture, Steady-State Inital Conditions (Degrees Celsius)

Figure 3.4.1-1 Temperature Contour Plot of Package Pre-Fire Fire Condition—HAC Pin Damage on Top Impact Limiter

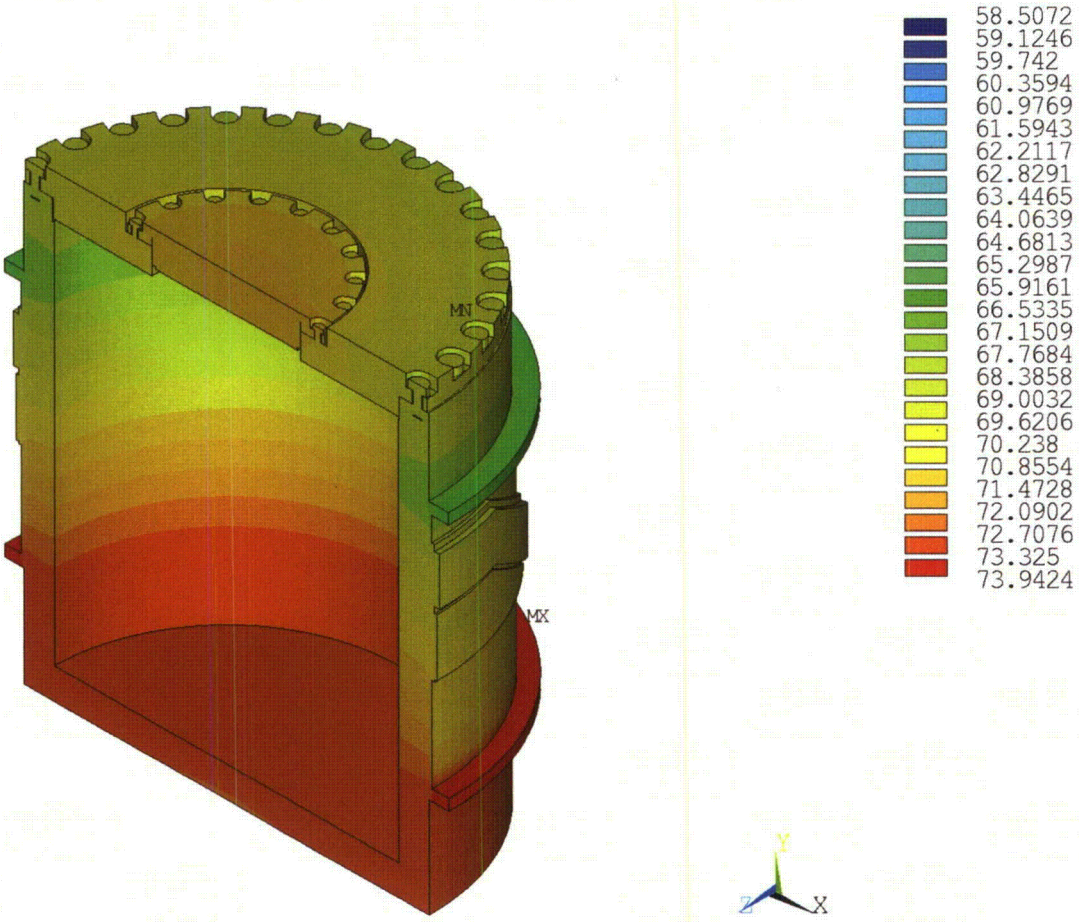

HAC--Fire Top Puncture, Steady-State Inital Conditions (Degrees Celsius)

Figure 3.4.1-2 Temperature Contour Plot of Cask Body Pre-Fire Condition—HAC Pin Damage on Top Impact Limiter

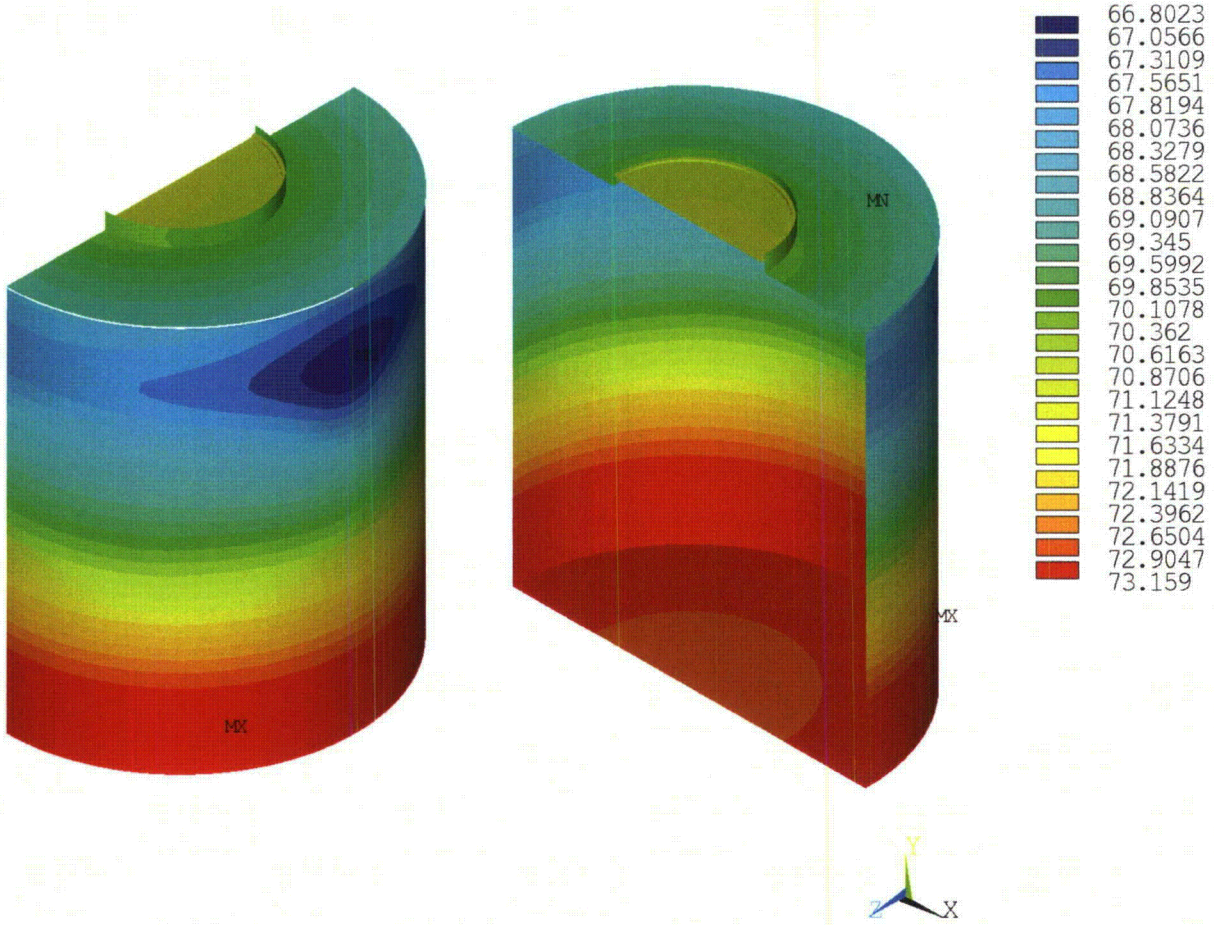

HAC--Fire Top Puncture, Steady-State Inital Conditions (Degrees Celsius)

Figure 3.4.1-3 Temperature Contour Plot of Inner Shell Pre-Fire Condition—HAC Pin Damage on Top Impact Limiter

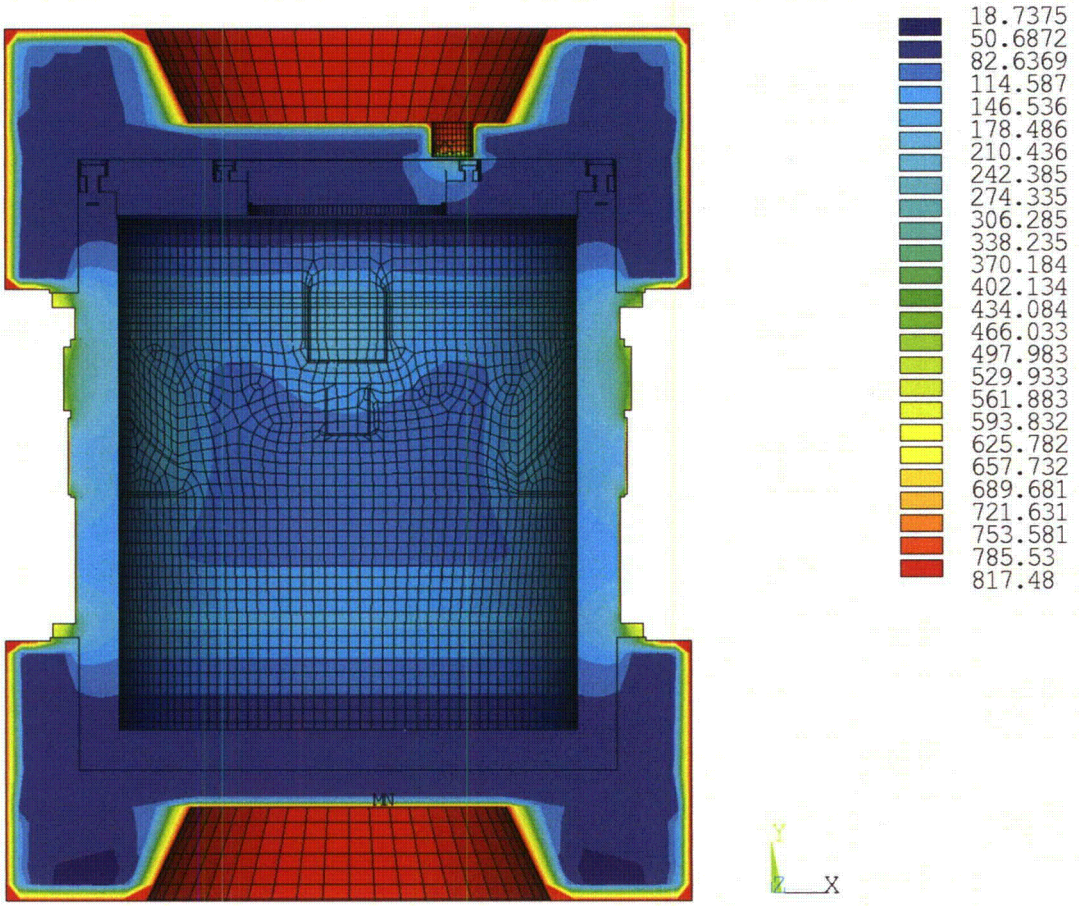

HAC--Fire Top Puncture, Steady-State Inital Conditions (Degrees Celsius)

Figure 3.4.1-4 Temperature Contour Plot of Package at the End of Fire—HAC Pin Damage on Top Impact Limiter

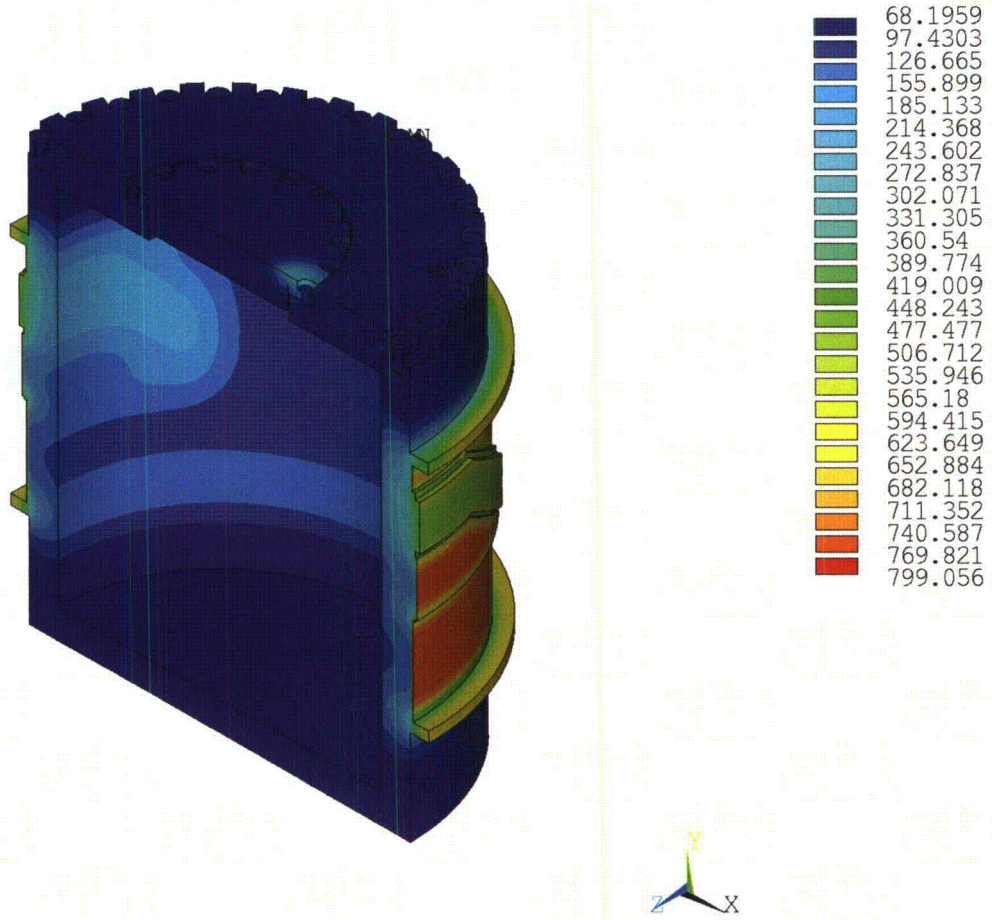

Figure 3.4.1-5 Temperature Contour Plot of Cask Body at the End of Fire—HAC Pin Damage on Top Impact Limiter

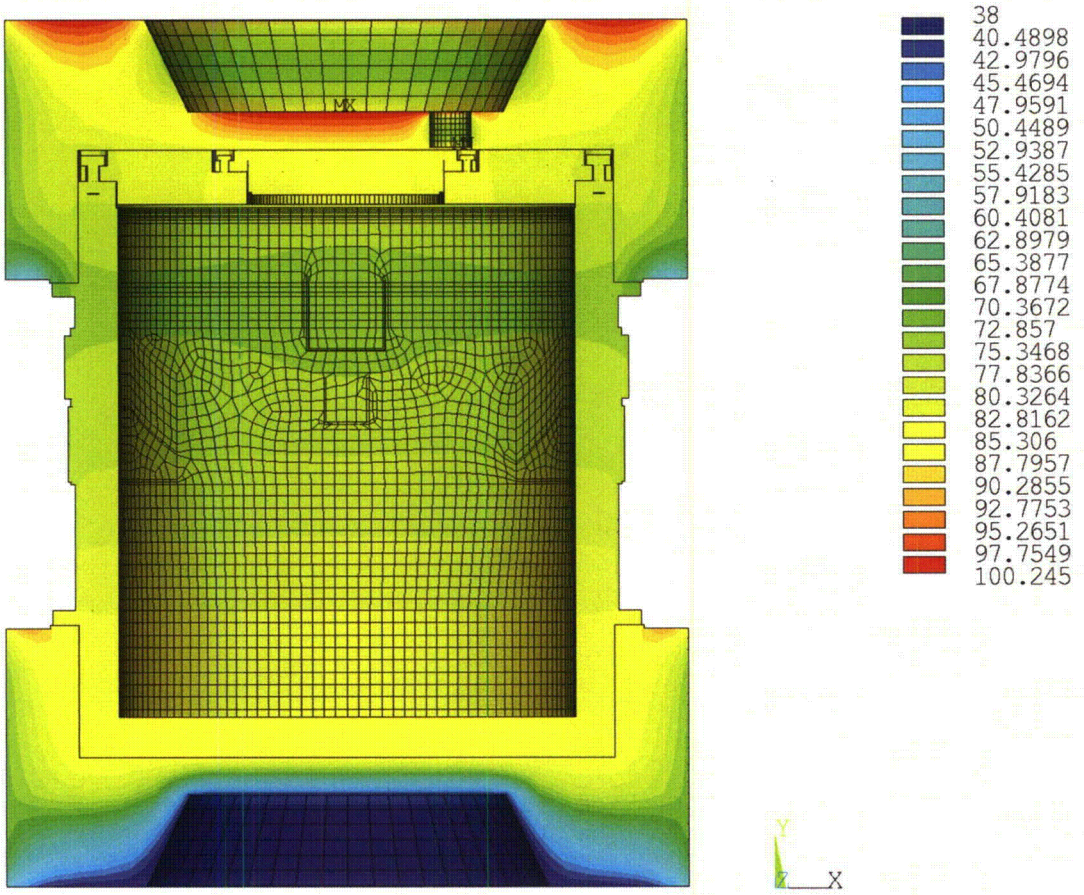

HAC--Fire Top Puncture, Steady-State Inital Conditions (Degrees Celsius)

Figure 3.4.1-6 Temperature Contour Plot of Package after Cool-Down—HAC Pin Damage on Top Impact Limiter

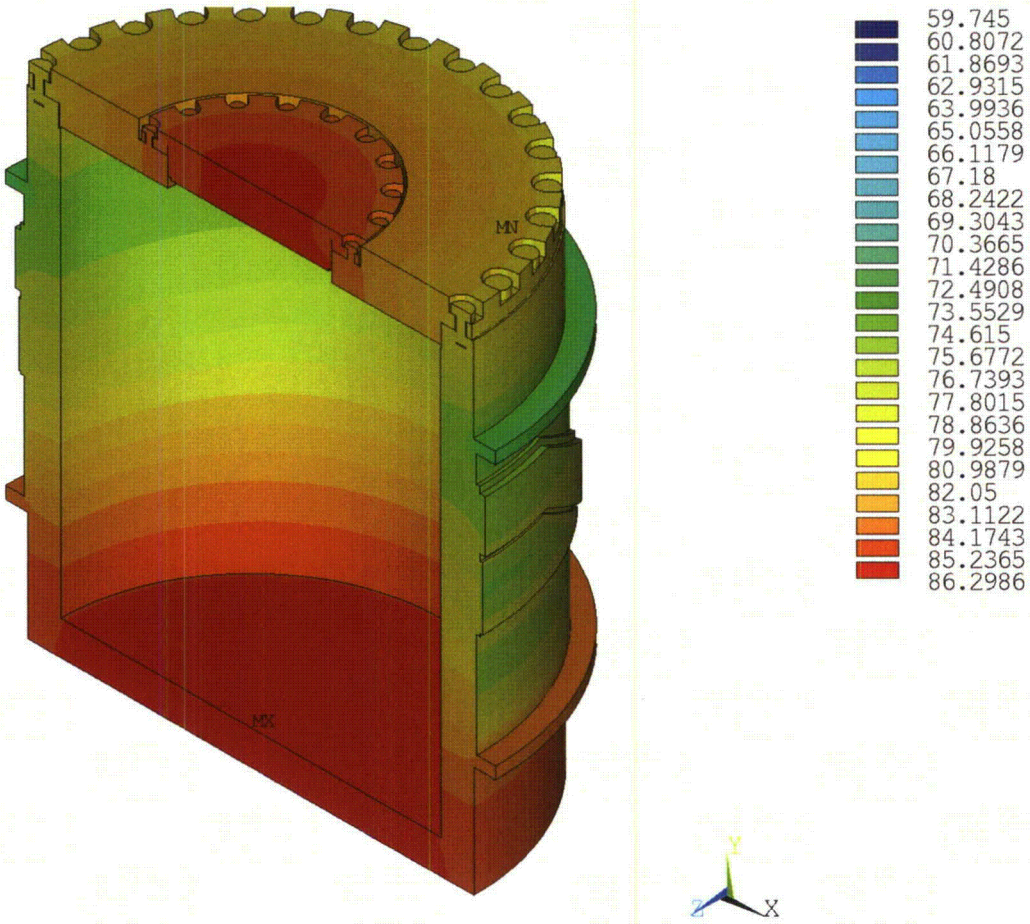

HAC--Fire Top Puncture, Steady-State Inital Conditions (Degrees Celsius)

Figure 3.4.1-7 Temperature Contour Plot of Cask Body after Cool-Down—HAC Pin Damage on Top Impact Limiter

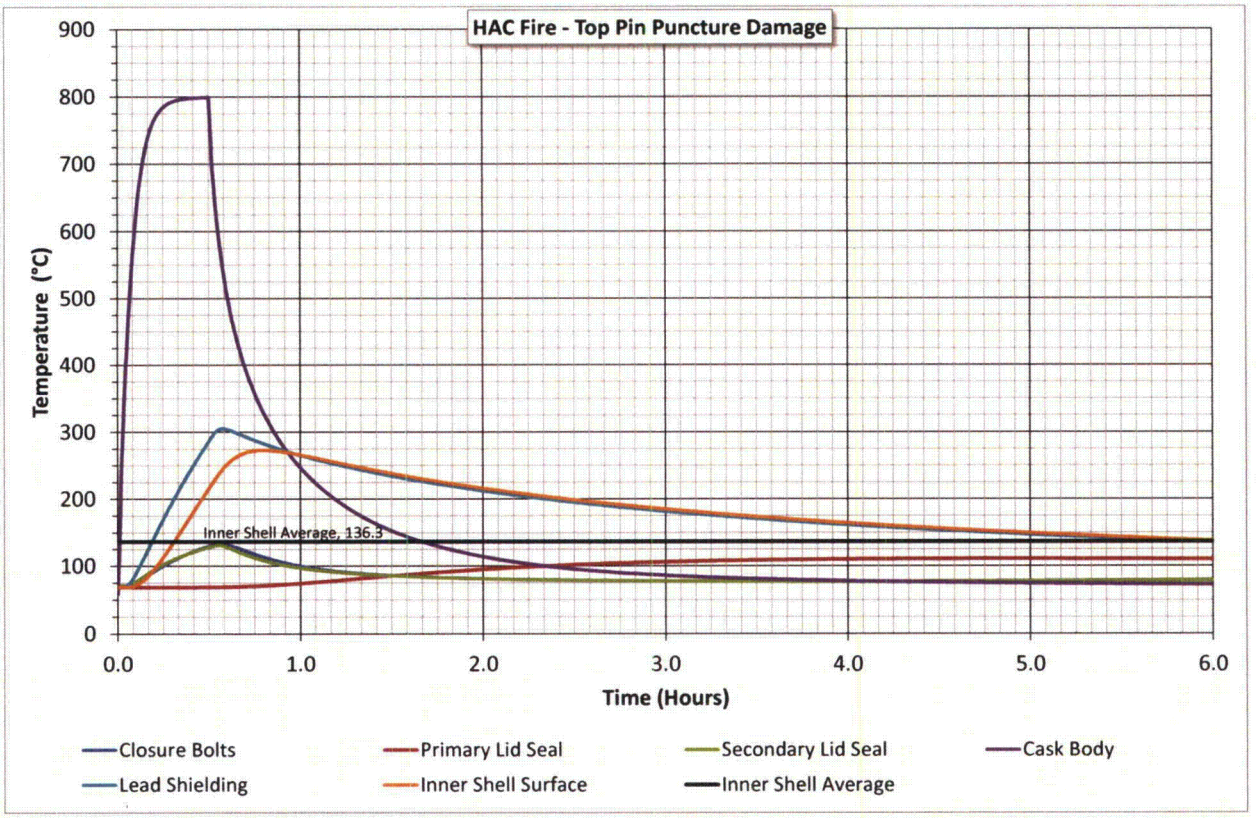

Figure 3.4.1-8 Time-History Plot of Critical Package Components—HAC Pin Damage on Top Impact Limiter

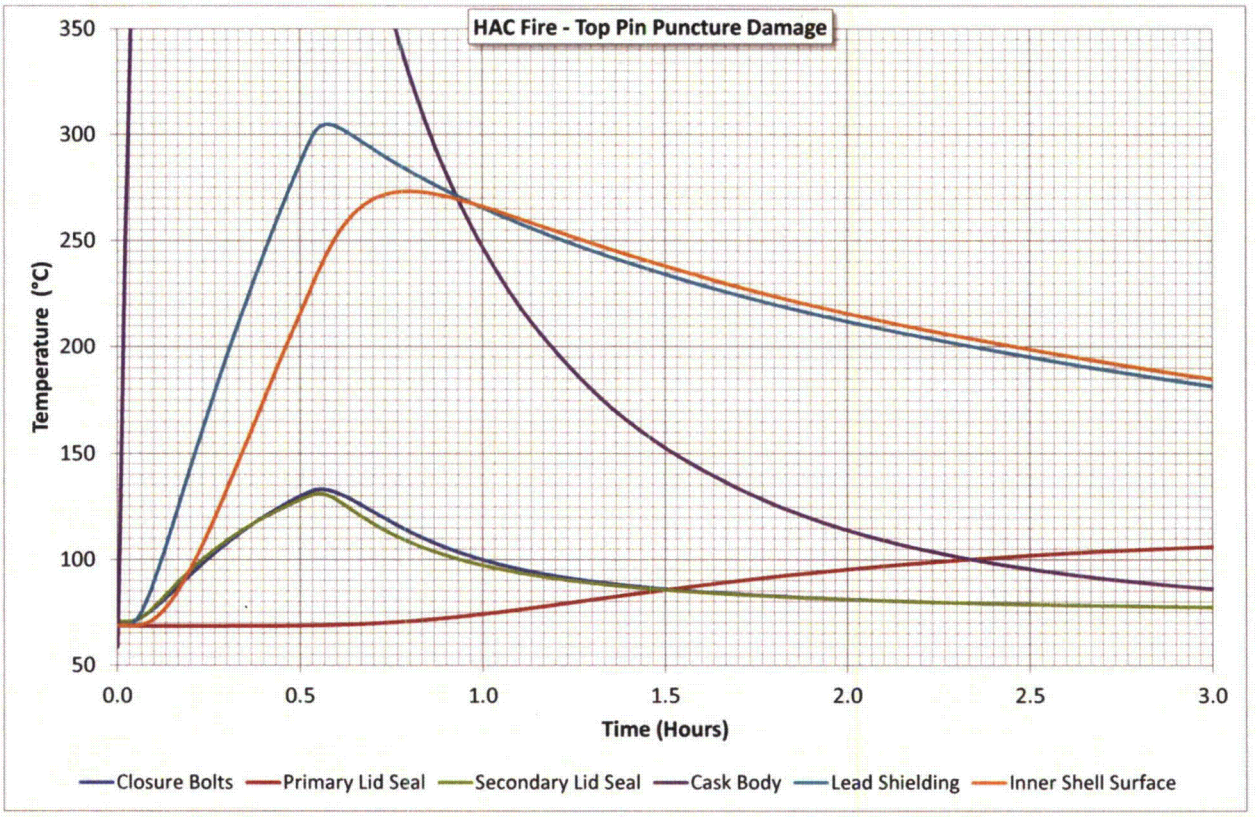

Figure 3.4.1-9 Time-History Enhanced View Plot of Critical Package Components—HAC Pin Damage on Top Impact Limiter

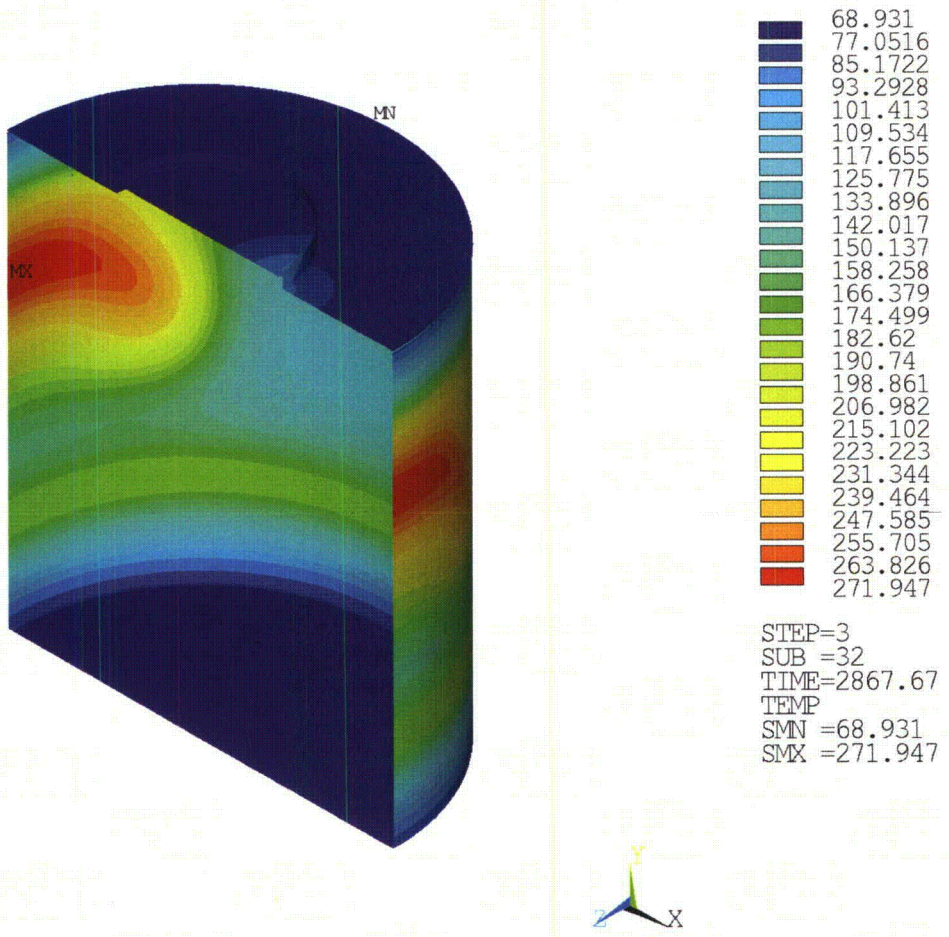

HAC--Fire Top Puncture, Steady-State Inital Conditions (Degrees Celsius)

Figure 3.4.1-10 Maximum Temperature of the Inner Shell—HAC Pin Damage on Top Impact Limiter

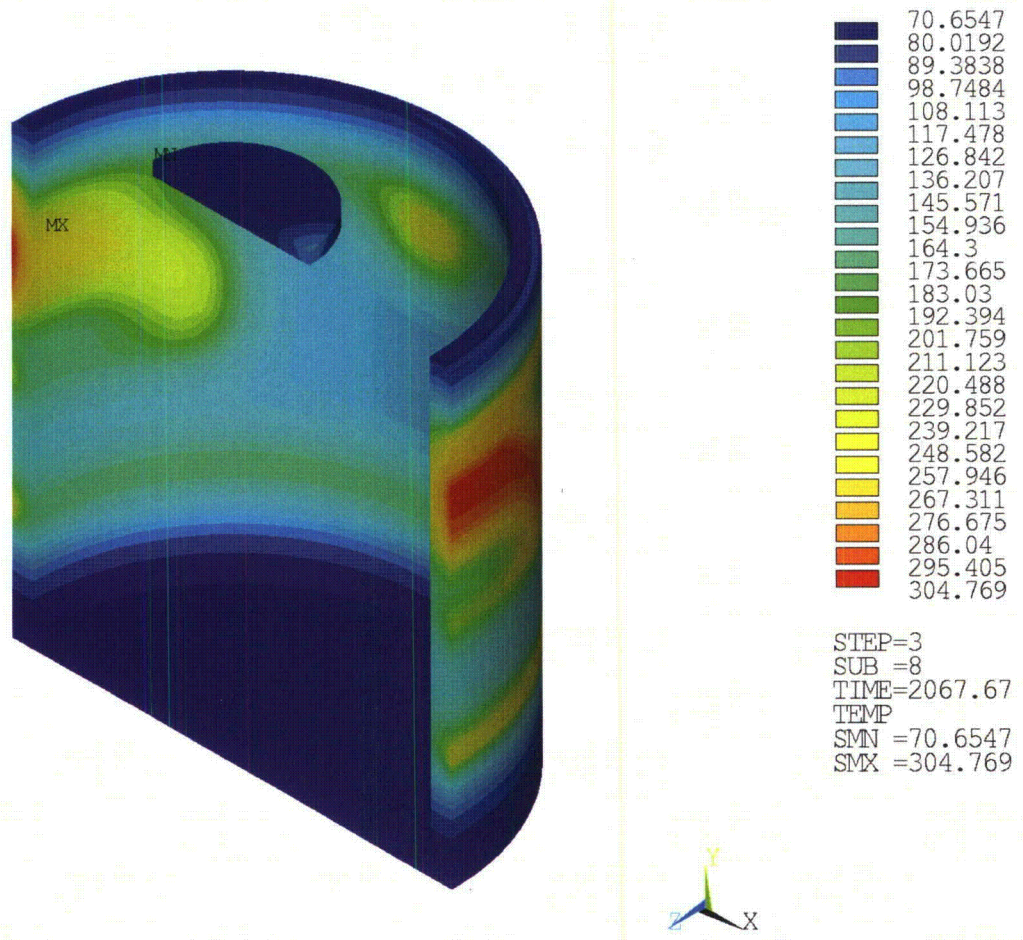

HAC--Fire Top Puncture, Steady-State Inital Conditions (Degrees Celsius)

Figure 3.4.1-11 Maximum Temperature of Lead Shielding—HAC Pin Damage on Top Impact Limiter

3.4.2 HAC Fire Evaluation—Pin Puncture Damage to the Side of the Cask Body

The analytical model described in Section 3.3.1.2 is used to evaluate the RT-100 with damage on the cask side wall. For this case, the limiting configuration considers the pin puncturing the thermal shield directly below the lifting block. This configuration increases the area of the outer shell of the cask that is not protected by the thermal shield and maximizes the heat input into the lead. The following section evaluates both pin puncture orientations to determine the effect to critical components such as the seal locations and lead shielding.

3.4.2.1 Initial Condition—Pin Puncture Damage to the Side of the Cask Body

Figure 3.4.2-1 shows the FE model of the cask body due to pin puncture damage on the side. The location of the damage is chosen below the lifting pocket in a region where no thermal insulation exists. Therefore, the heat flow is maximized into the package. The removed elements at this area cover a surface area greater than the area of the pin. As with the pin puncture on the top impact limiter case, NCT Hot case 1 steady state solution is used as the initial condition for the fire cases. The steady-state temperatures are applied as a boundary condition during the first

load step of the transient solution, prior to initiating the HAC fire transient. Figure 3.4.2-2 shows the package temperature distribution prior to the fire. The cask body and inner shell pre-fire temperatures are shown in Figure 3.4.2-3 and Figure 3.4.2-4.

3.4.2.2 HAC Fire Analysis—Pin Puncture Damage to the Side of the Cask Body

The thermal analysis for HAC includes a 30 minute transient fire followed by the prescribed post-fire cool-down period. The FE model described in Section 3.3.1.2 is analyzed by applying the following boundary conditions. Following the initial load step in which the steady-state temperatures are applied, the analysis proceeds with the HAC fire transient for 30 minutes (1,800 seconds) followed by a cool-down period with the boundary conditions associated with NCT hot case 1. The NCT hot case 1 boundary conditions are applied as constants, ignoring the day/night cool-down cycle. The following is a summary of the fire transient boundary conditions:

- Environment temperature, 800°C (1472°F)
- No solar insolation, 0 W/m^2
- Forced convection, heat transfer coefficient = 10 $W/m^2 \cdot °C$
- Radiation from the environment to package surface, flame emissivity = 0.9
- Internal heat load as a uniform heat flux, 13.04 W/m^2

The cool-down analysis is performed for 216,000 seconds (2.5 days) with the following boundary conditions:

- Environment temperature, 38°C (100°F)
- Solar insolation applied as constant, 776 W/m^2 for flat surfaces and 388 W/m^2 for curved surfaces.
- Natural convection, heat transfer coefficient = 5 $W/m^2 \cdot °C$
- Radiation from package surface to the environment, package emissivity = 0.8
- Internal heat load as a uniform heat flux, 13.04 W/m^2

3.4.2.3 HAC Fire and Cool-down Analysis—Pin Puncture Damage to the Side of the Cask Body

The boundary conditions for the top and side pin puncture cases are the same as the case with pin puncture damage at the top impact limiter described in Section 3.4.2.1. The temperature contour plots of the package and the cask body at the end of fire are shown in Figure 3.4.2-5 and Figure 3.4.2-6. Figure 3.4.2-6 shows the maximum temperature at the lifting pockets and puncture location. Figure 3.4.2-7 and Figure 3.4.2-8 shows the package and cask body after the cool-down period.

Time-history temperature data is obtained in the transient analysis for critical components of the package including the outer shell, inner shell, closure bolts, lead shield, and O-rings. Maximum temperature results are obtained during post-processing by selecting the FE model component or material of interest and sorting the nodal results. Figure 3.4.2-9 shows the temperature time-history from the start of the fire through the cool-down. As Figure 3.4.2-9 shows, the average inner shell temperature is 137°C and is representative of the contents during the fire/cool-down

transient. Figure 3.4.2-10 provides an enhanced view of the time-history data through the 30 minute fire and 2.5 hours of the cool down process. Figure 3.4.2-11 identifies the highest inner shell temperature at the instant it occurs, 48 minutes from the start of the fire. Figure 3.4.2-12 identifies the maximum lead shield temperature occurring 35 minutes after the start of the fire, at a point underneath the tie-down arms. This figure indicates that no melting of the lead shield occurs during the HAC fire.

Table 3.1.3-3 summarizes the maximum temperatures of the cask under HAC fire with pin puncture damage at the side of the cask body.

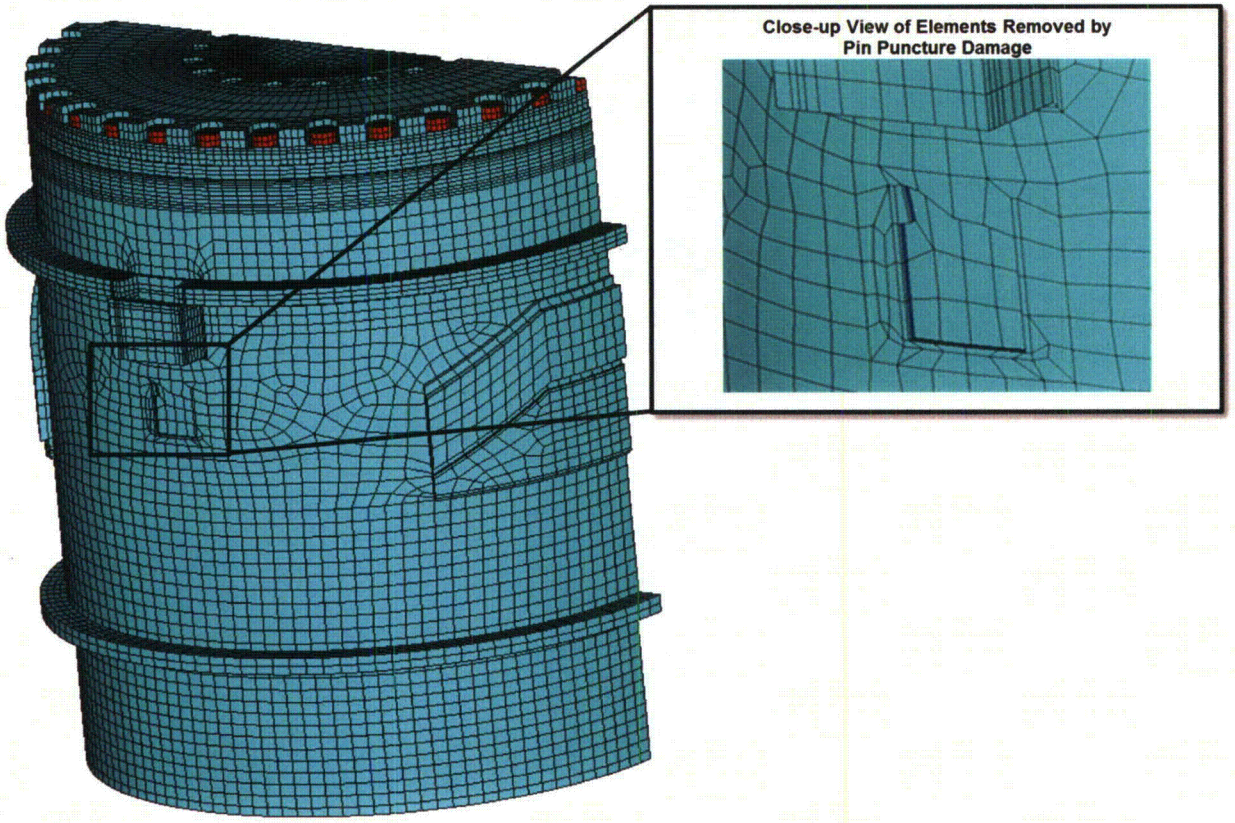

Figure 3.4.2-1 Cask Model-HAC Pin Damage on Cask Body Side

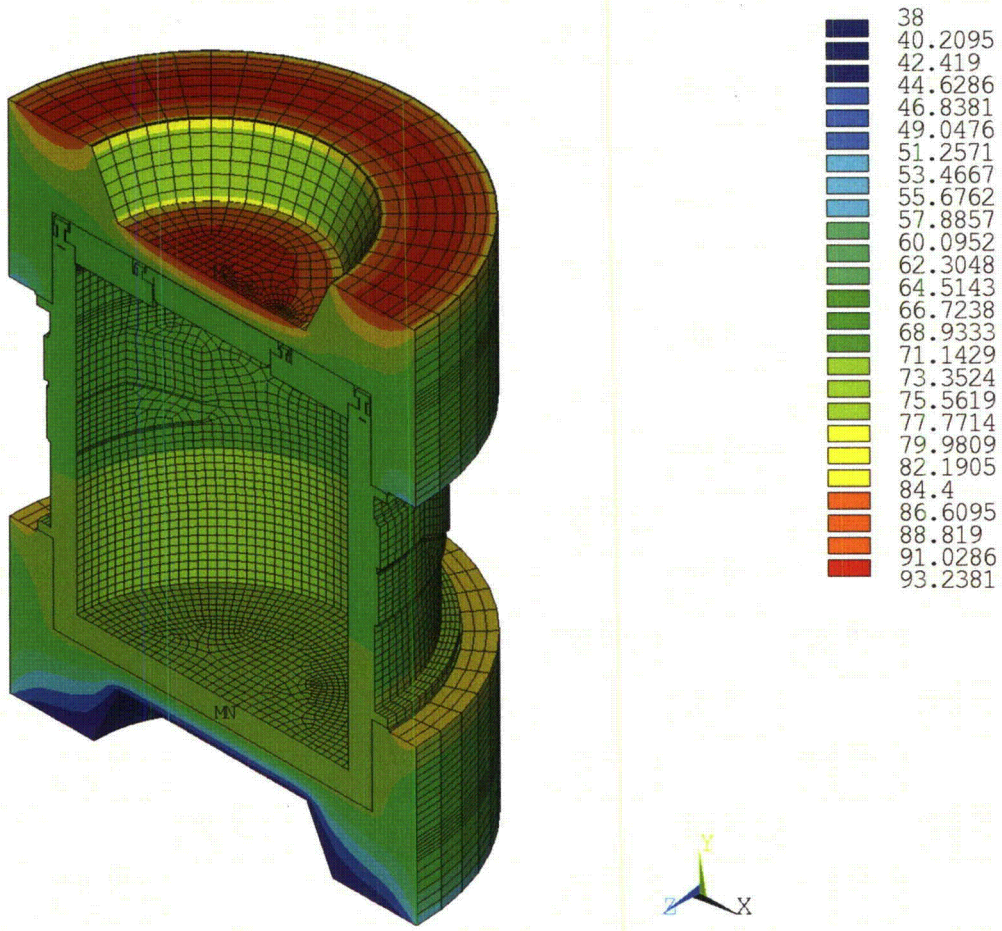

HAC—Fire Side Puncture, Steady-State Inital Conditions (Degrees Celsius)

Figure 3.4.2-2 Temperature Contour Plot of Package Pre-Fire Condition—HAC Pin Damage on Cask Body Side

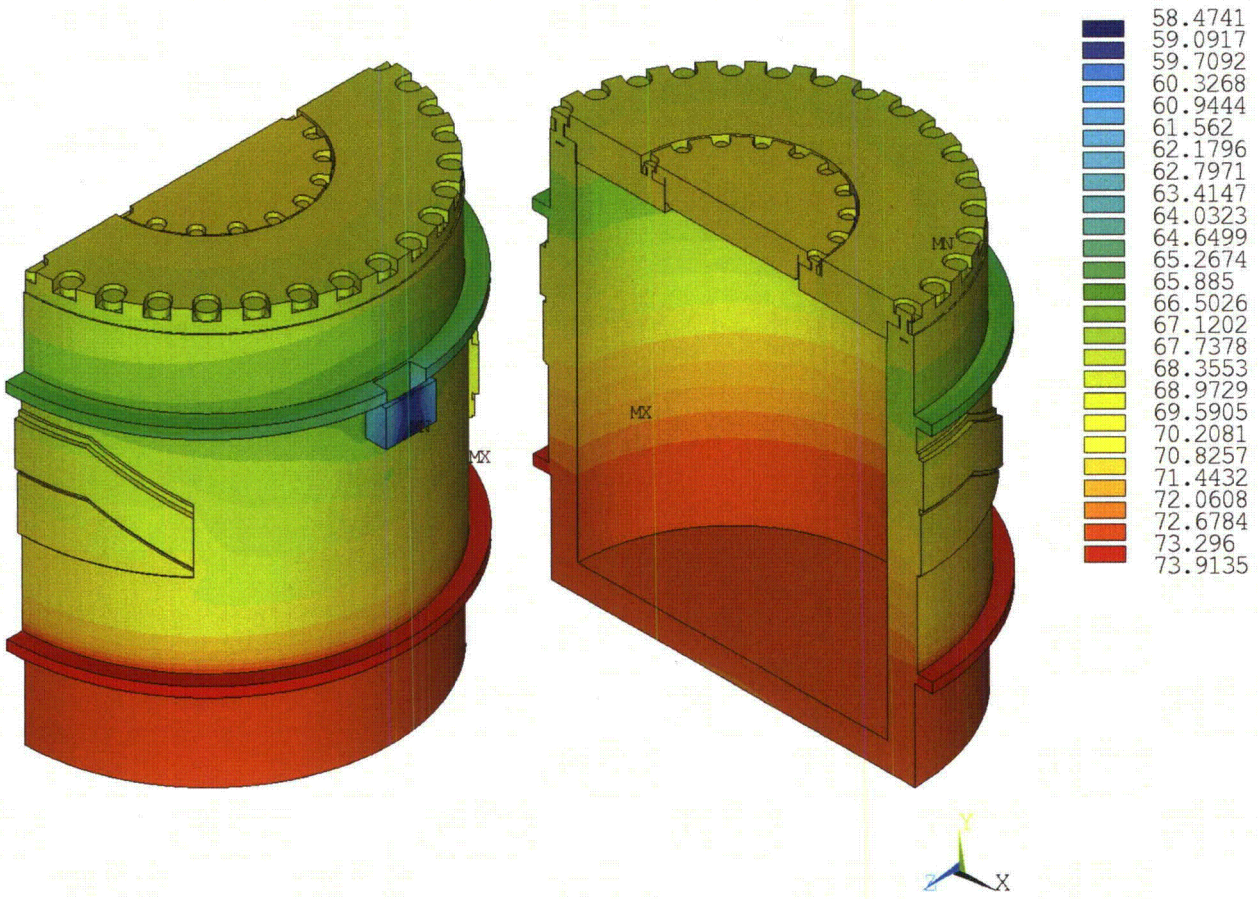

HAC--Fire Side Puncture, Steady-State Inital Conditions (Degrees Celsius)

Figure 3.4.2-3 Temperature Contour Plot of Cask Body Pre-Fire Condition—HAC Pin Damage on Cask Body Side

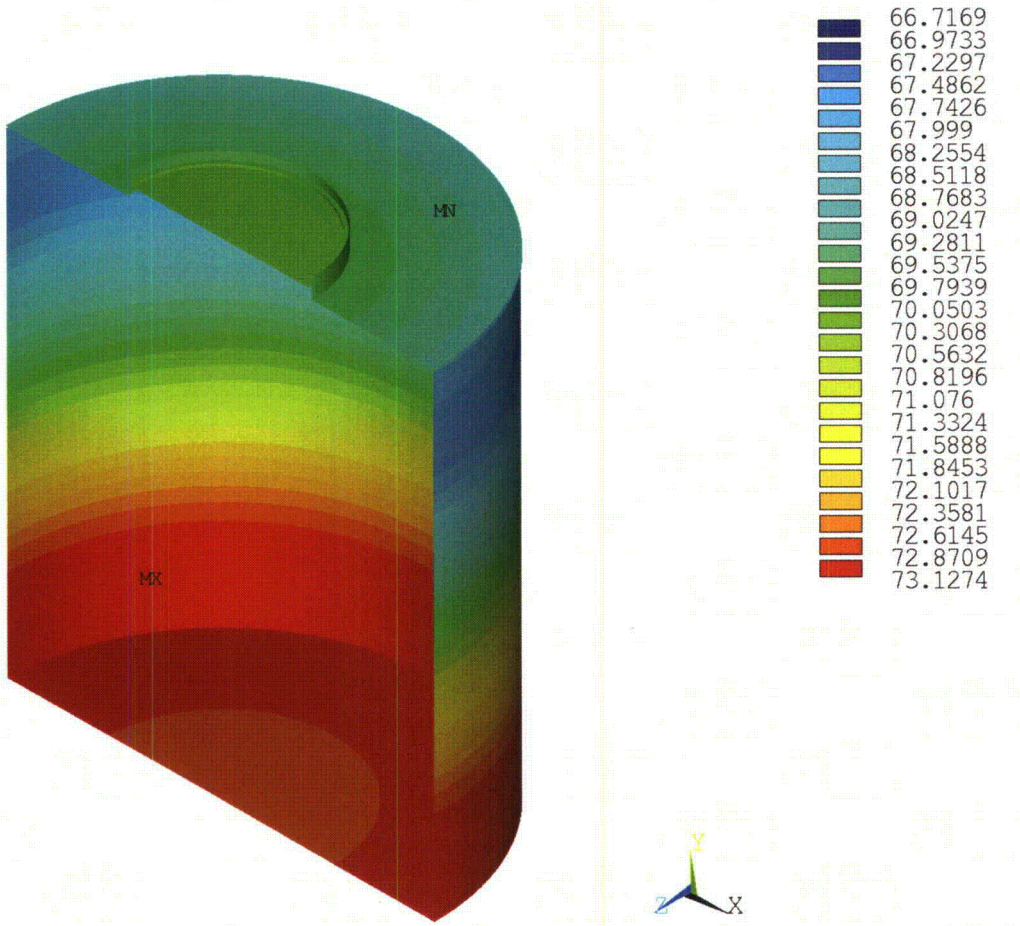

HAC--Fire Side Puncture, Steady-State Inital Conditions (Degrees Celsius)

Figure 3.4.2-4 Temperature Contour Plot of Inner Shell Pre-Fire Condition—HAC Pin Damage on Cask Body Side

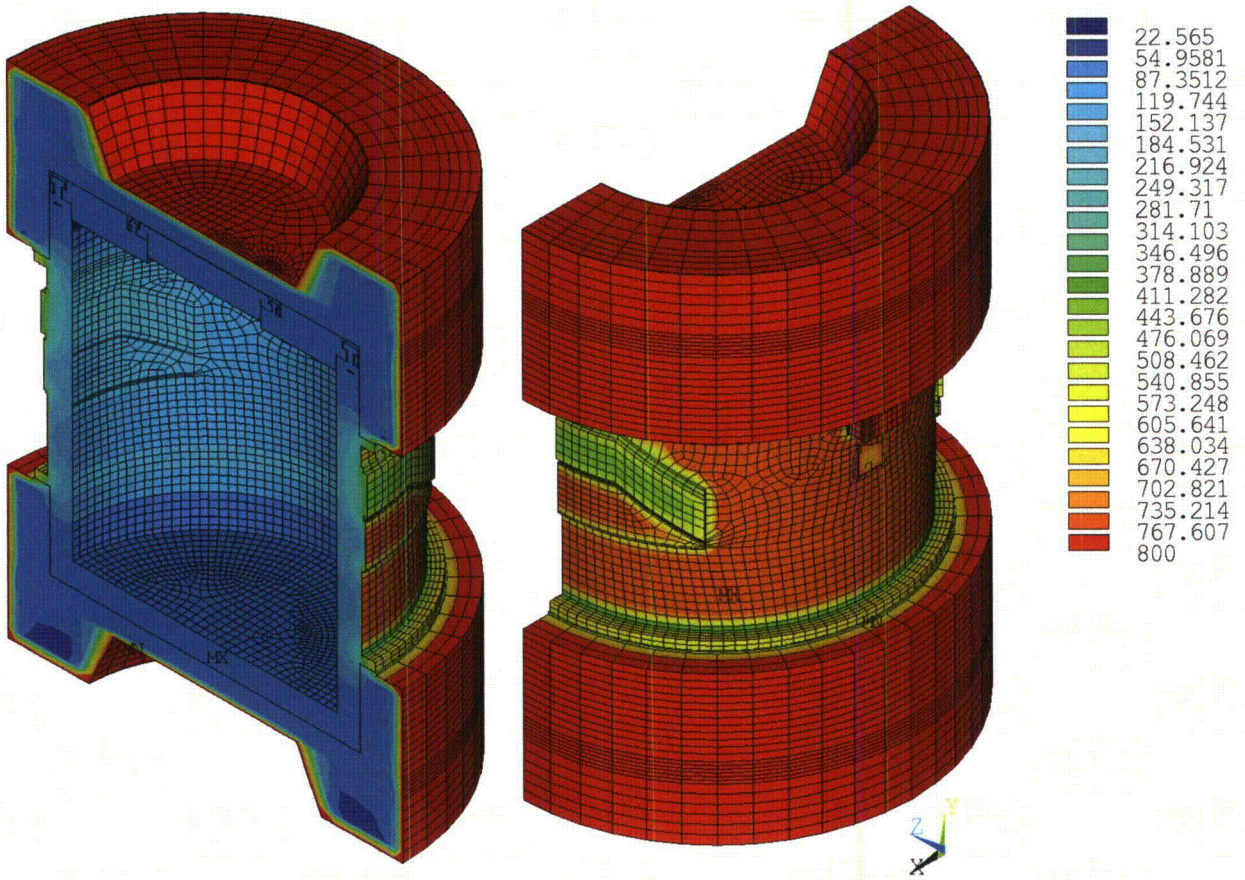

Figure 3.4.2-5 Temperature Contour Plot of Package at the End of Fire—HAC Pin Damage on Cask Body Side

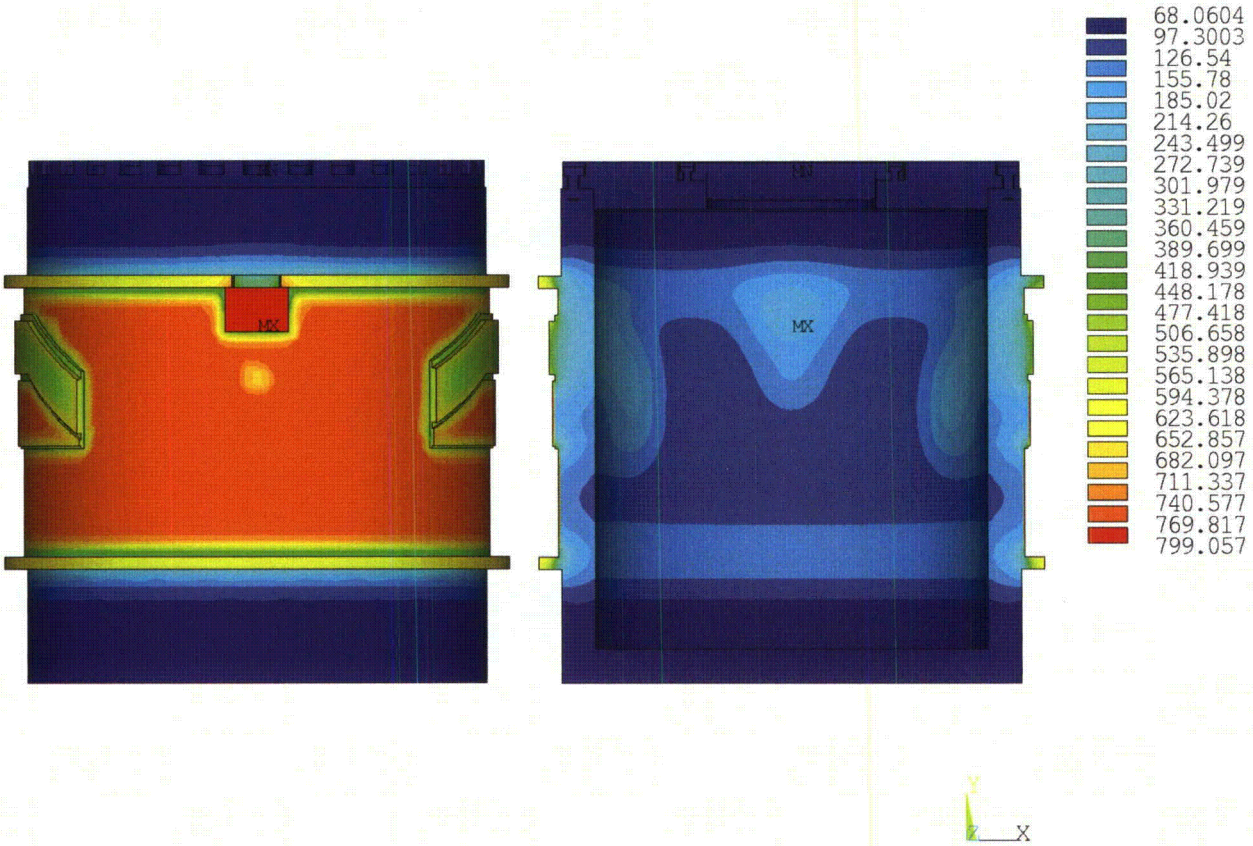

HAC—Fire Side Puncture, Steady-State Inital Conditions (Degrees Celsius)

Figure 3.4.2-6 Temperature Contour Plot of Cask Body at the End of Fire—HAC Pin Damage on Cask Body Side

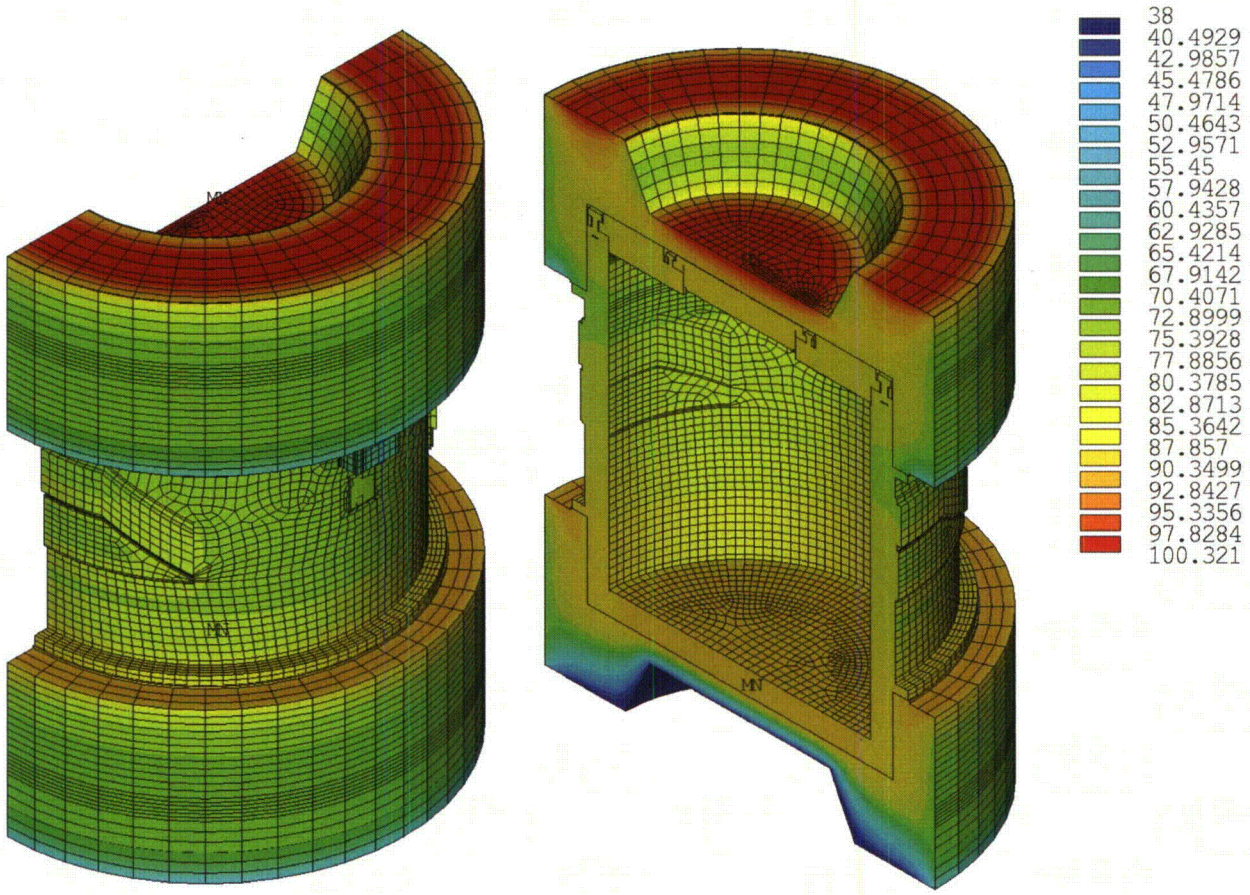

HAC--Fire Side Puncture, Steady-State Inital Conditions (Degrees Celsius)

Figure 3.4.2-7 Temperature Contour Plot of Package after Cool-Down—HAC Pin Damage on Cask Body Side

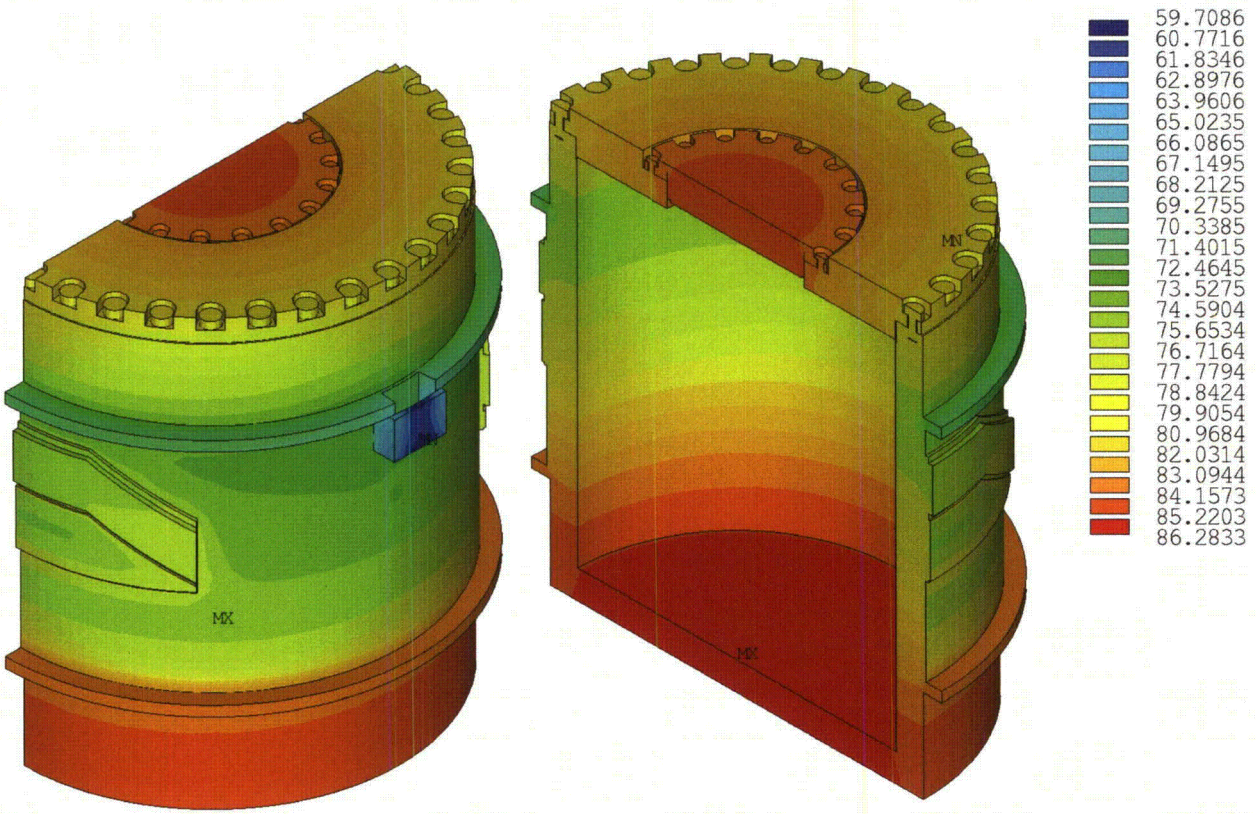

HAC--Fire Side Puncture, Steady-State Inital Conditions (Degrees Celsius)

Figure 3.4.2-8 Temperature Contour Plot of Cask Body After Cool-Down—HAC Pin Damage on Cask Body Side

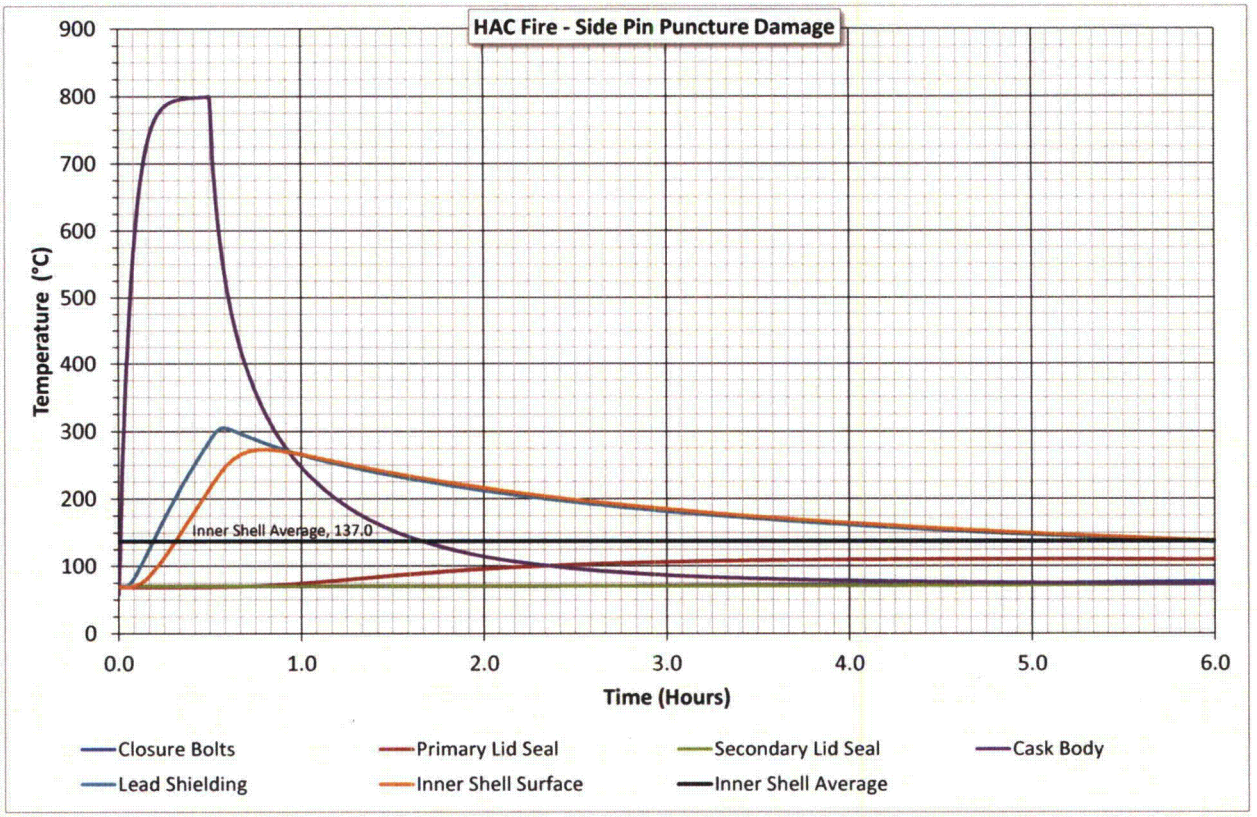

Figure 3.4.2-9 Time-History Plot of Critical Package Components—HAC Pin Damage on Cask Body Side

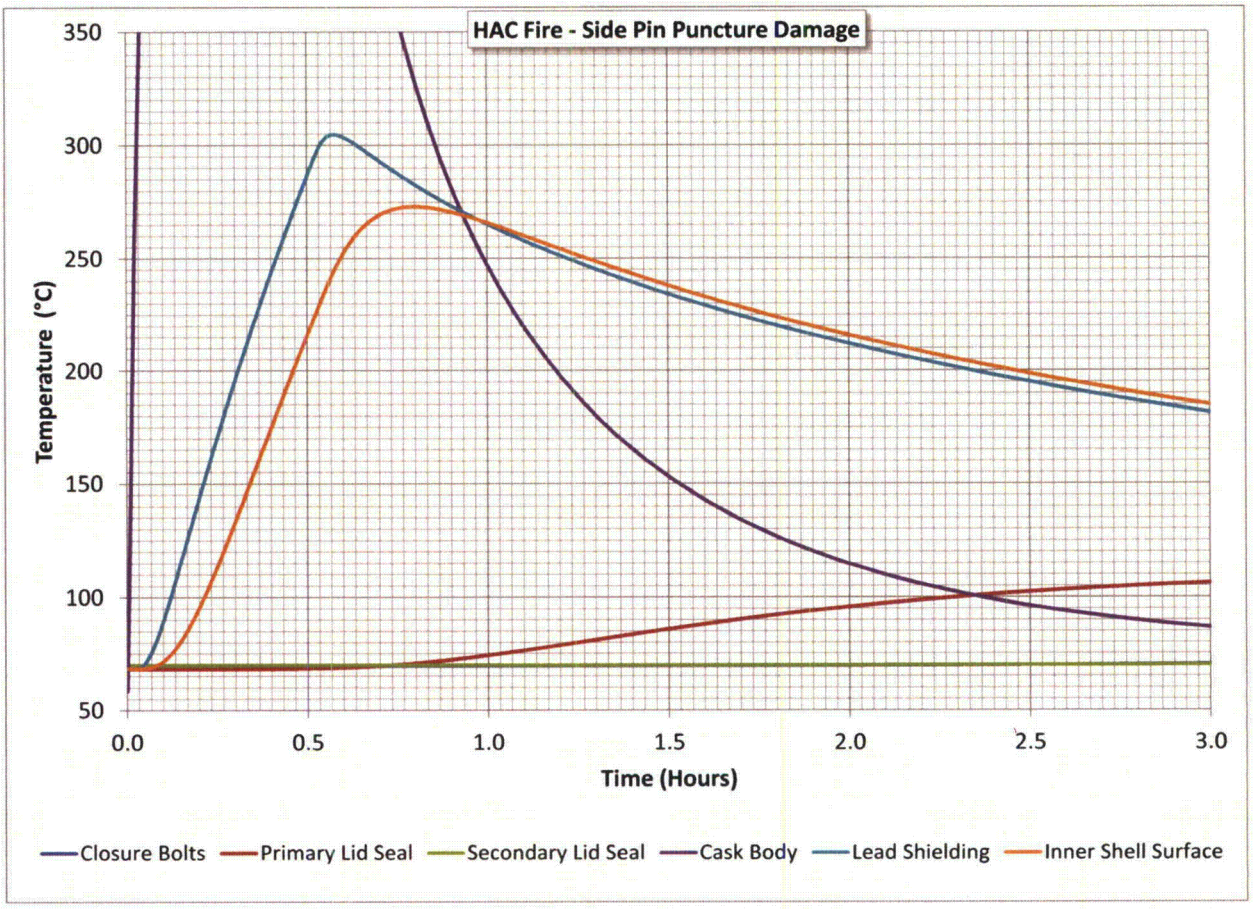

Figure 3.4.2-10 Time-History Enhanced View Plot of Critical Package Components—HAC Pin Damage on Cask Body Side

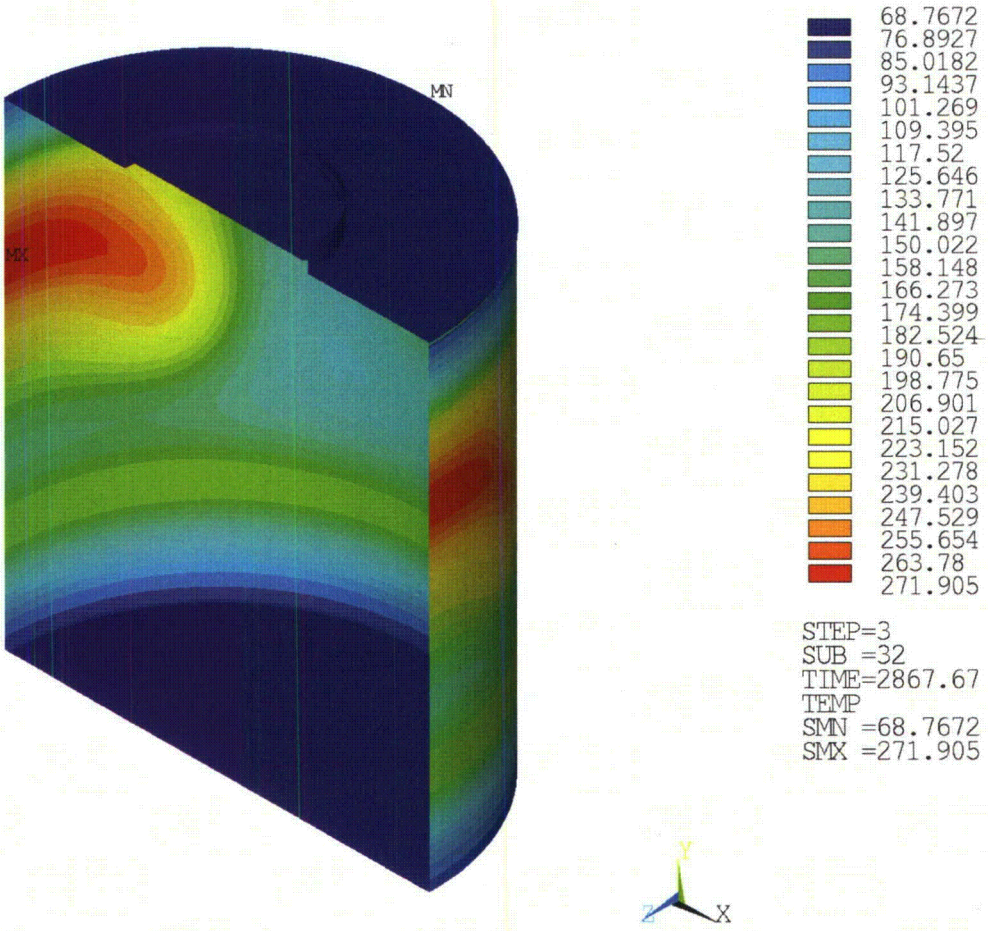

HAC--Fire Side Puncture, Steady-State Inital Conditions (Degrees Celsius)

Figure 3.4.2-11 Maximum Temperature of the Inner Shell—HAC Pin Damage on Cask Body Side

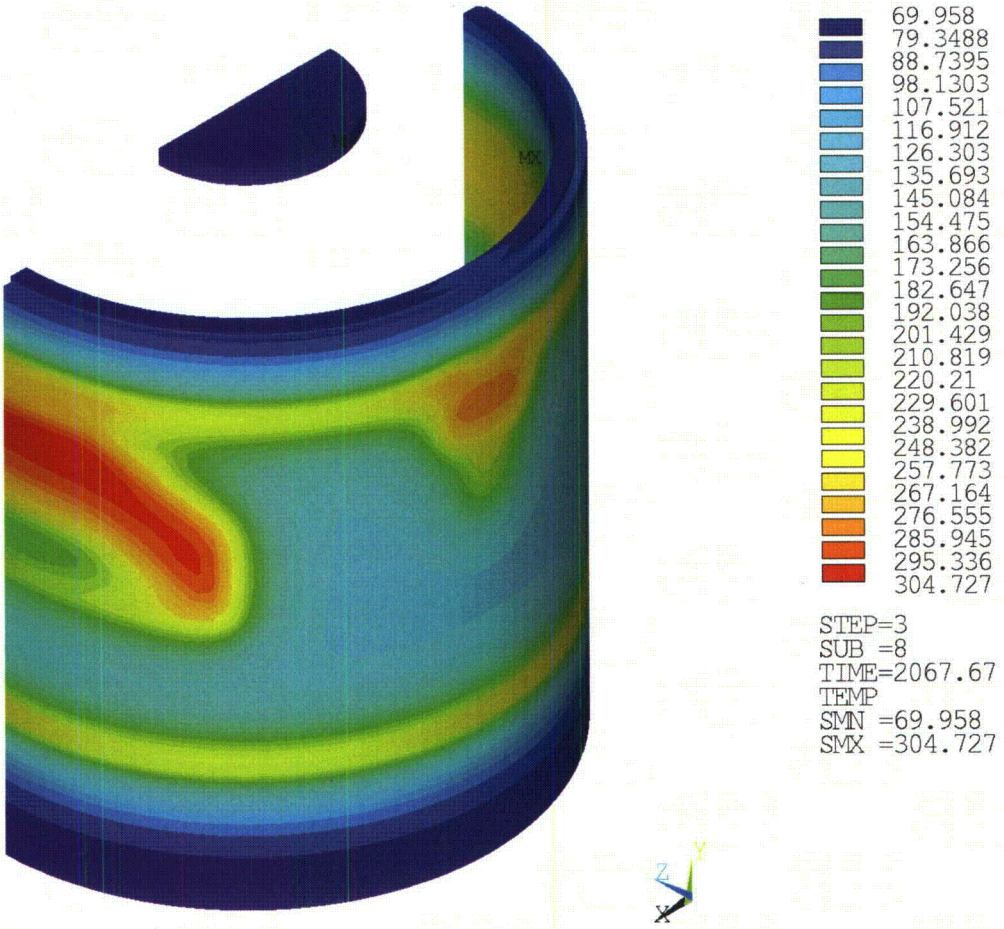

HAC--Fire Side Puncture, Steady-State Inital Conditions (Degrees Celsius)

Figure 3.4.2-12 Maximum Temperature of Lead Shielding—HAC Pin Damage on Cask Body Side